UCD 472-133
DOE Research and Development Report
UC-48, Biomedical and Environmental Research

1987 Annual Report

Laboratory for Energy-Related Health Research

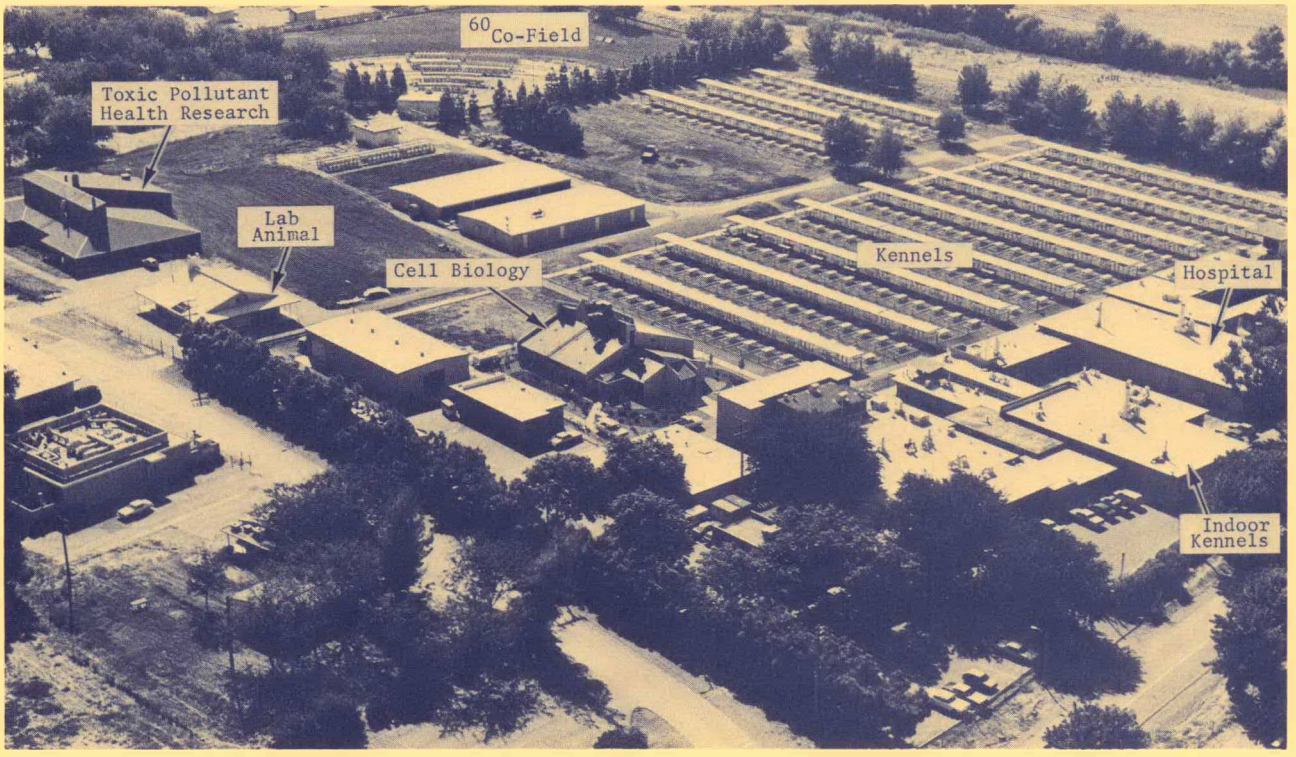

DO NOT MICROFILM THIS PAGE

Printed in the United States of America
Available from
National Technical Information Service
U. S. Department of Commerce
5285 Port Royal Road
Springfield, VA 22161

Printed copy: $21.95
Microfiche copy: A07

UCD--472-133

DE89 012234

LABORATORY FOR ENERGY-RELATED HEALTH RESEARCH

SCHOOL OF VETERINARY MEDICINE
UNIVERSITY OF CALIFORNIA, DAVIS

ANNUAL REPORT FISCAL YEAR 1987

Issued April 1989
By

THE STAFF OF THE LABORATORY FOR
ENERGY-RELATED HEALTH RESEARCH
JAMES W. OVERSTREET, DIRECTOR
OTTO G. RAABE, ASSOCIATE DIRECTOR FOR SCIENCE
DANA L. ABELL, EDITOR

Prepared under
Contract DE-AC03-76SF00472
for the
Department of Energy

FOREWORD

This report to the U.S. Department of Energy summarizes research activities for the period from 1 October 1986 to 30 September 1987 at the Laboratory for Energy-related Health Research (LEHR) which is operated by the University of California, Davis, for the Office of Health and Environmental Research of the Office of Energy Research of the U. S. Department of Energy via Contract No. DE-AC03-76SF00472 administered by the San Francisco Operations Office. Both Department of Energy programmatic research and selected related work for other agencies and organizations as approved by the Department of Energy are reported.

This is the twenty-second annual report of the Laboratory for Energy-related Health Research (LEHR) (formerly called the Radiobiology Laboratory). LEHR is an Organized Research Unit of the University of California, Davis, and is associated with the School of Veterinary Medicine. The Director reports to the Dean of Veterinary Medicine, Dr. Edward A. Rhode, concerning University administrative matters and to the Dean of Graduate Studies and Research, Dr. Allen G. Marr, concerning Laboratory research activities, including University collaborations and graduate student training at LEHR. The LEHR personnel summary, the Advisory Committee members, and names of research collaborators can be found at the back of this report.

The laboratory's research objective is to provide new knowledge for an improved understanding of the potential bioenvironmental and occupational health problems associated with energy utilization. Our purpose is to contribute to the safe and healthful development of energy resources for the benefit of mankind. This research encompasses several areas of basic investigation that relate to toxicological and biomedical problems associated with potentially toxic chemical and radioactive substances and ionizing radiation, with particular emphasis on carcinogenicity. Studies of systemic injury and nuclear-medical diagnostic and therapeutic methods are also involved. This program is interdisciplinary; it involves physics, chemistry, environmental engineering, biophysics and biochemistry, cellular and molecular biology, physiology, immunology, toxicology, both human and veterinary medicine, nuclear medicine, pathology, hematology, radiation biology, reproductive biology, oncology, biomathematics, and computer science.

The principal themes of the research at LEHR center around the biology, radiobiology, and health status of the skeleton and its blood-forming constituents; the toxicology and properties of airborne materials; the beagle as an experimental animal model; carcinogenesis; and the scaling of the results from laboratory animal studies to man for appropriate assessment of risk.

LEHR began as a small research project on the Davis campus of the University of California in 1951 in which studies were done of the biological effects of X-rays on laboratory animals under the support of the U.S. Atomic Energy Commission. In 1957 a major project was initiated by the Atomic Energy Commission to study the biological effects associated with low-level chronic exposure of the skeleton to beta particle irradiation from skeletal deposits of the bone seeking radionuclide, Sr-90, a fission product found in fallout from atmospheric tests of nuclear weapons and a constituent of nuclear wastes from nuclear power plants. The beagle was chosen as the experimental subject because it could be studied in sufficient detail to scale the results to predict the risk in human populations that might be exposed. To assist in this scaling from results in beagles to expected risks in people, parallel studies were planned utilizing the bone-seeking radionuclide Ra-226, to which some people had been exposed in watch-dial painting and in medicine earlier in this century. This main study was the basis for the formation of the Radiobiology Laboratory in 1965 under the direction of Leo K. Bustad as an Organized Research Unit of the University of California, Davis, and the building and administration of the Radiobiology Laboratory by the Atomic Energy Commission. The main study is now nearing completion after some twenty-five years since the first beagles were exposed to Sr-90 in the long-term experiments. The last beagle out of 1063 who were involved in all phases of this research died on February 27, 1986, at the age of 18.5 years (D05Y16); he had been exposed to radiostrontium at the lowest level of the study. The first section of this report documents the current status of this important lifetime study of internally deposited radionuclides in beagles.

The Radiobiology Laboratory grew as the main project expanded, and the research interests of the laboratory broadened to consider all aspects of the radiobiological effects of the irradiation of the skeleton. Special interest in cellular biology focused on the blood-forming and immunological functions of bone marrow cells and their alterations by ionizing radiation. In the early 1970's an outdoor Co-60 irradiator was designed and constructed (nominal source strength 6 TBq) for chronic exposure of beagles to up to about 3 mC/kg in air. This facility has been beneficially utilized for research on the cellular and systemic effects of penetrating gamma ray irradiation on the bone marrow in beagles and has been especially valuable for studies of the radiation induction of leukemia. A report on current research based on these external radiation effects studies is found herein as part of the cellular and molecular studies aimed at improving our understanding of the genetic and cellular nature of leukemia.

Construction of the new Toxic Pollutant Health Research Laboratory was completed and the facility was dedicated in 1983. This specialized building was designed for the total containment and safe study of highly toxic and/or carcinogenic agents, including both radioactive and chemical materials in toxicological studies with laboratory animals. This research may involve exposures to toxic materials by dermal, intravenous, oral-gastro-intestinal, intratracheal and inhalation routes. Current work in TPHRL includes studies of Pu-241 behavior in beagles and monkeys.

Also in 1983, studies began of the application of chemical and nuclear science to problems in nuclear medicine. These nuclear-medicine studies have centered on issues associated with the development of specifically bound, short-lived radionuclides that can be exclusively targeted to irradiate cancer cells and/or tumors in the body. The development of these so-called radiopharmaceuticals continues to be a major research activity, and it is the subject of one whole section of this report.

The report has been divided into several topical sections outlining the scope of research at LEHR, including "Radionuclide Toxicity Studies," "Skeletal Biology Studies," "Cellular and Molecular Studies," "Nuclear Medical Studies" and "Radiological Impacts." Emphasis at LEHR is placed on open literature publications. Open literature publications and oral presentations from national and international meetings are listed at the back.

We hope that this progress report will provide needed information concerning the status of the various funded projects at LEHR and reflect the intellectual and scientific pride and enthusiasm of the research faculty and staff concerning the important advances in knowledge that are resulting from this program. As always, we appreciate comments and suggestions concerning the content of this report and the direction of future research.

Respectively submitted,

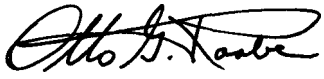

Otto G. Raabe
Associate Director for Science

ACKNOWLEDGMENTS

We thank Pamela Carroll for organizing, word processing and layout and Bobbi Jean Melbourn for typing this report. We wish to extend special thanks to Steve Maslowski, Scott Hammond and their assistants in animal care for their efforts in this most important area.

The active interest and advice of Dean Edward A. Rhode of the School of Veterinary Medicine, Dean Allen G. Marr of Graduate Studies and Research, our Advisory Committee and our consultants and collaborators are sincerely appreciated.

The research described in this report involved animals maintained in facilities approved by the American Association for the Accreditation of Laboratory Animal Care (AAALAC).

TABLE OF CONTENTS

RADIONUCLIDE TOXICITY STUDIES

STRONTIUM-90 AND RADIUM-226 TOXICITY IN BEAGLE DOGS: CURRENT STATUS

L. S. Rosenblatt
M. R. Culbertson
N. J. Parks
W. L. Spangler
M. Goldman

We are investigating biologic effects of ^{90}Sr and ^{226}Ra in the beagle in order to predict the possible long-term hazards to people from chronic exposure to low levels of irradiation. Animals received either radionuclide by several means of administration: (a) continual ingestion of ^{90}Sr, (b) a single intravenous injection of ^{90}Sr, or (c) a series of eight intravenous injections of ^{226}Ra. Although administration of ^{90}Sr and ^{226}Ra ended at 540 days of age, the animals continued to receive chronic, low-level radiation doses from these bone-seeking radionuclides throughout life. The last of the dogs died last year at age 18.5, but we are continuing to investigate the significance of these long-term exposures given at low dose rates with regard to cancer production, physiologic well-being, and shortening of life through the detailed records that were kept and by study of preserved materials.

The major goal of this study on the toxicity of ^{90}Sr and ^{226}Ra is to provide information on long-term consequences expected to occur in people from chronic exposure to α- and β-emitting bone-seeking radionuclides. To meet this goal, we are evaluating the biologic effects of the two radionuclides in the beagle. Similarities between dogs and people provide a valuable base for the scaling of potential hazards from radionuclide contamination from canine to human populations.

Experimental Design

Radium-226 was injected intravenously into dogs beginning at 435 days and every two weeks thereafter until 540 days of age. Activities over an approximately 500-fold range were administered to these animals in 6 treatment levels plus controls; together they comprise the R-dogs (Table 1).

Table 1. EXPERIMENTAL DESIGN AND STATUS OF RADIUM-226 TOXICITY STUDY

^{226}Ra Injection Series (8 Biweekly Injections Starting at 435 Days of Age)					
Treatment Code	Multiple of 10 level	kBq/kg/inj	Total (kBq/kg)	Number of Dogs	Median Survival (Years)
R00	0	0	0	85	14.6
R05	0.3	0.111	0.888	46	14.5
R10	1	0.296	2.37	40	13.8
R20	6	1.74	13.9	42	10.9
R30	18	5.18	41.4	40	7.4
R40	54	15.5	124.0	41	5.1
R50	162	46.3	370.0	41	4.3
				335	

The activity per injection ranged from 0.111 to 46.25 kBq/kg. The nominal quantity injected for a 10-kg dog ranged from 8.88 to 370 kBq of ^{226}Ra.

The activity at R10 was computed to represent the canine equivalent of 10 times the maximum permissible skeletal burden for man (3.7 kBq ^{226}Ra), based on the assumption of a 25% skeletal retention of the injected quantity. The time of injection, from 14 to 18 months of age, was chosen to approximate the temporal pattern of ^{226}Ra assimilation by the radium dial painters, a human population to which the experimental canine population would be compared. Strontium-90 was administered in the food, with the dietary concentration of ^{90}Sr maintained at a constant level with respect to dietary calcium levels. Activities were administered to 7 treatment groups (plus controls) over a 1500-fold range; these are the D-dogs (Table 2).

Table 2. EXPERIMENTAL DESIGN AND STATUS OF STRONTIUM-90 TOXICITY STUDY

^{90}Sr Ingestion Series (in utero to 540 days of Age)
Data include 15 dogs fed throughout life in D30, D40 and D50.

Treatment Code	Multiple of 10 Level	kBq ^{90}Sr per g dietary Ca	Ingested kBq/d	Total Ingested (kBq)	Number of Dogs	Median Survival (Years)
D00	0	0	0	0	80	14.5
D05	0.3	0.259	0.74	370	77	14.2
D10	1	0.777	2.59	1,480	42	13.5
D20	6	4.55	16.3	8,880	66	14.4
D30	18	13.7	48.1	25,900	64	14.1
D40	54	41.1	148.0	81,400	71	12.0
D50	162	123.0	444.0	241,000	65	5.2
D60*	486	370.0	1,332.0	718,000	19	2.2
					484	

*D60 dogs were not in the original experimental design but were added in 1967.

^{90}Sr Injection Series
(Single IV Injection at 540 Days of Age)

Treatment Code	Multiple of 10 Level	kBq/kg/inj	Total kBq/kg	Number of Dogs	Median Survival (Years)
S20	6	137	137	20	13.5
S40	54	1,220	1,220	26	13.3
				46	
Total				865	

Administration of ^{90}Sr began in utero at the beginning of the second trimester of gestation when the dams began to receive radioactive feed. Pups were nursed while their mothers continued on the dietary regimen, and they were weaned onto the same ^{90}Sr-containing diet. Feeding continued until 540 days of age, at which time the animals began to receive the standard (nonradioactive) laboratory ration. The nominal quantity ingested was 370 to 717,800 kBq ^{90}Sr. The time of administration, from prior to birth until 18 months of age, includes the period of skeletal maturation, and was chosen to represent human exposures by ingestion of ^{90}Sr-contaminated foods during early life.

Two additional small groups of dogs (S-) were given their ^{90}Sr as a single injection at 540 days of age, to serve in the comparison of the two modes of administration (injection vs. ingestion). These groups were included to also act as a common link between the project at Davis and a related DOE-funded study at the University of Utah.

Survival

The last surviving dog, D05Y16, died on 02/27/86 at 18.5 years

The cumulative survival rates of R05- and R10-level dogs appear indistinguishable from control animals through 17 years (Figure 1). Cumulative survival rates of other treatment groups are significantly different from controls ($p < 0.05$) after 7.5 years of age for R20 dogs, 6 years for R30s, 5 years for R40s, and 3 years for R50s.

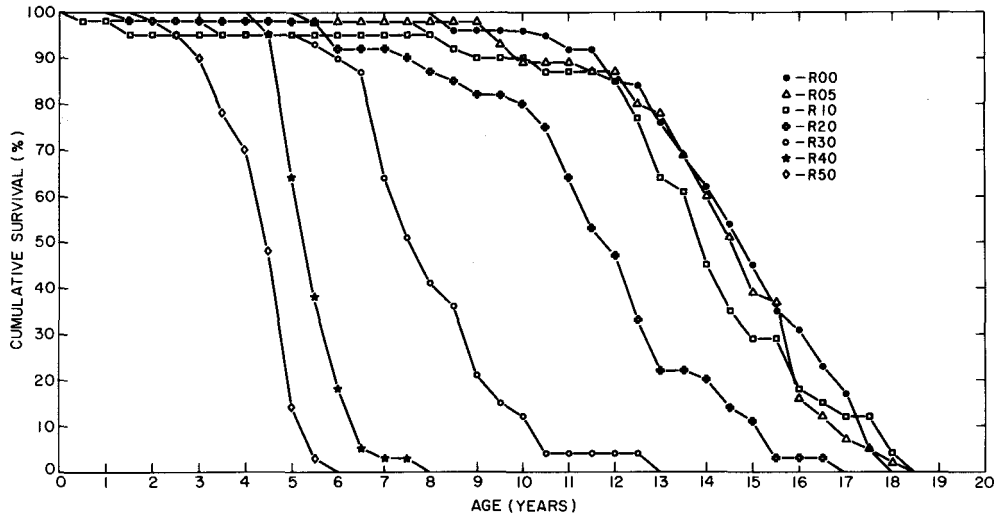

Fig. 1. Cumulative survival curves of beagle dogs given eight fortnightly intravenous injections of ^{226}Ra, the last of which occurred at 540 days of age.

Strontium-90 fed dogs at D05, D20, and D30 levels were not different from controls through 17 years of age (Figure 2), whereas D40s were significantly different from controls from 3 to 6 years and after 10 years of age; D50s after 3 years of age; and D60s after 2 years of age.

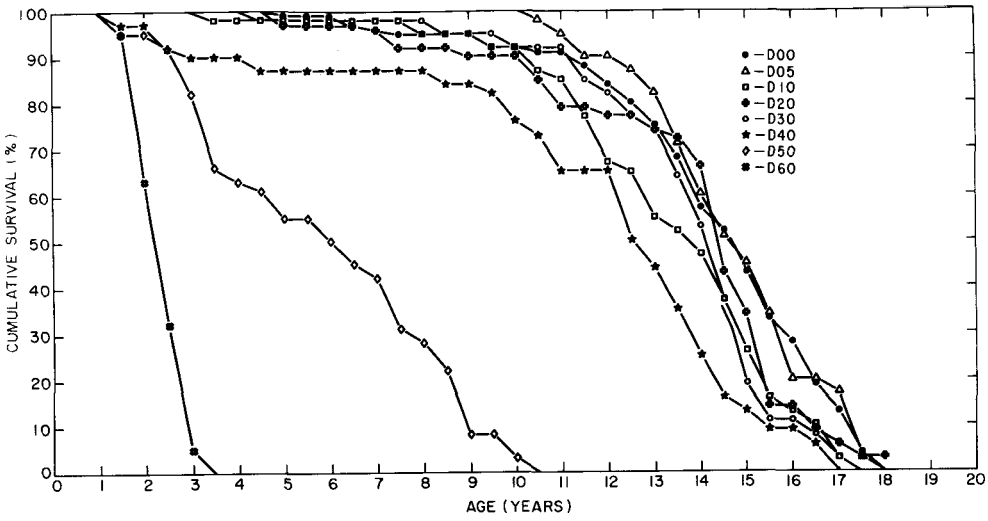

Fig. 2. Cumulative survival of beagles fed ^{90}Sr until 540 days of age.

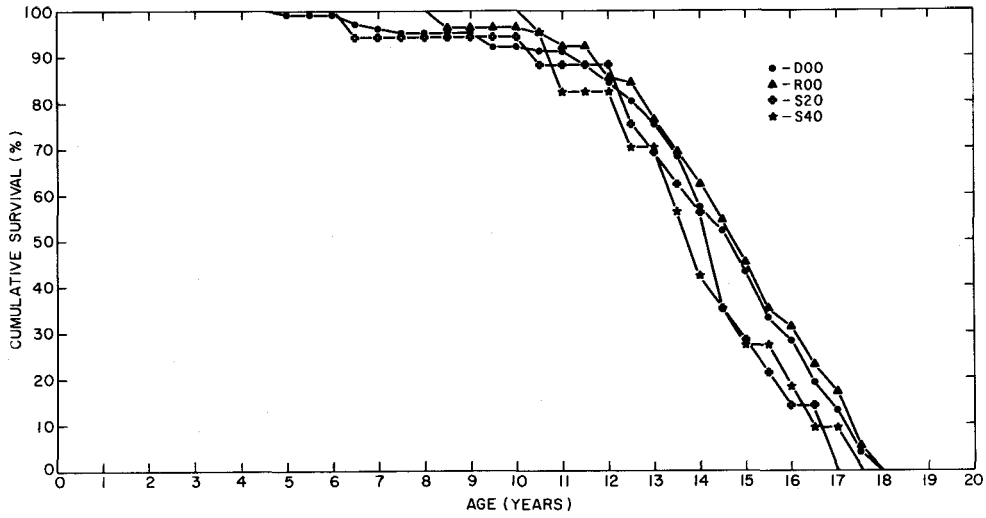

Fig. 3. Cumulative survival of beagles given a single intravenous injection of ^{90}Sr at 540 days of age.

The median survival time for unirradiated control beagles is 14.5 yr for D00's and 14.6 yr for R00's. Median survivals for each of the dose groups are given in Tables 1-3, above.

Radiation Doses

From the wide range of administered activities presented in Tables 1 and 2, variable body burdens of ^{226}Ra and ^{90}Sr were obtained. Soon after cessation of treatment, most of the radionuclides distributed in soft tissue were eliminated. The body burden, therefore, is essentially equivalent to the skeletal burden. Longer-term retention and, therefore, radiologic dose also varied among and within treatment levels.

Cumulative average skeletal doses (means for each group) are included in Table 3. Primarily because of differences in longevity, the 500-fold range of injected dosages for the radium dogs (Table 1) is reduced to a 180-fold range of average skeletal doses. Further, the 1500-fold range of ingested activities of ^{90}Sr is reduced to a 430-fold range.

Table 3. CUMULATIVE AVERAGE SKELETAL DOSES (MEAN VALUES FOR EACH GROUP).

Level	Mean (±SEM) Dose (centiGy.)	Level	Mean (±SEM) Dose (centiGy.)
R00	--	D00	--
R05	90 ± 3	D05	30 ± 2
R10	290 ± 20	D10	130 ± 5
R20	1400 ± 50	D20	800 ± 30
R30	3100 ± 110	D30	2600 ± 90
R40	7800 ± 330	D40	6100 ± 270
R50	16000 ± 700	D50	9700 ± 540
		D60	13000 ± 870
		S20	750 ± 70
		S40	6200 ± 420

Causes of Death of Control, ^{90}Sr-, and ^{226}Ra-Treated Beagles

The causes of death are presented as "Comments" in Table 4 (pages 10-33) of this report. The following description applies to the individual tabulated data:

The study evolved in three production runs. The "Pilot Series" was initiated in 1961-63 with ^{90}Sr feeding of D05-, D20-, D30-, D40-, and D50-level dogs prior to completion of construction of all facilities. In the "First Run," 1963-64, half of the controls, the ^{90}Sr-fed or -injected dogs, and the ^{226}Ra-injected dogs were treated, with maximum facility utilization. At this time, 15 dogs (7 D30s, 4 D40s, and 4 D50s) were fed ^{90}Sr, but instead of ^{90}Sr administration ending at 540 days of age, it continued for their lifetimes. These dogs are designated "continuous feeding" dogs and have been discussed recently (Book et al., 1982). The "Second Run," 1965-67, completed the required number of experimental animals. In 1967 a group of beagles was introduced at the D60 level to provide toxicity data for a higher exposure level. At about the same time, a small group of dogs (designated R5X) received their R50-level injections beginning at either 60 or 120 days of age, rather than at 435 days, for the study of ^{226}Ra effects in early life.

Dogs dying or otherwise removed from the study prior to weaning (at 42 days of age) are not included. No difference in mortality of young beagles before weaning was found between control and irradiated groups (Rosenblatt et al., 1972). Previous reference to

"scheduled sacrifice" dogs has been deleted because there were no "scheduled sacrifices." Special sacrifices are listed in the comments column of Table 4. Some unexposed R dogs and young D dogs previously listed have also been deleted.

In the individual data, both birthdate and age are given and litters are grouped. Dogs with the same 3 digits in the "Litter Number" column are littermates. "Age at Termination" refers to the age at which some treatment or procedure was initiated which may affect interpretation of the results--BCG therapy for mammary cancer, for example.

For each dog that received radioactivity, the peak body burden in kBq and in kBq/kg body weight is presented. Values are the highest actual counts determined by periodic whole body counting. For S-dogs, counts were made 3-4 weeks after the single injection of ^{90}Sr; hence, the "peak" in this instance is less than the quantity injected (Table 2).

"Exposure Days" refers to the time of exposure to radioactivity, equal to age for D-dogs, but equal to age minus 540 for S-dogs and age minus 435 for all R-dogs other than R5X. For the R5X dogs, exposure days is age minus 119 for F01, age minus 124 for M02 and M03, and age minus 63 for M04, M05, and M06. For dogs with termination dates, exposure ends at termination rather than at death.

"Total Dose" is the cumulative skeletal centiGrays received by each animal and is the lifetime integration of the skeletal rads/day curve determined by periodic counting of whole body radioactivity. For these calculations, we assumed the skeletal burden to be 100% of the body burden for ^{226}Ra, 98% of the body burden for ^{90}Sr after cessation of ^{90}Sr feeding, and 88% of the body burden for ^{90}Sr during ^{90}Sr feeding. Other aspects of dose calculations have been discussed previously (Raabe et al., 1981).

"Comments" summarize our assessment of the primary factor contributing to each animal's death. The diagnoses are not necessarily final and should be considered preliminary. As additional information is gained, the comments may require change. Hence, the reader should use caution when drawing conclusions from these data. In addition, these comments do not include secondary and complicating factors, some of which may have a radiation-related etiology. For instance, an animal that had died of a myeloproliferative disorder may also have had a microscopic bone tumor. Although induced by irradiation and so noted in the dog's records, this latter occurrence would not appear in this summary. The "Comments" in this report differ from previous reports in that they represent a reappraisal of the clinical and histopathologic records. Particular attention was paid to those deaths previously listed as accidental.

The following symbols are used:

MPS - myeloproliferative syndrome

C - continuous (lifetime) feeding of ^{90}Sr

BCG - treatment of mammary tumor with intralesional injection of BCG (Bacillus of Calmette Guerin)

A - indicates an amputation of a limb. A list of those dogs and reasons for amputation was given in the 1984 Annual Report (UCD 472-130, pp. 6-8).

REFERENCES

Book, S. A., W. L. Spangler and L. A. Swartz. Effects of lifetime ingestion of ^{90}Sr in beagle dogs. 1982. Rad. Res. 90:244.

Rosenblatt, L. S., S. W. Bielfelt and D. J. Della Rosa. 1972. In M. Goldman and L. K. Bustad (eds.), Biomedical Implications of Radiostrontium Exposures. AEC Symposium No. 25, p. 334.

Raabe, O. G., S. A. Book, N. J. Parks, C. E. Chrisp and M. Goldman. 1981. Lifetime studies of ^{226}Ra and ^{90}Sr toxicity in beagles - a status report. Rad. Res. 86:515-538.

Table 4. DATA FOR CONTROL BEAGLES AND BEAGLES EXPOSED TO ^{90}Sr AND ^{226}Ra.

(Table 4 follows on pages 10 - 33)

BEAGLE NUMBER	LITTER NUMBER	BIRTH DATE	AGE AT TERM.	AGE AT DEATH	PEAK BODY BURDEN (kBq)	(kBq/KG)	EXPOSURE DAYS	TOTAL DOSE (CENTIGRAYS)	C O M M E N T S
	FIRST RUN								
D00F01	307A	12/14/63		17.3					METASTATIC MAMMARY CARCINOMA
D00F02	307B	12/14/63		15.3					LEIOMYOSARCOMA-URETHRA
D00F03	307C	12/14/63		12.5					METASTATIC THYROID CARCINOMA
D00M04	307D	12/14/63		14.0					PERITONITIS SECONDARY TO DUODENAL ULCERS
D00F05	329A	3/11/64		15.5					METASTATIC MAMMARY CARCINOMA
D00M06	329B	3/11/64		17.0					METASTATIC SEMINOMA
D00F08	346B	4/23/64		14.4					METASTATIC HEMANGIOSARCOMA
D00M09	346C	4/23/64		15.6					LYMPHOSARCOMA
D00M10	346D	4/23/64		12.0					LYMPHOSARCOMA
D00F11	347A	4/23/64		13.7					METASTATIC MAMMARY CARCINOMA
D00F12	347B	4/23/64		11.2					MALIGNANT LYMPHOMA
D00M14	347D	4/23/64		6.9					CHRONIC PULMONARY DISEASE WITH COR PULMONALE
D00F16	353A	5/12/64		15.6					ACUTE NECROTIZING PNEUMONIA-ASPIRATION, AND LYMPHOSARCOMA
D00F19	353D	5/12/64		14.0					PITUITARY TUMOR
D00M20	353E	5/12/64		12.8					MALIGNANT LYMPHOMA
D00M21	353F	5/12/64		3.5					CONVULSIONS, IDEOPATHIC EPILEPSY, ASPIRATION PNEUMONIA
D00F24	364C	6/03/64		15.0					METASTATIC COMPLEX TUBULAR ADENOCARCINOMA-MAMMARY GLAND
D00M26	364E	6/03/64		14.9					METASTATIC PERIANAL ADENOCARCINOMA
D00M27	364F	6/03/64		14.4					DISSEMINATED BRONCHOGENIC CARCINOMA
D00M28	364G	6/03/64		15.0					ADRENAL CORTICAL ATROPHY
D00F29	373A	6/16/64		12.3					CHRONIC VALVULAR ENDOCARDITIS WITH CONGESTIVE HEART FAILURE
D00M31	373C	6/16/64		9.2					HYDROCEPHALUS, SECONDARY TO PITUITARY TUMOR
D00F32	375A	6/17/64		16.6					METASTATIC MAMMARY ADENOCARCINOMA (SQUAMOUS CELL) TO THE LUNG
D00F34	375C	6/17/64		11.4					METASTATIC MAMMARY CARCINOMA
D00F35	375D	6/17/64		12.3					METASTATIC SPLENIC HEMANGIOSARCOMA
D00M36	375E	6/17/64		11.5					CONGESTIVE HEART FAILURE SECONDARY TO ENDOCARDIOSIS
D00M37	375F	6/17/64		16.0					SENILE CEREBRAL ATROPHY
D00F39	376B	6/18/64		16.0					ADRENAL MEDULLARY NEOPLASM
D00M40 A	376C	6/18/64		14.7					SARCOMA NEAR VERTEBRA, ORIGIN UNKNOWN
D00M41	376D	6/18/64		12.7					TRANSITIONAL CELL CARCINOMA OF THE PROSTATIC URETHRA
D00M43	376F	6/18/64		17.7					PULMONARY THROMBOSIS
D00M47	380D	6/20/64		16.8					UNDETERMINED CNS DISEASE
D00M48	380E	6/20/64		6.0					COLONIC INFARCTION AND SHOCK
D00F49	404A	8/01/64		15.1					DISSEMINATED MAMMARY CARCINOMA
D00F50	404B	8/01/64	4.3						CULLED (EPILEPSY)
D00M51	404C	8/01/64		17.2					INTERSTITIAL PNEUMONIA AND BRONCHIECTASIS
D00M53	404E	8/01/64		13.4					SALIVARY GLAND ADENOCARCINOMA OR ORAL MELANOMA
D00F54	428A	10/08/64		13.0					METASTATIC MAMMARY CARCINOMA
D00M57	428D	10/08/64		13.3					METASTATIC TRANSITIONAL CELL CARCINOMA OF THE URINARY BLADDER
D00M58	428E	10/08/64		16.1					CHRONIC RENAL FAILURE/CNS DEFICIENCY

BEAGLE NUMBER	LITTER NUMBER	BIRTH DATE	AGE AT TERM.	AGE AT DEATH	PEAK BODY BURDEN (kBq)	(kBq/KG)	EXPOSURE DAYS	TOTAL DOSE (CENTIGRAYS)	C O M M E N T S
	SECOND RUN								
D00F62	490C	9/10/65		17.3					ACUTE ENDOCARDITIS AND MYOCARDITIS
D00M64	490E	9/10/65		17.5					INTERVERTEBRAL DISC DEGENERATION AND HERNIATION
D00F66	507A	11/05/65		14.1					VACUOLAR HEPATOPATHY-HEPATIC INSUFFICIENCY
D00F67	507B	11/05/65		17.0					DISSEMINATED MAMMARY ADENOCARCINOMA
D00F69	507D	11/05/65		16.4					SQUAMOUS CELL CARCINOMA, RIGHT TONSIL
D00M70	507E	11/05/65		14.7					SQUAMOUS CELL CARCINOMA--TONSIL
D00M71	507F	11/05/65		15.6					NECROTIZING MYOCARDITIS, ETIOLOGY UNKNOWN
D00F73	514B	12/22/65		17.7					CHRONIC RENAL DISEASE
D00F74	514C	12/22/65		13.6					CHRONIC SUPPURATIVE FOLLICULODERMATITIS (DEMODEX)
D00F75	514D	12/22/65		15.4					MPS
D00F78	549A	6/10/66		12.4					ACUTE ASPIRATION BRONCHOPNEUMONIA (ASPIRATED VOMITUS)
D00F80 A	549C	6/10/66		17.6					ORAL MALIGNANT MELANOMA WITH METASTASIS
D00M82	549E	6/10/66		13.2					METASTATIC HEART BASE TUMOR
D00M83	549F	6/10/66		16.0					CHRONIC SUPPURATIVE PNEUMONIA
D00F85	554A	6/25/66		13.6					ACUTE NECROTIZING PNEUMONIA-BACTERIAL
D00F86	554B	6/25/66		7.3					CHRONIC MEMBRANOPROLIFERATIVE GLOMERULONEPHRITIS
D00F87	554C	6/25/66		14.6					HEPATIC FAILURE SECONDARY TO LYMPHOSARCOMA/MYOCARDIAL NECROSIS
D00M88	554D	6/25/66		11.9					CONGESTIVE HEART FAILURE
D00M89	554E	6/25/66		16.4					MPS
D00M90	554F	6/25/66		17.5					OSTEOSARCOMA WITH METASTASIS
D00F91	559A	7/02/66		15.2					SENILE ENCEPHALOPATHY (CNS DEFICIENCY). ALSO ENDOCARDITIS?
D00F92	559B	7/02/66		9.3					METASTATIC HEMANGIOSARCOMA OF THE R ATRIUM
D00M94	559D	7/02/66		12.9					UNDETERMINED--POST MORTEM AUTOLYSIS
D00M96	559F	7/02/66		16.3					CHRONIC PYELONEPHRITIS
D00X03	565C	8/04/66		16.1					SEVERE PROGRESSIVE RENAL DISEASE
D00X04	565D	8/04/66		16.1					METASTATIC MAMMARY CARCINOMA
D00Y05	565E	8/04/66		10.3					TRANSITIONAL CELL CARCINOMA OF THE PROSTATIC URETHRA
D00Y06	565F	8/04/66		15.2					BACTERIAL ENDOCARDITIS
D00Y07	565G	8/04/66		17.4					SPINAL MYELOPATHY (LUMBAR). ALSO RENAL FAILURE
D00X08	577A	11/10/66		.3					ACCIDENTAL DEATH (ANESTHETIC DEATH)
D00Y10	577C	11/10/66		14.0					CONGESTIVE HEART FAILURE/BRONCHOPNEUMONIA
D00X13	579C	11/17/66		14.8					METASTATIC PANCREATIC ADENOCARCINOMA
D00X15	580A	11/18/66		17.4					METASTATIC MAMMARY CARCINOMA
D00Y17	580C	11/18/66		13.7					EMBOLIC PNEUMONIA
D00Y18	580D	11/18/66		13.4					METASTATIC ISLET CELL CARCINOMA
D00Y19	580E	11/18/66		17.1					INTRACTABLE COUGH / PULMONARY INTERSTITIAL FIBROSIS
D00X20	620A	6/05/67		14.3					ADRENAL CORTICAL ATROPHY
D00X23	638B	9/12/67		14.0					LYMPHOSARCOMA
D00X24	638C	9/12/67		16.7					LYMPHOCYTIC ENTERITIS - MALABSORPTION
D00X25	638D	9/12/67		5.0					ENTEROPATHY
D00Y27	638F	9/12/67		14.6					NASAL CARCINOMA

BEAGLE NUMBER	LITTER NUMBER	BIRTH DATE	AGE AT TERM.	AGE AT DEATH	PEAK BODY BURDEN (kBq)	(kBq/KG)	EXPOSURE DAYS	TOTAL DOSE (CENTIGRAYS)	C O M M E N T S
PILOT SERIES									
D05F02	098B	1/28/61		14.4	11.84	1.517	5267	20	METASTATIC CARCINOMA - HEPATOCELLULAR AND ADRENAL CORTICAL
D05F03	098C	1/28/61	7.8		16.65	1.591	2845	19	TERMINATED (EPILEPSY)
D05M04	098D	1/28/61		14.9	15.17	1.739	5443	22	MALIGNANT LYMPHOMA
D05M05	098E	1/28/61	7.8		15.17	1.406	2845	30	TERMINATED (EPILEPSY)
D05F08	099B	2/01/61		15.9	9.25	.888	5819	22	CENTRAL NERVOUS SYSTEMS SIGNS (SEVERE PURKINJE CELL DEGENERATION)
D05M10	099D	2/01/61		16.7	10.73	.999	6085	27	SEVERE POSTERIOR PARESIS, ACUTE SEVERE PROSTATIC INFECTION, PROGRESSIVE RENAL FAILURE
D05M11	099E	2/01/61		16.0	12.58	1.332	5850	34	CENTRAL NERVOUS SYSTEMS SIGNS (SEVERE PURKINJE CELL DEGENERATION)
D05F12	102A	2/16/61	16.1	16.1	9.25	1.924	5883	14	NEPHROSCLEROSIS AND CHRONIC BRONCHOPNEUMONIA
D05F14	102C	2/16/61		16.2	13.32	1.813	5929	23	BRONCHOPNEUMONIA, ACUTE, CHRONIC
D05F15	102D	2/16/61		13.3	17.76	3.700	4855	38	AORTIC THROMBOSIS
D05F17	209A	6/20/62		9.9	7.77	1.073	3621	18	HEPATOCELLULAR ADENOMA
D05F18	209B	6/20/62		12.8	9.25	1.517	4682	18	TRANSITIONAL CELL CARCINOMA OF THE URINARY BLADDER
D05F19	209C	6/20/62		10.8	10.73	1.332	3957	31	METASTATIC THYROID CARCINOMA
D05M20	209D	6/20/62		15.0	12.95	1.554	5482	30	CHRONIC PYELONEPHRITIS, DRUG REACTION, AND CARDIOMEGALY
D05M21	209E	6/20/62		16.5	14.06	1.443	6028	36	DISSEMINATED INTRAVASCULAR COAGULATION, CLOSTRIDIUM SEPTICEMIA, THROMBOSIS
D05M22	209F	6/20/62		14.3	13.32	1.258	5215	39	METASTATIC ADRENAL CARCINOMA WITH DISSEMINATED INTRAVASCULAR COAGULOPATHY
D05F23	227A	9/20/62		14.4	11.10	1.332	5270	30	METASTATIC MAMMARY CARCINOMA
D05F24	227B	9/20/62		9.4	12.58	1.295	3450	28	NASAL CARCINOMA
D05M26	227D	9/20/62		12.0	11.10	1.073	4401	32	MALIGNANT LYMPHOMA
D05M27	227E	9/20/62		6.6	18.13	1.369	2416	32	GRANULOMATOUS ENCEPHALITIS
D05F28	233A	11/12/62	5.3	15.6	10.73	1.036	5714	26	TERMINATED-BCG EXPERIMENT END STAGE RENAL DISEASE SECONDARY TO BILATERAL RENAL ARTERIOSCLEROSIS
D05M31	233D	11/12/62		5.1	12.21	1.184	1876	21	CLOSTRIDIAL SEPTICEMIA
D05F36	330A	3/12/64	13.1	14.9	11.10	1.443	5430	32	TERMINATED-BCG EXPERIMENT, BCG SACRIFICE
D05F37	330B	3/12/64		17.5	8.51	1.480	6383	15	CHRONIC PROGRESSIVE ARTHRITIS
D05F38	330C	3/12/64	3.8	3.8	8.88	1.295	1386	14	ACCIDENTAL DEATH (TERMINATED FOR POS. DIROFILARIASIS TEST)
D05F40	330E	3/12/64		14.9	13.69	1.443	5433	34	METASTATIC MAMMARY CARCINOMA
D05F42 A	338B	3/31/64	8.9	9.5	9.62	1.332	3485	20	METASTATIC UNDIFFERENTIATED MALIGNANT TUMOR OF THE L REAR 4TH DIGIT
FIRST RUN									
D05M43	338C	3/31/64		13.7	14.80	1.702	5013	43	CHOLETHIASIS (BILE DUCT OBSTRUCTION) AND MULTIPLE HEPATOCELLULAR ADENOMAS
D05M44	338D	3/31/64		16.5	15.91	1.813	6036	30	PHEOCHROMOCYTOMA
D05F46	349A	4/26/64		11.0	9.99	1.369	4029	26	IDIOPATHIC EPILEPSY
D05F47	349B	4/26/64		15.1	11.10	1.443	5514	24	CONGESTIVE HEART FAILURE
D05F48	349C	4/26/64		13.4	9.62	1.517	4894	21	ANESTHETIC DEATH WITH CARDIOMEGALY, TOOTH ABSCESS AND CUSHING'S DISEASE
D05M49	349D	4/26/64		10.9	8.14	1.073	3981	22	EPENDYMOMA OF THE THIRD VENTRICLE, BRAIN
D05M50	349E	4/26/64		15.1	13.69	1.369	5533	38	HEMANGIOSARCOMA
D05F53	367C	6/04/64		17.1	16.65	1.961	6258	84	METASTATIC MAMMARY CARCINOMA
D05F54	367D	6/04/64		10.1	17.39	1.739	3698	48	HEMANGIOSARCOMA OF THE SPLEEN
D05M59	367I	6/04/64		13.6	17.76	2.035	4956	55	CHRONIC PROSTATITIS

BEAGLE NUMBER	LITTER NUMBER	BIRTH DATE	AGE AT TERM.	AGE AT DEATH	PEAK BODY BURDEN (kBq)	(kBq/KG)	EXPOSURE DAYS	TOTAL DOSE (CENTIGRAYS)	C O M M E N T S
D05F60	383A	7/02/64		12.9	11.47	1.665	4702	32	CHRONIC PYELONEPHRITIS
D05F61	383B	7/02/64		15.4	6.66	1.110	5625	18	CNS DISEASE OF UNDETERMINED ORIGIN
D05M64	383E	7/02/64		17.6	11.10	1.480	6410	55	HEPATIC ATROPHY
D05F65	403A	7/31/64		13.4	20.72	2.627	4899	25	METASTATIC MAMMARY CARCINOMA
D05M66	403B	7/31/64		13.3	10.73	1.517	4843	31	METASTATIC PULMONARY ADENOCARCINOMA
D05M67	403C	7/31/64		13.2	13.69	1.702	4836	45	MALIGNANT LYMPHOMA
	SECOND RUN								
D05F68	491A	9/11/65		13.3	8.88	1.184	4857	30	MALIGNANT MELANOMA
D05M69	491B	9/11/65		14.5	12.58	1.147	5288	40	CONGESTIVE HEART FAILURE
D05M70	491C	9/11/65		13.6	13.69	1.591	4966	50	ADAMANTINOMA
D05M71	491D	9/11/65		1.8	21.09	1.369	649	10	ACCIDENTAL DEATH (ANESTHETIC DEATH - FOR WHOLE BODY COUNTING)
D05F72	500A	9/28/65		13.3	5.92	.962	4868	17	TRANSITIONAL CELL CARCINOMA-URETHRA
D05F73	500B	9/28/65		13.7	10.36	1.258	5011	45	METASTATIC MAMMARY CARCINOMA/CONGESTIVE HEART FAILURE
D05F74	500C	9/28/65	11.5	12.6	14.06	1.369	4585	43	TERMINATED-BCG EXPERIMENT METASTATIC MAMMARY CARCINOMA
D05F75	500D	9/28/65		11.3	10.36	1.184	4111	45	METASTATIC MAMMARY CARCINOMA
D05F76	500E	9/28/65		17.3	10.73	1.258	6315	36	CHRONIC INTERVERTEBRAL DISC DISEASE
D05M77	500F	9/28/65		1.2	13.69	1.406	433	5	PERITONITIS (FROM DOG BITE)
D05F85	569B	9/17/66		15.7	7.03	.814	5732	19	INTERVERTEBRAL DISC HERNIATION
D05F86	569C	9/17/66		15.1	7.40	.962	5499	19	METASTATIC PANCREATIC ADENOCARCINOMA
D05M88	569E	9/17/66		11.1	8.88	1.110	4037	27	NEPHROSCLEROSIS
D05M89	569F	9/17/66		17.2	10.73	1.110	6300	28	FOOT INFECTION WITH TOXEMIA/DIC
D05M90	569G	9/17/66		15.9	13.69	1.406	5798	43	INTERVERTEBRAL DISC HERNIATION
D05M91	569H	9/17/66		15.7	9.99	.999	5719	30	CHRONIC, ACUTE PERITONITIS, SEPTICEMIA
D05F92	592A	12/21/66		14.2	9.99	.962	5199	43	ACUTE BRONCHOPNEUMONIA
D05M93	592B	12/21/66		14.8	12.58	1.332	5422	50	DISSEMINATED HEMANGIOSARCOMA
D05M94	592C	12/21/66		11.4	12.58	1.554	4172	40	SUPPURATIVE PROSTATITIS
D05M95	592D	12/21/66		17.5	11.84	1.036	6389	50	LYMPHOSARCOMA
D05M96	592E	12/21/66		17.1	13.69	1.665	6245	55	CHRONIC RENAL DISEASE
D05X02	593B	12/23/66		11.9	9.99	1.443	4350	36	METASTATIC MAMMARY CARCINOMA
D05X03	593C	12/23/66		16.9	7.40	1.147	6164	29	CHRONIC SEVERE PYELONEPHRITIS
D05X04	593D	12/23/66		16.5	9.62	1.258	6032	39	CHRONIC RENAL DISEASE
D05X05 A	593E	12/23/66		13.4	6.66	.888	4885	19	INTERVERTEBRAL DISC DISEASE, CHRONIC ACUTE
D05Y06	593F	12/23/66		14.8	6.29	.925	5411	18	ORAL MALIGNANT MELANOMA WITH PULMONARY METASTASIS
D05Y07	593G	12/23/66		14.8	7.4	1.036	5416	30	METASTATIC RENAL CARCINOMA
D05X08	602A	3/16/67		14.4	10.73	1.406	5276	29	METASTATIC MAMMARY CARCINOMA
D05X09	602B	3/16/67		12.2	9.99	1.221	4452	26	INVASIVE ORAL NEOPLASM
D05Y11	602D	3/16/67		12.9	10.73	1.443	4712	43	CHRONIC INTERSTITIAL PNEUMONIA/ARTERIOSCLEROSIS
D05Y13	634B	8/22/67		15.9	17.02	1.258	5825	55	UNDETERMINED
D05Y14	634C	8/22/67		15.8	18.13	1.665	5770	50	ADRENAL CORTICAL CARCINOMA METASTATIC TO LUNGS
D05Y15	634D	8/22/67	11.3	11.3	13.69	1.184	4123	35	MALIGNANT LYMPHOMA (INTESTINAL)
D05Y16	634E	8/22/67		18.5	14.80	1.295	6764	42	SUPPURATIVE HEPATITIS (HEPATIC ABSCESS)
D05Y17	634F	8/22/67		15.9	12.95	1.332	5811	32	HEPATOCELLULAR CARCINOMA/LIVER FAILURE

BEAGLE NUMBER	LITTER NUMBER	BIRTH DATE	AGE AT TERM.	AGE AT DEATH	PEAK BODY BURDEN (kBq)	(kBq/KG)	EXPOSURE DAYS	TOTAL DOSE (CENTIGRAYS)	C O M M E N T S
FIRST RUN									
D10F02	310B	12/20/63		9.5	30.71	3.737	3454	97	PITUITARY TUMOR WITH CUSHING'S DISEASE
D10M04	310D	12/20/63		13.7	31.08	3.774	4993	134	METASTATIC RENAL CARCINOMA
D10M05	310E	12/20/63		14.4	36.63	3.774	5247	162	URETHRAL STRICTURE SECONDARY TO PROSTATECTOMY
D10F10	361B	5/24/64		11.9	26.64	3.219	4363	120	METASTATIC MAMMARY CARCINOMA
D10F11	361C	5/24/64		11.1	29.23	3.404	4069	118	METASTATIC PULMONARY ADENOCARCINOMA
D10M12	361D	5/24/64		14.2	41.81	4.477	5169	148	PRIMARY PULMONARY NEOPLASM OF BRONCHIOLAR ORIGIN
D10F17	386A	7/05/64		13.8	21.46	2.738	5027	97	ACCIDENTAL (ASPIRATED GLYCOL WHEN TREATED FOR GLAUCOMA--LED TO ASPIRATION PNEUMONIA)
D10F18	386B	7/05/64		15.0	19.24	2.590	5490	88	BRONCHOGENIC CARCINOMA
D10M19	386C	7/05/64		3.4	37.74	4.551	1241	55	MYELOMALACIA
D10M20	386D	7/05/64		15.3	37.00	3.626	5570	163	PITUITARY CARCINOMA
D10F22	409A	8/11/64		12.5	27.75	3.441	4559	119	METASTATIC MAMMARY CARCINOMA
D10F25	409D	8/11/64		12.8	29.60	3.367	4682	115	METASTATIC ADRENAL CARCINOMA
D10M26	409E	8/11/64		14.7	29.23	3.330	5355	128	CNS DISEASE OF UNDETERMINED ORIGIN
D10F36	423A	9/25/64		16.9	34.04	4.329	6173	153	INTERVERTEBRAL DISC DISEASE(DEGENERATIVE MYELOPATHY)
D10M39	423D	9/25/64		13.0	33.30	3.552	4732	127	TRANSITIONAL CELL CARCINOMA OF THE PROSTATIC URETHRA
D10M40	423E	9/25/64		14.7	36.26	4.107	5358	157	FIBROSARCOMA-NEURAL
D10F41	445A	12/07/64		10.7	28.12	2.812	3913	96	MYOCARDIAL DEGENERATION, CARDIAC HYPERTROPHY
D10F42	445B	12/07/64		11.2	39.22	3.848	4095	136	FOCAL ENCEPHALOMALACIA
D10M45	445E	12/07/64		11.9	47.73	4.625	4328	178	CONGESTIVE HEART FAILURE (RUPTURED CHORDA TENDONAE)
D10M46	445F	12/07/64		14.5	42.55	4.144	5281	180	METASTATIC HEMANGIOSARCOMA
SECOND RUN									
D10F52	510B	12/09/65		7.6	33.67	3.663	2794	83	INTESTINAL LYMPHANGIECTASIA
D10F53	510C	12/09/65		17.3	33.30	3.071	6328	135	LACRIMAL GLAND CARCINOMA
D10F54	510D	12/09/65		14.1	33.67	3.330	5147	134	ACUTE NECROTIZING ENTERITIS (PARVOVIRUS)
D10F55	510E	12/09/65		13.0	35.89	3.774	4761	136	CHRONIC PANCREATITIS
D10M58	510H	12/09/65		16.9	39.22	3.330	6157	145	CHRONIC INTERVERTEBRAL DISC DESEASE
D10M60	543B	5/19/66		12.8	40.33	4.181	4671	168	CONGESTIVE HEART FAILURE
D10M61	543C	5/19/66		15.3	31.82	3.589	5574	137	PLEURAL EFFUSION - ETIOLOGY UNKNOWN
D10M62	543D	5/19/66		10.5	38.85	3.663	3819	127	POSTERIOR PARALYSIS (UNDETERMINED CAUSE)
D10F64	561B	7/08/66		12.0	37.74	4.921	4367	140	METASTATIC MAMMARY CARCINOMA
D10M65	561C	7/08/66		12.9	44.40	4.958	4723	159	CARDIAC ARREST UNDER ANESTHESIA FOR HEMANGIOSARCOMA-SPLEEN
D10M66	561D	7/08/66		12.7	30.71	3.145	4654	119	CHRONIC PYELONEPHRITIS
D10M69	562C	7/13/66		11.4	45.14	4.958	4180	142	MALIGNANT LYMPHOMA
D10F71	581B	11/19/66		16.9	19.98	2.220	6166	98	INTERVERTEBRAL DISC DISEASE
D10M72	581C	11/19/66		10.2	21.46	2.849	3713	86	MULTIPLE ENDOCRINOPATHY (HYPOPLASIA OR ATROPHY)
D10M73	581D	11/19/66		15.4	35.52	3.700	5638	157	PRIMARY LYMPHOSARCOMA OF BRAINSTEM
D10M74	581E	11/19/66		14.7	25.16	2.590	5360	120	METASTATIC HEMANGIOSARCOMA
D10F75	618A	5/23/67		11.7	17.76	2.590	4287	90	METASTATIC MAMMARY CARCINOMA
D10F76	618B	5/23/67		15.7	25.53	3.219	5726	136	CUSHING'S DISEASE
D10F77	618C	5/23/67		16.1	34.41	3.515	5895	175	CUSHING'S DISEASE
D10M82	618H	5/23/67		14.6	40.70	3.515	5323	167	ACUTE EXUDATIVE INTERSTITIAL PNEUMONIA

BEAGLE NUMBER	LITTER NUMBER	BIRTH DATE	AGE AT TERM.	AGE AT DEATH	PEAK BODY BURDEN (kBq)	(kBq/KG)	EXPOSURE DAYS	TOTAL DOSE (CENTIGRAYS)	C O M M E N T S
PILOT SERIES									
D20F02	103B	2/16/61		15.6	86.21	16.946	5713	646	HEPATIC ABSCESS
D20M04	103D	2/16/61		15.7	152.07	20.831	5731	845	METASTATIC MALIGNANT MELANOMA OF THE BUCCAL CAVITY
D20F06	104A	2/20/61		17.3	162.43	21.275	6336	776	LEUKOENCEPHALOMALACIA
D20M09	104D	2/20/61		.7					ACCIDENTAL DEATH (ANESTHETIC DEATH - FOR DEBARKING)
D20M10	104E	2/20/61		14.1	169.83	15.947	5149	692	ACUTE PULMONARY COAGULOPATHY, CHRONIC PULMONARY AND HEPATIC THROMBOSIS, PULMONARY VASCULITIS
D20M11	104F	2/20/61		2.9	194.99	20.905	1066	221	EPILEPSY
D20F15	149B	9/30/61		10.2	115.07	20.572	3720	615	CHRONIC PULMONARY DISEASE
D20F16	149C	9/30/61		13.7	177.23	25.234	5014	939	METASTATIC AORTIC BODY TUMOR
D20F17	149D	9/30/61		11.7	189.07	22.237	4259	830	PYOMETRA AND ACUTE PERITONITIS
D20F21	167D	1/01/62	10.0	10.0	218.30	22.052	3668	652	MALIGNANT LYMPHOMA
D20M22	167E	1/01/62		16.3	189.44	20.128	5937	911	SEVERE CNS DISEASE
D20M24	167G	1/01/62		14.2	257.15	19.684	5204	796	INTERVERTEBRAL DISC HERNIATION
D20F25	197A	5/19/62		17.6	189.81	19.240	6433	778	METASTATIC MAMMARY CARCINOMA
D20F26	197B	5/19/62		14.2	195.36	17.686	5197	784	CONGESTIVE HEART FAILURE (RUPTURED CHORDA TENDONAE)
D20M28	197D	5/19/62		9.8	237.91	20.276	3590	655	RENAL CARCINOMA
D20M29	197E	5/19/62		13.4	268.25	25.086	4900	887	METASTATIC HEPATOCELLULAR CARCINOMA
D20M30	197F	5/19/62		15.3	239.39	21.201	5570	849	METASTATIC RENAL CARCINOMA
D20M31	197G	5/19/62		15.9	254.19	22.496	5807	1001	SENILITY
D20F32	263A	6/25/63		13.7	219.78	27.121	5001	1137	HEPATOCELLULAR ADENOMA AND ASPIRATION PNEUMONIA
D20F33	263B	6/25/63		10.6	176.12	23.606	3889	765	HEPATOCELLULAR ADENOMA
D20M34	263C	6/25/63		9.5	233.47	21.016	3453	736	HEPATOCELLULAR CARCINOMA
D20M35	263D	6/25/63		14.7	223.85	22.163	5374	998	ACUTE PERITONITIS SECONDARY TO PROSTATITIS
D20M36	263E	6/25/63		16.6	219.04	28.527	6047	1360	INTERVERTEBRAL DISC DISEASE
FIRST RUN									
D20F40	288B	11/03/63		14.1	119.14	13.690	5163	614	UNDETERMINED
D20F41	288C	11/03/63		13.8	131.72	14.652	5026	598	BRONCHOPNEUMONIA
D20M42	288D	11/03/63		12.8	162.43	17.797	4685	739	NASAL CARCINOMA
D20F53	354D	5/12/64		3.6	143.93	17.649	1319	278	ASPIRATION PNEUMONIA-SECONDARY TO CONVULSIONS
D20F54	354E	5/12/64	12.8	14.5	198.69	20.498	5295	913	TUBERCULOSIS CAUSED BY BCG (GRANULOMATOUS PLEURITIS AND PERICARDITIS)
D20M55	354F	5/12/64		10.6	214.23	19.758	3868	712	ASPIRATION PNEUMONIA DUE TO CRANIAL ABSCESS SECONDARY TO CHRONIC OTITIS INTERNA
D20M56	354G	5/12/64		15.2	281.57	25.900	5552	1097	TRANSITIONAL CELL CARCINOMA-PROSTATIC URETHRA
D20F57	357A	5/20/64		16.4	126.17	19.314	5972	869	NEPHROSCLEROSIS, CHRONIC PYELONEPHRITIS
D20M59	357C	5/20/64		15.3	136.90	23.791	5599	993	INTERVERTEBRAL DISC DISEASE
D20M60	357D	5/20/64		8.9	215.71	23.199	3248	707	MALIGNANT LYMPHOMA
D20F62	358A	5/22/64		10.6	163.54	18.722	3854	618	PULMONARY ABSCESS
D20M63	358B	5/22/64		10.2	214.60	25.900	3736	775	MALIGNANT LYMPHOMA
D20F66	378A	6/19/64		14.4	163.17	16.872	5263	808	POST-SURGICAL SHOCK/PYOMETRA
D20F67	378B	6/19/64		14.4	167.98	21.053	5266	844	ACUTE NECROTIZING ENTERITIS (PARVOVIRUS)

BEAGLE NUMBER	LITTER NUMBER	BIRTH DATE	AGE AT TERM.	AGE AT DEATH	PEAK BODY BURDEN (kBq)	(kBq/KG)	EXPOSURE DAYS	TOTAL DOSE (CENTIGRAYS)	C O M M E N T S
D20M69	378D	6/19/64		14.0	182.04	22.237	5114	952	HEART FAILURE (CLINICAL THIRD DEGREE HEART BLOCK) MYOCARDIAL INFARCTION
D20M70	378E	6/19/64		15.5	173.16	19.758	5661	888	CONGESTIVE HEART FAILURE
D20F71	405A	8/03/64	12.7	14.5	192.03	19.425	5293	843	TERMINATED-BCG EXPERIMENT, BCG SACRIFICE
D20F73	405C	8/03/64		15.4	163.91	16.983	5635	762	UNDETERMINED
D20M75	405E	8/03/64		7.4	259.37	30.377	2692	725	METASTATIC SPLENIC LEIOMYOSARCOMA
D20M76	405F	8/03/64		16.5	193.88	19.721	6011	808	CHOLANGIOHEPATITIS(COMMON BILE DUCT OBSTRUCTION)
SECOND RUN									
D20F78	480A	8/29/65		14.8	225.70	21.682	5415	979	PITUITARY ADENOMA
D20F79	480B	8/29/65		15.4	147.26	16.132	5632	723	MPS
D20F80	480C	8/29/65		14.4	154.29	17.649	5255	695	PANCREATIC INSUFFICIENCY/MALABSORPTION
D20M82	480E	8/29/65		17.1	195.36	21.904	6262	1002	CHRONIC RENAL DISEASE
D20F84	533B	3/26/66		6.8	97.31	16.724	2475	330	NEPHROSCLEROSIS
D20F89	546A	5/28/66		15.3	122.84	18.500	5584	827	CONGESTIVE HEART FAILURE
D20F90	546B	5/28/66		14.9	108.41	19.092	5425	834	CONGESTIVE HEART FAILURE
D20F91	546C	5/28/66		4.0	135.42	19.166	1465	302	ACCIDENTAL DEATH (HEAT EXHAUSTION)
D20M94	546F	5/28/66		14.2	155.40	19.129	5187	884	CONGESTIVE HEART FAILURE/SUBACUTE BACTERIAL ENDOCARDITIS
D20M95	546G	5/28/66		14.1	166.87	21.830	5149	878	HEPATOCELLULAR ADENOMA WITH HEMORRHAGE COAGULATION
D20X01	582A	11/23/66		14.9	183.89	19.832	5430	853	CHRONIC BRONCHIECTASIS
D20X03	582C	11/23/66		11.8	251.60	20.202	4320	804	PITUITARY NEOPLASM
D20Y04	582D	11/23/66		16.9	213.86	22.385	6173	928	INTERVERTEBRAL DISC DISEASE
D20Y05	582E	11/23/66	13.5	13.5	229.40	21.053	4943	869	SQUAMOUS CELL CARCINOMA-TONSIL
D20X06	586A	12/09/66		4.7	148.37	22.089	1722	316	ENTEROPATHY & BRONCHIAL PNEUMONIA
D20X07	586B	12/09/66		15.1	133.57	14.652	5523	711	ULTIMOBRANCHIAL NEOPLASM
D20Y09	586D	12/09/66		14.3	149.48	18.426	5232	821	MALIGNANT HEART BASE TUMOR (CHEMODECTOMA)
D20X12	596B	1/04/67		14.1	146.89	19.943	5151	744	COMPLEX ADENOCARCINOMA
D20X13	596C	1/04/67		13.1	219.04	23.162	4767	823	BRONCHOGENIC CARCINOMA
D20Y15	596E	1/04/67		15.6	292.30	25.974	5697	1331	ADRENAL NECROSIS/UNDETERMINED
D20Y16	596F	1/04/67		10.0	262.33	25.826	3662	849	HEPATOCELLULAR ADENOMA
D20Y17	596G	1/04/67		17.8	296.74	26.418	6502	1292	1) PROGRESSIVE POSTERIOR PARALYSIS; 2) CHRONIC RENAL DISEASE
PILOT SERIES									
D30F02 A	114B	4/27/61		14.4	543.53	69.856	5277	2814	LYMPHOSARCOMA, HISTIOCYTIC TYPE
D30M10	115F	5/01/61		15.2	544.64	58.571	5567	2766	CONGESTIVE HEART FAILURE (RUPTURED CHORDA TENDONAE)
D30F16	121D	6/11/61		16.6	651.57	81.548	6078	3558	CEREBRAL ATROPHY
D30F19	122A	6/14/61		14.4	646.02	78.662	5250	3012	METASTATIC PULMONARY CARCINOMA
D30F20	122B	6/14/61		15.2	509.12	65.083	5536	2570	MALIGNANT LYMPHOMA
D30M21	122C	6/14/61		1.5	931.66	82.806	540	469	TERMINATED (EPILEPSY)
D30M22	122D	6/14/61		12.0	810.67	78.884	4389	2933	ACCIDENTAL (ANESTHETIC DEATH)
D30F25	194C	5/10/62		13.8	448.81	46.990	5033	1779	MALIGNANT LYMPHOMA
D30F26	194D	5/10/62	14.9	16.7	483.22	57.646	6088	2283	TERMINATED-BCG EXPERIMENT, BCG SACRIFICE

BEAGLE NUMBER	LITTER NUMBER	BIRTH DATE	AGE AT TERM.	AGE AT DEATH	PEAK BODY BURDEN (kBq)	(kBq/KG)	EXPOSURE DAYS	TOTAL DOSE (CENTIGRAYS)	C O M M E N T S
D20M69	378D	6/19/64		14.0	182.04	22.237	5114	952	HEART FAILURE (CLINICAL THIRD DEGREE HEART BLOCK) MYOCARDIAL INFARCTION
D20M70	378E	6/19/64		15.5	173.16	19.758	5661	888	CONGESTIVE HEART FAILURE
D20F71	405A	8/03/64	12.7	14.5	192.03	19.425	5293	843	TERMINATED-BCG EXPERIMENT, BCG SACRIFICE
D20F73	405C	8/03/64		15.4	163.91	16.983	5635	762	UNDETERMINED
D20M75	405E	8/03/64		7.4	259.37	30.377	2692	725	METASTATIC SPLENIC LEIOMYOSARCOMA
D20M76	405F	8/03/64		16.5	193.88	19.721	6011	808	CHOLANGIOHEPATITIS(COMMON BILE DUCT OBSTRUCTION)
SECOND RUN									
D20F78	480A	8/29/65		14.8	225.70	21.682	5415	979	PITUITARY ADENOMA
D20F79	480B	8/29/65		15.4	147.26	16.132	5632	723	MPS
D20F80	480C	8/29/65		14.4	154.29	17.649	5255	695	PANCREATIC INSUFFICIENCY/MALABSORPTION
D20M82	480E	8/29/65		17.1	195.36	21.904	6262	1002	CHRONIC RENAL DISEASE
D20F84	533B	3/26/66		6.8	97.31	16.724	2475	330	NEPHROSCLEROSIS
D20F89	546A	5/28/66		15.3	122.84	18.500	5584	827	CONGESTIVE HEART FAILURE
D20F90	546B	5/28/66		14.9	108.41	19.092	5425	834	CONGESTIVE HEART FAILURE
D20F91	546C	5/28/66		4.0	135.42	19.166	1465	302	ACCIDENTAL DEATH (HEAT EXHAUSTION)
D20M94	546F	5/28/66		14.2	155.40	19.129	5187	884	CONGESTIVE HEART FAILURE/SUBACUTE BACTERIAL ENDOCARDITIS
D20M95	546G	5/28/66		14.1	166.87	21.830	5149	878	HEPATOCELLULAR ADENOMA WITH HEMORRHAGE COAGULATION
D20X01	582A	11/23/66		14.9	183.89	19.832	5430	853	CHRONIC BRONCHIECTASIS
D20X03	582C	11/23/66		11.8	251.60	20.202	4320	804	PITUITARY NEOPLASM
D20Y04	582D	11/23/66		16.9	213.86	22.385	6173	928	INTERVERTEBRAL DISC DISEASE
D20Y05	582E	11/23/66	13.5	13.5	229.40	21.053	4943	869	SQUAMOUS CELL CARCINOMA-TONSIL
D20X06	586A	12/09/66		4.7	148.37	22.089	1722	316	ENTEROPATHY & BRONCHIAL PNEUMONIA
D20X07	586B	12/09/66		15.1	133.57	14.652	5523	711	ULTIMOBRANCHIAL NEOPLASM
D20Y09	586D	12/09/66		14.3	149.48	18.426	5232	821	MALIGNANT HEART BASE TUMOR (CHEMODECTOMA)
D20X12	596B	1/04/67		14.1	146.89	19.943	5151	744	COMPLEX ADENOCARCINOMA
D20X13	596C	1/04/67		13.1	219.04	23.162	4767	823	BRONCHOGENIC CARCINOMA
D20Y15	596E	1/04/67		15.6	292.30	25.974	5697	1331	ADRENAL NECROSIS/UNDETERMINED
D20Y16	596F	1/04/67		10.0	262.33	25.826	3662	849	HEPATOCELLULAR ADENOMA
D20Y17	596G	1/04/67		17.8	296.74	26.418	6502	1292	1) PROGRESSIVE POSTERIOR PARALYSIS; 2) CHRONIC RENAL DISEASE
PILOT SERIES									
D30F02 A	114B	4/27/61		14.4	543.53	69.856	5277	2814	LYMPHOSARCOMA, HISTIOCYTIC TYPE
D30M10	115F	5/01/61		15.2	544.64	58.571	5567	2766	CONGESTIVE HEART FAILURE (RUPTURED CHORDA TENDONAE)
D30F16	121D	6/11/61		16.6	651.57	81.548	6078	3558	CEREBRAL ATROPHY
D30F19	122A	6/14/61		14.4	646.02	78.662	5250	3012	METASTATIC PULMONARY CARCINOMA
D30F20	122B	6/14/61		15.2	509.12	65.083	5536	2570	MALIGNANT LYMPHOMA
D30M21	122C	6/14/61		1.5	931.66	82.806	540	469	TERMINATED (EPILEPSY)
D30M22	122D	6/14/61		12.0	810.67	78.884	4389	2933	ACCIDENTAL (ANESTHETIC DEATH)
D30F25	194C	5/10/62		13.8	448.81	46.990	5033	1779	MALIGNANT LYMPHOMA
D30F26	194D	5/10/62	14.9	16.7	483.22	57.646	6088	2283	TERMINATED-BCG EXPERIMENT, BCG SACRIFICE
D30M27	194E	5/10/62		11.4	513.19	52.392	4180	1663	MALIGNANT MELANOMA OF THE GINGIVA
D30F28	228A	9/20/62		13.8	475.08	53.391	5053	2188	METASTATIC MAMMARY CARCINOMA

BEAGLE NUMBER	LITTER NUMBER	BIRTH DATE	AGE AT TERM.	AGE AT DEATH	PEAK BODY BURDEN (kBq)	(kBq/KG)	EXPOSURE DAYS	TOTAL DOSE (CENTIGRAYS)	C O M M E N T S
D30F29	228B	9/20/62		12.2	474.71	51.282	4459	1719	METASTATIC MAMMARY CARCINOMA
D30M30	228C	9/20/62		16.9	857.29	72.335	6158	3987	INTERVERTEBRAL DISC DISEASE
D30M31	228D	9/21/62		7.8	820.29	59.755	2859	1758	MALIGNANT LYMPHOMA
D30F33	250B	2/27/63		17.1	488.77	69.634	6236	3216	SQUAMOUS CELL CARCINOMA-GINGIVA
D30F34	250C	2/27/63		11.9	525.77	60.421	4332	2091	MPS
D30F35	250D	2/27/63		15.7	570.17	64.380	5739	2922	ACUTE NECROTIZING ENTERITIS (PARVOVIRUS)
D30F36	250E	2/27/63		10.6	589.04	64.528	3870	2158	ACCIDENTAL (ANESTHETIC DEATH - DURING DIAGNOSTIC X-RAYS) FOR LIPOMA REMOVAL)
D30M40	250I	2/27/63		7.9	514.67	63.566	2872	1575	MPS
	FIRST RUN								
D30F41	296A	11/30/63		16.4	368.89	49.099	5997	1974	CHRONIC RENAL FAILURE/NEPHROSCLEROSIS
D30F43	296C	11/30/63		11.2	418.10	58.164	4099	1841	CHRONIC ACTIVE HEPATITIS
D30M46	296F	11/30/63		8.3	657.86	60.532	3041	1781	MALIGNANT LYMPHOMA
D30F49	299C	12/10/63		14.7	531.32	50.542	5371	2066	SQUAMOUS CELL CARCINOMA-GINGIVA
D30F50	299D	12/10/63		13.7	530.58	58.645	5005	2301	METASTATIC MAMMARY CARCINOMA
D30F51 C	299E	12/10/63		14.5	510.97	52.133	5302	3531	METASTATIC MAMMARY CARCINOMA
D30F52	299F	12/10/63		13.0	550.56	54.353	4758	2185	METASTATIC MAMMARY CARCINOMA
D30M54	299H	12/10/63		14.5	748.51	70.411	5286	2315	NASAL CARCINOMA
D30M55	299I	12/10/63		14.7	607.54	69.116	5376	2683	INTERVERTEBRAL DISC DISEASE WITH SPINAL MYELOPATHY
D30M56 C	299J	12/10/63		15.8	543.16	52.688	5768	3746	NASAL ADENOCARCINOMA
D30F57	327A	3/06/64		11.0	573.13	74.037	4030	2413	NASAL CARCINOMA
D30M58	327B	3/06/64		13.6	608.65	73.149	4980	2774	PITUITARY TUMOR WITH CUSHING'S DISEASE
D30M59	327C	3/06/64		14.4	660.82	76.516	5247	3165	INTERVERTEBRAL DISC DISEASE
D30M60	327D	3/06/64		14.9	636.77	76.738	5424	3455	CHRONIC RENAL DISEASE AND MYELOPATHY
D30M61 C	327E	3/06/64		5.3	817.70	69.116	1918	2188	MPS
D30F62 C	369A	6/09/64		13.9	404.41	46.694	5091	2916	CEREBRAL EDEMA SECONDARY TO CHRONIC ENTERITIS
D30F63	369B	6/09/64		14.5	357.05	56.240	5311	2112	DISSEMINATED INTRAVASCULAR COAGULATION PULMONARY ADENOCARCINOMA OR SUBCUT. HEMANGIOMA
D30F65	369D	6/09/64	12.8	14.3	527.62	60.939	5228	2464	TERMINATED-BCG EXPERIMENT, MALIGNANT LYMPHOMA
D30M66 C	369E	6/09/64		12.5	429.94	48.322	4563	2901	METASTATIC MALIGNANT MELANOMA OF THE BUCCAL CAVITY
D30M67	369F	6/09/64		14.3	579.05	62.604	5225	2437	PROSTATITIS, RUPTURED PROSTATIC ABSCESS
D30M68	369G	6/09/64		16.6	513.19	59.607	6075	2719	BRONCHOGENIC CARCINOMA
D30M78	443D	12/06/64		14.4	674.51	77.256	5276	3104	RENAL AMYLOIDOSIS
D30F79	450A	1/19/65		13.6	570.17	62.382	4973	2861	MALIGNANT LYMPHOMA
D30F80	450B	1/19/65		15.2	473.97	68.672	5538	2905	TRANSITIONAL CELL CARCINOMA
D30M81 C	450C	1/19/65		9.6	696.34	74.555	3508	2614	CONGESTIVE HEART FAILURE
D30M82 C	450D	1/19/65		6.1	844.34	93.018	2233	1993	MPS
D30M83	450E	1/19/65		12.9	636.77	72.631	4720	2780	HEPATOCELLULAR ADENOMA
	SECOND RUN								
D30F86	482C	8/30/65		11.4	529.84	63.862	4174	2457	TRANSITIONAL CELL CARCINOMA OF THE URINARY BLADDER
D30F87	482D	8/30/65		11.7	422.54	44.807	4257	1978	CHRONIC INTERSTITIAL PULMONARY FIBROSIS
D30M88	482E	8/30/65		9.9	675.99	85.544	3634	2629	OSTEOSARCOMA OF THE 10TH THORACIC VERTEBRA

BEAGLE NUMBER	LITTER NUMBER	BIRTH DATE	AGE AT TERM.	AGE AT DEATH	PEAK BODY BURDEN (kBq)	PEAK BODY BURDEN (kBq/KG)	EXPOSURE DAYS	TOTAL DOSE (CENTIGRAYS)	C O M M E N T S
D30M89	482F	8/30/65		6.9	619.75	67.525	2533	1780	ACCIDENTAL DEATH (NEPHROTIC SYNDROME SECONDARY TO ANESTHESIA, AFTER SURGERY FOR IV DISK PROTRUSION)
D30M90	482G	8/30/65		4.5	772.56	67.858	1628	1215	CHRONIC DERMATITIS, DEMODEX INFECTION
D30F92	492B	9/12/65		13.3	567.58	72.372	4846	2637	NASAL CARCINOMA
D30F93	492C	9/12/65		15.0	611.98	77.663	5481	2996	DISSEMINATED INTRAVASCULAR COAGULATION
D30M94	492D	9/12/65		17.4	633.44	79.217	6340	3476	CHRONIC RENAL DISEASE (NEPHROSCLEROSIS AND MEDULLARY NECROSIS)
D30F95	506A	11/03/65		14.5	567.21	75.813	5306	3421	BILIARY CYSTADENOCARCINOMA
D30F96	506B	11/03/65		14.6	487.29	61.235	5347	2868	MALIGNANT MAMMARY TUMOR
D30M97	506C	11/03/65		15.5	700.04	84.027	5655	3945	HEMANGIOSARCOMA, BONE-RIB
D30M98	506D	11/03/65		14.8	682.65	83.953	5405	3906	SQUAMOUS CELL CARCINOMA-GINGIVA
D30M99 A	506E	11/03/65		13.9	717.43	90.132	5083	3710	HEPATITIS WITH BILIARY STASIS
D30X01	600A	3/09/67		14.3	597.92	67.858	5224	2779	CONGESTIVE HEART FAILURE
D30X02	600B	3/09/67		12.3	673.03	75.295	4497	2583	METASTATIC MAMMARY CARCINOMA
D30X03	600C	3/09/67		14.4	628.26	61.938	5244	2582	SENILE CNS DISEASE
D30Y04	600D	3/09/67		13.3	812.89	64.454	4863	2820	CONGESTIVE HEART FAILURE
D30Y05	600E	3/09/67		14.8	875.79	77.108	5418	3627	POST-SURGICAL BRONCHOPNEUMONIA (AFTER SURGERY TO ENUCLEATE EYE FOR SEVERE KERATITIS)
D30Y06	600F	3/09/67		15.1	920.56	79.698	5525	4128	CONGESTIVE HEART FAILURE
D30Y07	600G	3/09/67		15.6	1009.73	87.283	5697	3699	OSTEOSARCOMA OF THE SPINE AT L1-2
D30Y08	600H	3/09/67		11.8	990.49	77.404	4306	3155	FIBROSARCOMA-GINGIVA
D30Y11	617C	5/21/67		12.4	534.65	69.079	4518	2506	SEVERE VEGETATIVE ENDOCARDITIS
D30Y12	617D	5/21/67		16.5	399.60	64.158	6030	2366	PANCREATIC ACINAR ADENOCARCINOMA
D30Y13	628A	7/16/67		13.4	740.37	54.612	4897	2563	LEUKOENCEPHALOPATHY, SPONGY, CAUSE UNKNOWN
PILOT SERIES									
D40F03 A	152C	10/28/61		12.1	1333.11	169.793	4426	6471	METASTATIC OSTEOSARCOMA
D40M04	152D	10/28/61		9.7	1642.80	214.748	3555	6285	TONSILLAR CARCINOMA
D40M05	152E	10/28/61		5.9	1890.70	233.729	2161	5084	MPS
D40M06	152F	10/28/61		10.7	1860.73	245.791	3903	8392	METASTATIC TONSILLAR CARCINOMA
D40F08	153B	10/31/61		15.1	1646.50	199.837	5506	8813	HYPOTHYROIDISM, NEPHROSCLEROSIS
D40M09	153C	10/31/61		8.4	2284.75	191.031	3081	4851	MALIGNANT LYMPHOMA
D40M10	153D	10/31/61		13.3	2343.95	169.238	4867	6939	METASTATIC OSTEOSARCOMA OF THE L MANDIBLE
D40F11	161A	12/17/61		14.5	1257.63	136.530	5290	4842	INTERVERTEBRAL DISC HERNIATION, OSTEOSARCOMA OF THE 4TH LUMBAR VERTEBRA, RENAL DISEASE
D40F12	161B	12/17/61		10.7	1240.61	177.230	3925	4681	INVASIVE SQUAMOUS CELL CARCINOMA OF THE L MANDIBLE
D40F14	161D	12/17/61		8.1	1383.06	140.415	2971	4222	FIBROSARCOMA OF THE MAXILLA
D40F15	161E	12/17/61		11.0	1787.84	247.974	4022	5798	TONSILLAR CARCINOMA
D40M25	198F	5/25/62		8.2	1713.10	149.221	3002	3561	MAXILLARY FIBROSARCOMA
D40F32	276A	8/28/63		13.1	1865.91	189.033	4801	7011	SQUAMOUS CELL CARCINOMA OF THE GINGIVA
D40F33	276B	8/28/63		8.6	2152.66	181.041	3151	6021	NASAL CARCINOMA
D40F34 A	276C	8/28/63		14.4	1605.43	159.766	5256	6424	MALIGNANT LYMPHOMA
D40F35	276D	8/28/63	15.0	15.2	1950.64	181.818	5553	8289	BCG TREATMENT, CHRONIC HEPATIC FIBROSIS
D40M37	276F	8/28/63	11.7	11.7	2724.68	261.257	4277	8080	MPS
D40M38	276G	8/28/63		13.0	2721.72	245.643	4754	8489	NASAL CARCINOMA

BEAGLE NUMBER	LITTER NUMBER	BIRTH DATE	AGE AT TERM.	AGE AT DEATH	PEAK BODY BURDEN (kBq)	(kBq/KG)	EXPOSURE DAYS	TOTAL DOSE (CENTIGRAYS)	C O M M E N T S
FIRST RUN									
D40F42	285D	10/26/63		14.1	1419.69	141.821	5155	5775	RUPTURED GALL BLADDER AND ACUTE PERITONITIS
D40M44	285F	10/26/63		12.2	2208.53	194.916	4454	7619	SPINAL MENINGIOMA
D40M45	285G	10/26/63		16.1	1905.13	171.014	5879	8185	SQUAMOUS CELL CARCINOMA-GINGIVA
D40F49	316D	1/04/64		2.8	1312.02	156.769	1010	1665	ACCIDENTAL DEATH (CHOKED)
D40F50	316E	1/04/64		9.2	1222.48	152.995	3361	3759	RENAL AMYLOIDOSIS
D40M51	316F	1/04/64		13.5	1377.14	169.164	4937	6192	METASTATIC HEMANGIOSARCOMA (PRIMARY SITE UNKNOWN)
D40F52	333A	3/24/64		10.8	1722.35	194.398	3942	7129	HEPATOCELLULAR ADENOMA
D40M53	333B	3/24/64		13.2	1483.70	164.872	4804	6840	BRONCHOGENIC CARCINOMA
D40M54	333C	3/24/64		13.5	2016.50	192.252	4929	7735	NASAL CARCINOMA
D40M55 C	333D	3/24/64		10.1	1912.16	192.733	3677	9231	MPS
D40M56	333E	3/24/64		1.2	1871.83	214.193	426	888	MPS
D40F62 C	368A	6/07/64		9.3	1024.53	147.223	3405	5661	METASTATIC TRANSITIONAL CELL CARCINOMA OF THE RENAL PELVIS
D40F63	368B	6/07/64		16.6	1144.04	128.094	6078	6010	METASTATIC PANCREATIC ADENOCARCINOMA
D40F64	368C	6/07/64		16.9	1216.93	155.437	6169	7384	TRANSITIONAL CELL CARCINOMA
D40F67 C	411A	8/22/64		3.6	1798.94	181.337	1332	2332	EPILEPSY
D40F68	411B	8/22/64		4.4	1557.70	168.424	1590	2845	ACCIDENTAL DEATH (STRANGULATION ON CHAIN)
D40M69	411C	8/22/64		12.2	1739.00	195.397	4468	8367	PITUITARY TUMOR WITH CUSHING'S DISEASE
D40M70	411D	8/22/64		12.1	2220.74	200.096	4422	8312	HEPATOCELLULAR ADENOMA
D40M71 C	411E	8/22/64		2.8	1737.52	180.634	1014	1883	EPILEPSY
D40M72	411F	8/22/64		12.5	2232.95	163.207	4573	7311	SQUAMOUS CELL CARCINOMA OF THE GINGIVA
D40F74	429B	10/11/64		12.3	1064.12	174.455	4502	6257	METASTATIC CARCINOMA OF UNDETERMINED ORIGIN
D40F75	429C	10/11/64		15.5	1195.47	204.018	5659	8732	SQUAMOUS CELL CARCINOMA-GINGIVA
D40M76	429D	10/11/64		2.3	1667.96	224.812	840	1958	MPS
SECOND RUN									
D40F79	481C	8/30/65	12.9	13.4	1153.66	163.873	4880	6386	BCG SACRIFICE
D40F80	481D	8/30/65		9.7	1391.57	157.398	3530	5428	METASTATIC SQUAMOUS CELL CARCINOMA OF THE GINGIVA
D40F81	481E	8/30/65		2.1	1517.37	178.932	771	1446	PROGRESSIVE APLASTIC ANEMIA
D40F90	517C	1/03/66		13.7	1252.82	180.523	5016	6267	METASTATIC MAMMARY CARCINOMA
D40M91 A	517D	1/03/66	10.9	12.6	2298.07	216.191	4588	8498	OSTEOSARCOMA (TO FREDERICK CANCER RESEARCH CENTER)
D40M92	517E	1/03/66		8.4	2618.12	258.963	3062	7283	METASTATIC FIBROSARCOMA OF THE HEAD (MALAR AREA)
D40M93	517F	1/03/66		12.7	2020.94	183.039	4624	7296	AORTIC THROMBOSIS
D40X02	558B	7/02/66		4.4	1502.57	188.996	1593	2952	BRONCHOPNEUMONIA & MPS
D40X03	558C	7/02/66		10.3	1408.59	141.266	3775	5805	METASTATIC MAMMARY CARCINOMA
D40X04	558D	7/02/66	11.9	12.0	1955.82	205.868	4367	6761	MALIGNANT LYMPHOMA (LEUKEMIC)
D40Y10 A	594A	1/01/67		14.1	1805.60	165.649	5136	7185	DISSEMINATED HEMANGIOSARCOMA
D40Y11	594B	1/01/67		9.8	1734.93	163.836	3566	5561	NEUROFIBROSARCOMA OF THE GINGIVA
D40Y12	594C	1/01/67		12.3	1942.87	164.502	4505	6704	RUPTURED PROSTATIC CYST
D40X14	598B	3/03/67		13.5	1253.19	153.957	4940	6668	BACTERIAL ENDOCARDITIS
D40Y15	598C	3/03/67		10.6	2214.82	209.124	3870	7252	SQUAMOUS CELL CARCINOMA OF THE GINGIVA
D40Y16	598D	3/03/67		13.1	2167.46	209.013	4773	8859	SQUAMOUS CELL CARCINOMA-TONSIL

BEAGLE NUMBER	LITTER NUMBER	BIRTH DATE	AGE AT TERM.	AGE AT DEATH	PEAK BODY BURDEN (kBq)	(kBq/KG)	EXPOSURE DAYS	TOTAL DOSE (CENTIGRAYS)	C O M M E N T S
D40X18	637B	9/10/67		5.7	1497.76	202.945	2097	4124	MALIGNANT LYMPHOMA
D40X19	637C	9/10/67		10.8	1283.90	160.469	3945	6227	HEMANGIOSARCOMA
D40X20	637D	9/10/67		14.7	1632.81	194.398	5373	7613	MENINGIOMA SPINAL CANAL
D40X21	637E	9/10/67		9.5	1460.39	196.840	3461	5668	METASTATIC MAMMARY CARCINOMA
D40Y22	637F	9/10/67		2.7	2236.65	171.532	976	1997	MPS
D40Y23	637G	9/10/67		14.2	2099.01	201.428	5204	9028	SQUAMOUS CELL CARCINOMA OF THE GINGIVA
PILOT SERIES									
D50F01	134A	7/23/61		7.5	3397.71	407.000	2742	9970	SQUAMOUS CELL CARCINOMA OF THE GINGIVA
D50F04	138A	7/26/61		1.6	4347.50	455.174	576	2492	ACUTE NECROTIZING ENTERITIS
D50F06	138C	7/26/61		3.0	4544.71	478.410	1092	5577	ACCIDENTAL (ANESTHETIC DEATH - DURING RADIOGRAPHIC SURVEY)
D50M08	138E	7/26/61		5.3	7414.80	563.880	1929	11781	ENTERITIS
D50F14	164E	12/25/61		1.5	2869.35	378.510	549	2054	MPS
D50M21	189B	4/13/62		4.7	5003.88	594.294	1703	10330	CEREBRAL HEMORRHAGE
D50M26	191E	4/24/62		6.6	3893.51	483.664	2417	10280	OSTEOSARCOMA OF THE R MANDIBLE
D50F29	193C	4/26/62		3.2	4051.50	479.890	1174	5928	MPS
D50F30	193D	4/26/62		3.6	4266.10	497.761	1331	6094	MPS
D50M31	193E	4/26/62		8.8	4874.01	532.800	3197	13890	METASTATIC OSTEOSARCOMA
D50M32	193F	4/26/62		2.3	4266.10	493.210	827	4171	MPS
D50M33	193G	4/26/62		1.6	5746.10	607.281	571	3292	MPS
D50F34	254A	4/21/63		6.0	2694.34	338.032	2180	6498	SQUAMOUS CELL CARCINOMA OF THE GINGIVA
D50F36	254C	4/21/63		10.1	3796.20	394.161	3672	12142	SQUAMOUS CELL CARCINOMA OF THE GINGIVA
D50F37	254D	4/21/63		8.9	4491.80	458.800	3256	13000	OSTEOSARCOMA OF THE L ISCHIUM
D50M39	254F	4/21/63		2.7	5746.10	573.870	971	5553	MPS
FIRST RUN									
D50M41	305B	12/12/63		3.5	4935.80	606.948	1276	7737	MPS
D50M42	305C	12/12/63		6.6	5020.90	595.700	2412	13572	SQUAMOUS CELL CARCINOMA OF THE GINGIVA
D50M43	305D	12/12/63		6.4	5233.28	603.618	2337	13960	SQUAMOUS CELL CARCINOMA OF THE R MANDIBLE
D50F45	314B	12/25/63		7.1	4348.98	563.510	2604	13073	OSTEOSARCOMA OF THE R MANDIBLE
D50F46 A	314C	12/25/63		8.6	3586.04	451.030	3144	12310	SQUAMOUS CELL CARCINOMA OF L MANDIBLE
D50F51	332C	3/23/64		7.6	3966.77	533.170	2787	13480	OSTEOSARCOMA OF THE 1ST CERVICAL VERTEBRA
D50F52 C	332D	3/23/64		6.0	4788.54	437.340	2187	13790	MPS
D50F53	332E	3/23/64		4.9	4943.20	672.364	1799	9891	OSTEOSARCOMA OF THE L MANDIBLE
D50M55	332G	3/23/64		9.0	5795.68	763.680	3287	19050	METASTATIC HEMANGIOSARCOMA (PRIMARY SITE NOT IN BONE)
D50F56 A	336A	3/28/64		8.4	3698.52	374.440	3076	10640	OSTEOSARCOMA OF THE L FEMUR & L MANDIBLE
D50M57	336B	3/28/64		9.6	3726.64	428.460	3511	11634	OSTEOSARCOMA OF THE R PETROUS TEMPORAL BONE
D50M58	336C	3/28/64		5.0	4240.20	517.038	1825	9316	GRANULOMATOUS MENINGOENCEPHALITIS
D50F60 A	362A	5/25/64		9.9	3514.63	466.200	3608	13470	METASTATIC OSTEOSARCOMA
D50F61	362B	5/25/64		8.6	3829.50	448.218	3138	12253	OSTEO OF L TEMPORAL BONE
D50F62	362C	5/25/64		8.9	5217.74	756.280	3242	16942	SQUAMOUS CELL CARCINOMA OF THE GINGIVA
D50M63	362D	5/25/64		10.0	3903.50	452.880	3658	14600	SQUAMOUS CELL CARCINOMA OF THE GINGIVA
D50M64	362E	5/25/64		3.5	6290.74	617.530	1278	8353	MPS

BEAGLE NUMBER	LITTER NUMBER	BIRTH DATE	AGE AT TERM.	AGE AT DEATH	PEAK BODY BURDEN (kBq)	(kBq/KG)	EXPOSURE DAYS	TOTAL DOSE (CENTIGRAYS)	C O M M E N T S
D50F65 C	394A	7/14/64		6.5	5026.08	548.710	2361	14684	OSTEOSARCOMA OF THE R ULNA
D50F66	394B	7/14/64		7.1	4558.40	534.317	2586	13000	OSTEOSARCOMA OF THE PELVIS
D50M67 C	394C	7/14/64		2.9	4399.67	597.920	1042	6363	EPILEPSY
D50M68	394D	7/14/64		7.4	6050.61	657.120	2715	16862	OSTEOSARCOMA OF THE L MANDIBLE
D50M69 C	394E	7/14/64		4.2	4843.30	549.080	1533	9915	MPS
D50M70	394F	7/14/64		3.0	6660.00	568.320	1095	6853	EPILEPSY
SECOND RUN									
D50M73	479C	8/29/65		3.3	6445.77	634.550	1215	8619	MPS
D50M74	479D	8/29/65		6.0	6512.00	647.130	2181	15222	SQUAMOUS CELL CARCINOMA OF THE MAXILLA
D50F75	495A	9/21/65		8.6	3172.75	446.960	3130	12293	PATHOLOGIC FRACTURES R TIBIA AND R MANDIBLE
D50F76	495B	9/21/65		3.5	3974.54	464.350	1275	6113	MPS
D50M77	495C	9/21/65		4.4	5181.48	558.367	1599	9446	MPS
D50F79	516B	1/02/66		3.0	6256.70	737.780	1083	7578	MPS
D50F80	516C	1/02/66		1.3	5464.90	625.300	467	2571	MPS
D50M81	516D	1/02/66		3.3	6952.30	623.450	1193	7754	MPS
D50M82	516E	1/02/66		2.5	7163.20	707.810	926	6847	MPS
D50F83	528A	2/25/66		7.1	4033.00	437.340	2611	2513	MPS (APLASTIC ANEMIA)
D50F84	528B	2/25/66		5.6	4566.54	566.581	2049	11952	SQUAMOUS CELL CARCINOMA OF THE GINGIVA
D50M86	528D	2/25/66		6.4	4880.30	629.740	2331	14852	ACCIDENTAL (HYPERTHERMIA AFTER ANESTHESIA FOR BIOPSY, EPULIS)
D50M87	528E	2/25/66		3.0	6564.54	756.317	088	7621	MPS
D50F89	560B	7/06/66		8.4	3725.90	490.028	3058	15620	RADIATION OSTEODYSTROPHY R FEMUR AND OSTEOSARCOMA R ISCHIUM
D50F92	622A	6/13/67		3.1	4584.30	500.610	1123	6730	MPS
D50M94	622C	6/13/67		6.1	4950.60	541.680	2219	11212	LYMPHOID HYPOPLASIA
D50M95	622D	6/13/67		2.3	5135.60	511.340	836	5020	MPS
D50M96	622E	6/13/67		3.6	5087.50	645.650	1325	7871	MPS
D50X01	644A	10/09/67		4.2	2811.26	450.660	1549	6193	MPS
D50X02 A	644B	10/09/67		9.7	3421.39	423.391	3526	13140	ULCERATIVE GASTRITIS
D50X03	644C	10/09/67		9.2	3201.24	433.751	3369	12740	CARCINOMA OF R FRONTAL SINUS
D50Y05	644E	10/09/67		1.8	4729.34	479.668	667	3389	MPS
D50Y09	645C	10/15/67		2.5	4414.47	507.418	898	5082	MPS
FIRST RUN									
D60F01	520A	1/09/66		.4					SCHEDULED SACRIFICE (SPECIAL STUDY)
D60M03	520C	1/09/66		.4					SCHEDULED SACRIFICE (SPECIAL STUDY)
D60M04	520D	1/09/66		.1					UNDETERMINED
D60M05	520E	1/09/66		.4					SCHEDULED SACRIFICE (SPECIAL STUDY)
D60M06	520F	1/09/66		.4					SCHEDULED SACRIFICE (SPECIAL STUDY)
D60F07	521A	1/11/66		.4					SCHEDULED SACRIFICE (SPECIAL STUDY)
D60F08	521B	1/11/66		.4					SCHEDULED SACRIFICE (SPECIAL STUDY)
D60F09	521C	1/11/66		.4					SCHEDULED SACRIFICE (SPECIAL STUDY)
D60M10	521D	1/11/66		.4					SCHEDULED SACRIFICE (SPECIAL STUDY)
D60F11	524A	2/02/66		.4					SCHEDULED SACRIFICE (SPECIAL STUDY)

BEAGLE NUMBER	LITTER NUMBER	BIRTH DATE	AGE AT TERM.	AGE AT DEATH	PEAK BODY BURDEN (kBq)	(kBq/KG)	EXPOSURE DAYS	TOTAL DOSE (CENTIGRAYS)	C O M M E N T S
D60F12	524B	2/02/66		.4					SCHEDULED SACRIFICE (SPECIAL STUDY)
D60M13	524C	2/02/66		.4					SCHEDULED SACRIFICE (SPECIAL STUDY)
D60M14	524D	2/02/66		.4					SCHEDULED SACRIFICE (SPECIAL STUDY)
D60M15	524E	2/02/66		.4					SCHEDULED SACRIFICE (SPECIAL STUDY)
D60F16	526A	2/10/66		.4					SCHEDULED SACRIFICE (SPECIAL STUDY)
D60F17	526B	2/10/66		.4					SCHEDULED SACRIFICE (SPECIAL STUDY)
D60M19	526D	2/10/66		.4					SCHEDULED SACRIFICE (SPECIAL STUDY)
D60M20	526E	2/10/66		.4					SCHEDULED SACRIFICE (SPECIAL STUDY)
D60M21	526F	2/10/66		.4					SCHEDULED SACRIFICE (SPECIAL STUDY)
SECOND RUN									
D60F22	610A	5/06/67		3.0	13608.6	1595.44	1080	18910	OSTEOSARCOMA OF THE L HUMERUS & L ULNA
D60F23	610B	5/06/67		1.6	14048.9	1481.89	586	8462	MPS
D60M24	610C	5/06/67		2.0	26514.2	2087.91	731	15700	MPS
D60M25	610D	5/06/67		1.4	16564.9	1680.17	496	7605	PANCYTOPENIA
D60M26	610E	5/06/67		3.0	14637.6	1567.32	1111	19363	CHONDROSARCOMA OF THE 1ST CERVICAL VERTEBRA
D60M30	612D	5/12/67		2.5	16897.9	1953.38	926	14480	HEMANGIOSARCOMA OF THE L HUMERUS
D60M31	612E	5/12/67		1.6	15458.6	1702.44	579	9160	POSTERIOR PARALYSIS (UNKNOWN ETIOLOGY
D60F32	627A	7/12/67		2.5	11251.7	1358.79	902	12882	SQUAMOUS CELL CARCINOMA OF THE GINGIVA
D60F33	627B	7/12/67		2.8	12513.4	1563.99	1009	17564	OSTEOSARCOMA OF THE PELVIS
D60F35	627D	7/12/67		2.4	12254.4	1289.97	868	12551	OSTEOSARCOMA OF THE PELVIS
D60M36	627E	7/12/67		1.6	14379.3	1751.58	602	10190	APLASTIC ANEMIA
D60M37 A	627F	7/12/67		2.8	11303.9	1278.72	1009	14840	OSTEOSARCOMA OF THE SKULL
D60M38	627G	7/12/67		2.2	17253.1	1526.69	799	14430	OSTEOSARCOMA OF THE L TIBIA
D60M39	627H	7/12/67		1.6	16539.0	1680.91	576	10263	OSTEOSARCOMA OF THE R HUMERUS
D60M40	627I	7/12/67		2.1	20250.1	1962.22	763	16130	OSTEOSARCOMA OF THE L HUMERUS
D60F41	636A	9/02/67		1.6	7311.2	1234.80	594	6823	PANCYTOPENIA
D60F42	636B	9/02/67		2.3	7355.6	929.847	844	8323	MPS
D60M43	636C	9/02/67		1.9	17523.2	2467.90	681	11820	MPS
D60M44	636D	9/02/67		2.6	11163.3	1172.64	958	12760	OSTEOSARCOMA OF THE L FEMUR & L TIBIA
FIRST RUN									
R00F03	282C	10/20/63		14.3					METASTATIC MAMMARY CARCINOMA
R00F04	282D	10/20/63		14.9					TRANSITIONAL CELL CARCINOMA METASTATIC TO LUNGS
R00M05	282E	10/20/63		16.1					CHRONIC PROSTATITIS
R00F11	322A	2/22/64		12.7					METASTATIC MAMMARY CARCINOMA
R00M12	322B	2/22/64		14.7					MALIGNANT LYMPHOMA
R00M13	322C	2/22/64		13.2					MALIGNANT LYMPHOMA
R00M14	322D	2/22/64		17.2					BRONCHOGENIC CARCINOMA
R00F15	323A	2/27/64		14.4					DIABETES MELLITIS
R00F16	323B	2/27/64		11.9					METASTATIC MAMMARY CARCINOMA

BEAGLE NUMBER	LITTER NUMBER	BIRTH DATE	AGE AT TERM.	AGE AT DEATH	PEAK BODY BURDEN (kBq)	PEAK BODY BURDEN (kBq/KG)	EXPOSURE DAYS	TOTAL DOSE (CENTIGRAYS)	COMMENTS
R00M17	323C	2/27/64		17.4					CHRONIC PNEUMONIA
R00M18	323D	2/27/64		16.5					MENINGIOMA
R00F20	326A	3/03/64		13.4					DISSEMINATED MAMMARY CARCINOMA
R00F21	326B	3/03/64		5.0					NORMAL SACRIFICE
R00M22	326C	3/03/64		14.8					NEPHROSCLEROSIS
R00M23	326D	3/03/64		11.9					CEREBRAL HEMORRHAGE
R00M24	326E	3/03/64		15.2					RUPTURED PROSTATIC ABSCESS
R00M28	340C	4/02/64	13.3	13.6					MALIGNANT LYMPHOMA, AND FIBRINOLYTIC SYNDROME SECONDARY TO DRUG TREATMENT FOR LYMPHOMA
R00M30	340E	4/02/64		16.8					CHRONIC BRONCHOPNEUMONIA
R00M33	350C	5/02/64		16.4					CHRONIC RENAL DISEASE/NEPHROSCLEROSIS
R00M34	350D	5/02/64		1.6					ACCIDENTAL (ANESTHETIC DEATH - FOR WHOLE BODY COUNTING)
R00M35	350E	5/02/64		15.0					METASTATIC BILE DUCT CARCINOMA
R00F38	370C	6/11/64		13.8					METASTATIC MAMMARY CARCINOMA
R00F42	393A	7/14/64		10.6					CHRONIC ACTIVE PNEUMONIA AND RENAL AMYLOIDOSIS
R00F43	393B	7/14/64		17.0					SENILE CNS DISEASE
R00F44	393C	7/14/64		15.2					DEGENERATIVE ENCEPHALOPATHY
R00F45	393D	7/14/64	12.7	13.1					METASTATIC MAMMARY TUMORS
R00M46	393E	7/14/64		17.4					UNDETERMINED CNS DISEASE-SENILE ENCEPHALOPATHY
R00F48	401A	7/26/64		17.1					MYELOPATHY, TERMINAL
R00M50	401C	7/26/64		17.4					RENAL CARCINOMA
R00F52	418A	9/14/64		5.8					ACCIDENTAL (UTERINE PERFORATION DURING ANTIBIOTIC INFUSION)
R00M54	418C	9/14/64		14.9					MALIGNANT LYMPHOMA
R00M55	418D	9/14/64		16.3					PERFORATING ESOPHAGEAL ULCER
R00F57	419B	9/17/64	13.1	14.3					BCG SACRIFICE
R00F58	419C	9/17/64		16.4					METASTATIC MAMMARY CARCINOMA
R00F59	419D	9/17/64		11.6					METASTATIC MAMMARY CARCINOMA
R00M60	419E	9/17/64		13.7					FIBROSARCOMA OF THE GINGIVA
R00M61	419F	9/17/64		13.5					METASTATIC UNDIFFERENTIATED SPLENIC TUMOR
R00F63	441B	12/03/64		8.3					METASTATIC TRANSITIONAL CELL CARCINOMA (RENAL PELVIS)
R00F64	441C	12/03/64		14.4					METASTATIC MAMMARY CARCINOMA
R00M67	441F	12/03/64		17.6					CHRONIC NEPHROSCLEROSIS/RENAL ARTERIOSCLEROSIS
SECOND RUN									
R00F70	472C	8/03/65		15.7					FIBROSARCOMA-ORAL CAVITY, METASTATIC TO LUNG
R00M73	472F	8/03/65		14.4					MELANOMA
R00M75	472H	8/03/65		15.5					CHOLANGIOHEPATITIS (COMMON BILE DUCT OBSTRUCTION)
R00M76	472I	8/03/65		15.2					THYMOMA, PLEURAL CAVITY/CARDIAC TAMPONADE
R00F82	527A	2/23/66		17.1					ACUTE PERITONITIS
R00F83	527B	2/23/66		11.5					PYOMETRA AND CONGESTIVE HEART FAILURE
R00M86	527E	2/23/66		18.0					SEVERE CHRONIC CHOLECYSTITIS

BEAGLE NUMBER	LITTER NUMBER	BIRTH DATE	AGE AT TERM.	AGE AT DEATH	PEAK BODY BURDEN (kBq)	(kBq/KG)	EXPOSURE DAYS	TOTAL DOSE (CENTIGRAYS)	COMMENTS
R00M87	527F	2/23/66		17.4					CHRONIC RENAL DISEASE (NEPHROSCLEROSIS)
R00M89	529B	3/01/66		12.0					ORAL MELANOMA (NEAR FRENULUM)
R00M90	529C	3/01/66		16.1					PNEUMONIA
R00M91	529D	3/01/66		16.9					DISSEMINATED LYMPHOSARCOMA
R00F94	548B	6/07/66		13.5					ACUTE RENAL FAILURE-IATROGENIC
R00F95	548C	6/07/66		15.4					METASTATIC MAMMARY CARCINOMA
R00M98	548F	6/07/66		15.8					DISSEMINATED LYMPHOSARCOMA
R00X02	555B	6/26/66		1.9					ACCIDENTAL DEATH (STRANGULATION ON NECK CHAIN)
R00X03	555C	6/26/66		14.0					MALIGNANT MAMMARY CARCINOMA
R00X08	575C	10/17/66		.2					ENTERITIS
R00Y12	576A	11/07/66		13.7					CONGESTIVE HEART FAILURE
R00Y13	576B	11/07/66		15.1					SUPPURATIVE HEPATITIS (HEPATIC ABSCESSATION)
R00Y14	576C	11/07/66		17.8					LYMPHOSARCOMA
R00X18	583D	12/01/66		14.9					METASTATIC MAMMARY CARCINOMA
R00Y19	583E	12/01/66		.3					ACCIDENTAL DEATH (ANESTHETIC DEATH)
R00Y20	583F	12/01/66		8.1					IDIOPATHIC EPILEPSY
R00Y21	583G	12/01/66		15.5					ACUTE CONGESTIVE HEART FAILURE? RUPTURED CHORDAE TENDINAE
R00X22	595A	1/03/67		8.3					CHRONIC ACTIVE INTERSTITIAL PNEUMONIA
R00X24	595C	1/03/67		13.0					CONGESTIVE HEART FAILURE
R00Y25	595D	1/03/67		12.6					CONGESTIVE HEART FAILURE, RUPTURED CHORDAE TENDINAE
R00X26	611A	5/11/67		12.9					INTERVERTEBRAL DISC DISEASE
R00X27	611B	5/11/67		12.3					ADRENAL CARCINOMA
R00X28	611C	5/11/67		13.2					PITUITARY CARCINOMA
R00Y30	611E	5/11/67		10.6					MALIGNANT LYMPHOMA
R00X32	621B	6/07/67		14.3					PITUITARY CARCINOMA
R00X33	621C	6/07/67		14.9					METASTATIC MAMMARY CARCINOMA
R00Y34	621D	6/07/67		10.3					ADRENOCORTICAL ATROPHY
R00X36	625A	7/04/67	10.6	11.5					BCG SACRIFICE
R00X37	625B	7/04/67		12.6					DIABETES MELLITUS
R00Y39	625D	7/04/67		13.3					MALIGNANT ORAL MELANOMA
R00Y41	625F	7/04/67		16.5					CHRONIC HEART DISEASE/LIVER DISEASE/KIDNEY DISEASE
R00X42	629A	7/15/67		17.3					PROGRESSIVE POSTERIOR PARALYSIS/CHRONIC RENAL DISEASE
R00X43	629B	7/15/67		12.6					HEPATIC ABSCESS RUPTURE/ABDOMINAL HEMORRHAGE
R00X44	629C	7/15/67		14.2					ACUTE CONGESTIVE HEART FAILURE
R00Y45	629D	7/15/67		16.2					CHRONIC RENAL DISEASE
	FIRST RUN								
R05F03	293C	11/19/63		14.2	2.96	.333	4767	91	METASTATIC MAMMARY CARCINOMA
R05F04	293D	11/19/63		12.6	2.59	.296	4180	90	METASTATIC SALIVARY GLAND ADENOCARCINOMA
R05M05	293E	11/19/63		14.1	3.33	.296	4727	113	HEPATOCELLULAR ADENOMA
R05M06	293F	11/19/63		14.7	3.33	.259	4927	126	METASTATIC TESTICULAR SEMINOMA

BEAGLE NUMBER	LITTER NUMBER	BIRTH DATE	AGE AT TERM.	AGE AT DEATH	PEAK BODY BURDEN (kBq)	(kBq/KG)	EXPOSURE DAYS	TOTAL DOSE (CENTIGRAYS)	C O M M E N T S
R05F07	300A	12/10/63		13.5	2.59	.259	4510	88	NEPHROSCLEROSIS, ACUTE PNEUMONIA AND CARDIOMEGALY
R05F08	300B	12/10/63		18.5	2.22	.333	6319	103	MAMMARY ADENOCARCINOMA
R05M09	300C	12/10/63		16.6	3.33	.333	5613	122	CUSHINGS DISEASE (PITUITARY ADENOMA)
R05M10	300D	12/10/63		15.0	2.96	.333	5026	109	CEREBRAL HEMORRHAGE
R05F24	392A	7/12/64		5.4	2.22	.222	1544	26	METASTATIC PANCREATIC ADENOCARCINOMA
R05F25	392B	7/12/64		9.5	2.22	.259	3043	55	CHRONIC INTERSTITAL PNEUMONIA
R05M27	392D	7/12/64		15.2	2.59	.370	5101	75	INTRAVASCULAR THROMBOSIS/MYOCARDIAL AND RENAL INFARCTION
R05F29	412B	8/27/64		13.0	3.33	.333	4324	91	MALIGNANT LYMPHOMA
R05F30	412C	8/27/64		14.1	2.22	.259	4711	86	METASTATIC MAMMARY CARCINOMA
R05M31	412D	8/27/64		13.7	2.59	.296	4574	74	TRANSITIONAL CELL CARCINOMA IN PROSTATIC URETHRA
R05M32	412E	8/27/64	14.1	14.3	2.96	.259	4801	98	MALIGNANT LYMPHOMA
R05F34	417B	9/07/64		16.0	1.85	.222	5392	72	CHRONIC RENAL FAILURE/NEPHROSCLEROSIS
R05F35	417C	9/07/64		15.7	3.33	.370	5299	118	PANCREATIC ATROPHY/FIBROSIS
R05M37	417E	9/07/64		15.9	2.96	.296	5378	96	MESENTERIC INFARCTION
R05M38	417F	9/07/64		15.0	2.59	.222	5040	108	UNDETERMINED NEUROLOGIC DISEASE - CONVULSIONS
R05M39	417G	9/07/64		15.7	3.33	.296	5301	102	PYELONEPHRITIS
R05F40	427A	10/07/64		9.2	2.59	.222	2933	53	SQUAMOUS CELL CARCINOMA OF THE GINGIVA
R05F41	427B	10/07/64		15.9	2.59	.222	5390	94	MAMMARY CARCINOMA
R05M43	427D	10/07/64		15.5	2.59	.222	5232	83	BRONCHIECTASIS/CHRONIC SUPPURATIVE PNEUMONIA
	SECOND RUN								
R05F44	483A	8/31/65		11.2	3.33	.407	3663	69	METASTATIC MAMMARY CARCINOMA
R05F45	483B	8/31/65		14.6	2.59	.333	4881	87	ACUTE NECROTIZING PNEUMONIA-ASPIRATION
R05F47	483D	8/31/65	11.5	13.4	2.96	.259	4465	88	TERMINATED-BCG EXPERIMENT
R05F48	483E	8/31/65		13.4	2.59	.296	4468	64	METASTATIC MAMMARY CARCINOMA
R05M49	483F	8/31/65		16.1	3.33	.296	5446	102	GINGIVAL FIBROSARCOMA
R05F51	494B	9/16/65		12.0	3.33	.333	3953	102	METASTATIC MALIGNANT MELANOMA OF THE EYE
R05M52	494C	9/16/65		9.3	4.07	.407	2965	98	NASAL CHONDROSARCOMA
R05M53	494D	9/16/65		13.2	4.44	.444	4381	107	STRANGULATION OF LARGE BOWEL
R05M54	494E	9/16/65		13.6	3.33	.333	4528	135	PROSTATIC ABSCESS
R05F56	547B	6/01/66		9.5	2.96	.296	3036	56	MALIGNANT LYMPHOMA
R05F57	547C	6/01/66		13.6	2.22	.259	4514	74	HISTIOCYTIC LYMPHOSARCOMA, DISSEMINATED
R05M58	547D	6/01/66		14.4	2.96	.333	4832	97	ADRENAL CORTICAL NECROSIS-ADDISONIAN CRISIS
R05M59	547E	6/01/66		16.2	3.33	.370	5499	120	INTERVETEBRAL DISC HERNIATION/PARAPLEGIA
R05F61	568B	9/14/66		17.6	2.22	.222	5979	64	CHRONIC SPINAL DISEASE
R05M63	568D	9/14/66		15.9	2.96	.333	5371	87	CHRONIC PYELONEPHRITIS
R05M64	568E	9/14/66		15.9	2.96	.296	5368	80	METASTATIC MALIGNANT MELANOMA, ORAL
R05F68	588D	12/11/66		12.5	2.22	.296	4129	63	NECROTIZING PNEUMONIA WITH SECONDARY PULMONARY THROMBOSIS
R05M70	588F	12/11/66		12.0	2.22	.296	3957	78	CONGESTIVE HEART FAILURE
R05F71	623A	6/16/67		13.1	3.70	.444	4352	99	METASTATIC MAMMARY CARCINOMA
R05F72	623B	6/16/67		17.0	2.59	.370	5763	77	CHRONIC PYELONEPHRITIS

BEAGLE NUMBER	LITTER NUMBER	BIRTH DATE	AGE AT TERM.	AGE AT DEATH	PEAK BODY BURDEN (kBq)	(kBq/KG)	EXPOSURE DAYS	TOTAL DOSE (CENTIGRAYS)	C O M M E N T S
R05F73	623C	6/16/67		14.8	2.59	.370	4962	86	CHRONIC RENAL DISEASE/PYELONEPHRITIS
R05F74	623D	6/16/67		17.2	2.96	.370	5865	102	CHRONIC RENAL FAILURE
R05M76	623F	6/16/67		16.0	2.96	.370	5401	111	INTERVERTEBRAL DISC DISEASE
	FIRST RUN								
R10F01	298A	12/07/63		14.8	9.25	.888	4972	331	CONGESTIVE HEART FAILURE, PULMONARY EDEMA
R10M02	298B	12/07/63		12.7	9.62	.888	4201	302	PITUITARY TUMOR WITH SECONDARY CUSHING'S DISEASE AND DISSEMINATED INTRAVASCULAR COAGULOPATHY
R10M04	298D	12/07/63		17.0	11.10	.925	5764	364	MALIGNANT LYMPHOMA
R10M05	298E	12/07/63		14.3	9.25	.740	4806	243	CHONDROSARCOMA OF VERTEBRA
R10M07	355B	5/13/64		15.7	5.55	.999	5283	276	EOSINOPHILIC TRACHEITIS/BRONCHITIS-PARASITIC
R10M09	355D	5/13/64	14.6	16.4	7.03	.851	5537	293	LYMPHOMA
R10F14	395A	7/14/64	12.7	14.5	5.18	.851	4871	219	TERMINATED-BCG EXPERIMENT, BCG SACRIFICE
R10F15	395B	7/14/64		14.4	4.44	.740	4825	219	ACUTE NECROTIZING ENTERITIS (PARVOVIRUS)
R10F17	395D	7/14/64		13.8	3.70	.629	4618	153	CUSHING'S DISEASE
R10F18	395E	7/14/64		13.4	4.44	.555	4458	141	DUODENAL ULCERS AND CHRONIC PERITONITIS
R10M20	395G	7/14/64		12.8	5.92	.740	4248	190	CARDIAC AND PULMONARY THROMBOSIS
R10M21	395H	7/14/64		11.6	7.77	.814	3817	208	MALIGNANT LYMPHOMA
R10F22	402A	7/26/64		14.8	5.55	.703	4967	224	DEMYELINATING ENCEPHALOPATHY
R10F23	402B	7/26/64		17.5	6.29	.777	5974	289	DIFFUSE ARTERIOSCLEROSIS, CHRONIC RENAL DISEASE
R10F24	402C	7/26/64		12.9	6.66	.777	4294	218	CONGESTIVE HEART FAILURE
R10M26	402E	7/26/64		12.9	7.40	.851	4260	221	METASTATIC HEMANGIOSARCOMA OF THE L ILEUM
R10M27	402F	7/26/64		15.5	7.03	.666	5238	299	MALIGNANT MELANOMA-LIP
R10M33	415D	9/02/64		18.2	5.18	.592	6228	174	HEPATIC NECROSIS AND ABSCESSATION/PERITONITIS
	SECOND RUN								
R10F38	478B	8/29/65		12.3	5.18	.592	4068	181	METASTATIC BILE DUCT CARCINOMA
R10M39	478C	8/29/65		8.2	5.55	.592	2563	157	PRIMARY BRAIN TUMOR
R10F41	534B	4/06/66		12.7	8.88	.888	4214	217	HEPATOCELLULAR ADENOMA
R10M43	534D	4/06/66		13.6	10.73	.925	4535	306	SALIVARY GLAND SARCOMA
R10M44	534E	4/06/66		14.4	11.84	.962	4830	311	BRONCHOGENIC CARCINOMA
R10F46	570B	9/17/66		16.0	8.14	.888	5399	280	PITUITARY TUMORS
R10F47	570C	9/17/66	10.6	12.3	8.14	.777	4046	267	TERMINATED-BCG EXPERIMENT, SEPTICEMIA SECONDARY TO TRANSITIONAL CELL CARCINOMA OF URINARY BLADDER AND URETHRA
R10M49	570E	9/17/66		12.3	12.21	1.147	4041	369	TRANSITIONAL CELL CARCINOMA-BLADDER/URETHRA
R10F53	574A	10/15/66		15.7	8.51	1.221	5300	364	CEREBRAL INFARCTION/NON-SUPPURATIVE ENCEPHALITIS
R10F54	574B	10/15/66		13.6	11.47	1.258	4538	429	ACUTE BRONCHOPNEUMONIA-BACTERIAL
R10M55	574C	10/15/66		10.2	16.28	1.406	3280	404	METASTATIC TRANSITIONAL CELL CARCINOMA OF URINARY BLADDER
R10M56	574D	10/15/66		17.8	17.02	1.813	6062	730	SUBDURAL HEMATOMA OF THE BRAINSTEM
R10F58	608B	4/28/67		13.7	5.55	.814	4553	259	CONGESTIVE HEART FAILURE

BEAGLE NUMBER	LITTER NUMBER	BIRTH DATE	AGE AT TERM.	AGE AT DEATH	PEAK BODY BURDEN (kBq)	(kBq/KG)	EXPOSURE DAYS	TOTAL DOSE (CENTIGRAYS)	C O M M E N T S
R10M59	608C	4/28/67		13.9	7.40	.999	4657	291	OSTEOSARCOMA THORACIC VERTEBRA
R10M60	608D	4/28/67		12.4	10.36	.999	4106	267	CONGESTIVE HEART FAILURE
R10F61	615A	5/19/67		8.5	7.03	1.184	2686	251	METASTATIC MAMMARY CARCINOMA
R10F62	615B	5/19/67		16.1	8.14	1.184	5451	383	CHRONIC RENAL DISEASE
R10F63	615C	5/19/67		17.9	8.88	1.221	6087	433	OSTEOSARCOMA OF THE LEFT FEMUR
R10M65	615E	5/19/67		14.3	9.62	1.221	4783	375	FIBROSARCOMA, RIB AND SPINE
R10M66	615F	5/19/67		13.7	8.88	.962	4578	382	CHRONIC PROSTATITIS
FIRST RUN									
R20F01 A	295A	11/30/63		15.5	34.41	3.737	5220	1526	INTERVERTEBRAL DISC DISEASE
R20F02	295B	11/30/63		13.9	35.89	4.144	4651	1427	ASTROCYTOMA (GRADE IV) AND NEUROFIBROSARCOMA
R20M03	295C	11/30/63		11.0	38.11	3.774	3580	1103	OSTEOSARCOMA OF THE R ILIUM
R20M04	295D	11/30/63		14.8	32.19	3.478	4962	1290	CONGESTIVE HEART FAILURE
R20F05	297A	12/02/63		12.4	29.23	3.367	4076	928	HEPATOCELLULAR ADENOMA
R20F06	297B	12/02/63		12.8	43.66	5.032	4250	1522	OSTEOSARCOMA OF THE 5TH LUMBAR VERTEBRA
R20F07 A	297C	12/02/63		11.3	49.58	4.699	3676	1264	OSTEOSARCOMA R FRONT LEG
R20M09	297E	12/02/63		10.3	81.77	6.068	3332	1706	MALIGNANT MELANOMA OF GINGIVA
R20F12 A	303B	12/11/63	9.6	9.7	54.02	4.810	3092	1124	METASTATIC OSTEOSARCOMA
R20F18	377A	6/19/64	11.4	12.1	29.23	4.625	4000	1434	OSTEOSARCOMA OF THE L ILEUM
R20F20	377C	6/19/64		12.9	45.14	4.625	4274	1491	SQUAMOUS CELL CARCINOMA OF THE GINGIVA
R20F21 A	377D	6/19/64		12.2	37.00	4.329	4015	1366	MALIGNANT MELANOMA OF THE BUCCAL CAVITY
R20M22	377E	6/19/64		12.7	56.24	5.439	4218	2089	OSTEOSARCOMA OF THE R FEMUR AND R HUMERUS
R20M23 A	377F	6/19/64		12.4	41.07	4.144	4076	1409	HEPATOCELLULAR ADENOMA
R20F24 A	407A	8/08/64		10.7	45.88	5.402	3487	1162	METASTATIC OSTEOSARCOMA
R20M26	407C	8/08/64		10.9	38.85	5.217	3561	1032	OSTEOSARCOMA OF THE 10TH THORACIC VERTEBRA
R20M27 A	407D	8/08/64		10.0	36.63	4.403	3210	991	METASTATIC OSTEOSARCOMA (L FEMUR)
R20M28	407E	8/08/64		5.8	47.36	5.217	1690	769	MALIGNANT LYMPHOMA
R20M32 A	438D	11/25/64		11.4	42.18	4.033	3714	1271	OSTEOSARCOMA L HUMERUS AND PULMONIC STENOSIS
SECOND RUN									
R20F34	488B	9/08/65		8.8	39.22	5.254	2785	1132	OSTEOSARCOMA OF THE 4TH R RIB
R20F35	488C	9/08/65		9.4	36.26	3.515	3003	879	METASTATIC PANCREATIC ADENOCARCINOMA
R20F36	488D	9/08/65		10.0	40.70	3.922	3232	1061	MALIGNANT LYMPHOMA
R20M37	488E	9/08/65		14.0	39.22	3.700	4691	1456	CONGESTIVE HEART FAILURE
R20F40 A	493B	9/14/65		7.9	40.70	4.514	2451	985	METASTATIC OSTEOSARCOMA
R20F41	493C	9/14/65		8.4	55.50	5.994	2634	1290	OSTEOSARCOMA OF THE L & R HUMERI
R20M44 A	493F	9/14/65		15.0	33.67	5.106	5060	1844	TRANSITIONAL CELL CARCINOMA (URINARY OBSTRUCTION)
R20M45	493G	9/14/65		15.0	37.74	4.699	5056	1957	MALIGNANT MELANOMA-ORIGIN UNDETERMINED
R20F48	501C	10/03/65		11.5	24.42	4.292	3756	1001	OSTEOSARCOMA OF THE SACRUM
R20F51	501F	10/03/65		14.4	30.34	4.847	4832	1601	CHRONIC SUPPURATIVE DERMATITIS
R20F52 A	501G	10/03/65		16.6	29.23	4.551	5639	1625	MAMMARY ADENOCARCINOMA WITH PULMONARY METASTASIS

BEAGLE NUMBER	LITTER NUMBER	BIRTH DATE	AGE AT TERM.	AGE AT DEATH	PEAK BODY BURDEN (kBq)	(kBq/KG)	EXPOSURE DAYS	TOTAL DOSE (CENTIGRAYS)	C O M M E N T S
R20F53	587A	12/10/66		10.9	41.07	5.143	3558	1242	OSTEOSARCOMA OF THE 4TH CERVICAL VERTEBRA
R20M54 A	587B	12/10/66		12.1	59.94	5.587	3984	1928	METASTATIC OSTEOSARCOMA-RIGHT RADIUS
R20M55	587C	12/10/66		7.5	81.77	6.956	2286	1667	METASTATIC FIBROSARCOMA OF THE 8TH THORACIC VERTEBRA
R20F58	606A	4/13/67		11.3	47.36	6.956	3710	1549	OSTEOSARCOMA-RIB
R20F60	606C	4/13/67		12.2	46.62	6.697	4008	1554	OSTEOSARCOMA-MANDIBLE
R20F61	606D	4/13/67	8.6	8.6	61.42	6.845	2714	1381	OSTEOSARCOMA OF THE L ILIUM
R20M63 A	606F	4/13/67		11.4	80.29	7.585	3731	1905	OSTEOSARCOMA-TIBIA
R20M66	613B	5/15/67		11.9	44.03	4.440	3916	932	PYELONEPHRITIS/PROSTATITIS
R20M68	613D	5/15/67		11.6	50.69	5.106	3806	1285	POLIOENCEPHALOMALACIA
R20M69 A	613E	5/15/67		6.0	69.93	5.994	1753	1085	METASTATIC OSTEOSARCOMA
R20M70	613F	5/15/67		12.6	48.84	3.959	4168	1474	RENAL CARCINOMA
	FIRST RUN								
R30F01	287A	10/28/63		8.7	103.97	12.247	2733	2871	RADIATION OSTEODYSTROPHY L ULNA & L RADIUS
R30M02	287B	10/28/63		6.9	172.05	12.580	2086	2487	SCLEROSING OSTEOSARCOMA OF VERTEBRA C-2
R30F04 A	302B	12/11/63		7.5	155.03	16.835	2302	3163	OSTEOSARCOMA WITH HEPATIC METASTASIS
R30M05	302C	12/11/63		7.2	171.31	15.873	2198	3212	OSTEOSARCOMA OF THE 4TH CERVICAL VERTEBRA
R30M06 A	302D	12/11/63		7.3	145.41	12.543	2218	2765	METASTATIC OSTEOSARCOMA
R30F09	342B	4/13/64		10.1	72.52	13.801	3236	2640	PATHOLOGIC FRACTURE OF THE L MANDIBLE
R30M10 A	342C	4/13/64		9.0	118.77	14.134	2844	3041	INTERVERTEBRAL DISC HERNIATION (C 5-6)
R30F13	365A	6/03/64		7.3	83.25	11.877	2219	1933	RADIATION OSTEODYSTROPHY L TEMPORAL BONE
R30F14 A	365B	6/03/64		10.1	75.48	11.729	3260	2756	METASTATIC OSTEOSARCOMA
R30F15	365C	6/03/64		8.8	1544.75	253.228	2773	2209	OSTEOSARCOMA OF THE 2ND CERVICAL VERTEBRA
R30M16 A	365D	6/03/64		6.8	159.10	18.685	2059	3115	METASTATIC OSTEOSARCOMA
R30M17	365E	6/03/64		7.0	123.95	14.245	2111	2576	OSTEOSARCOMA OF THE R ISCHIUM
R30F19	396B	7/14/64		12.9	84.36	10.952	4278	2544	OSTEOSARCOMA OF THE L MANDIBLE
R30M23 A	396F	7/14/64		10.0	152.07	19.980	3215	4144	OSTEOSARCOMA OF THE 4TH CERVICAL VERTEBRA
R30F25	413B	8/30/64		5.5	151.33	14.689	1571	2374	OSTEOSARCOMA OF THE PELVIS
R30F26 A	413C	8/30/64	8.2	9.2	103.23	12.728	2923	2857	OSTEO R RADIUS (LOW GRADE) OSTEO 6TH CERVICAL VERTEBRA
	SECOND RUN								
R30F29	477B	8/24/65		8.7	108.04	16.243	2749	3303	OSTEOSARCOMA OF THE 3RD CERVICAL VERTEBRA
R30M30	477C	8/24/65		6.7	174.64	17.760	2030	3371	SQUAM CELL CARCINOMA OF THE GINGIVA & OSTEOSARCOMA L FEMUR
R30M31 A	477D	8/24/65		8.3	160.21	18.167	2583	3863	METASTATIC OSTEOSARCOMA
R30M32	477E	8/24/65		7.7	193.14	19.647	2364	4145	OSTEOSARCOMA OF THE R ISCHIUM
R30M33	477F	8/24/65		2.3	220.89	19.573	413	864	CULLED
R30F34 A	489A	9/10/65		9.0	114.33	14.837	2862	3177	METASTATIC OSTEOSARCOMA OF THE L FRONTAL BONE
R30F35 A	489B	9/10/65		8.4	146.52	18.019	2644	3169	SQUAMOUS CELL CARCINOMA OF THE GINGIVA
R30F36	489C	9/10/65		5.9	119.14	16.206	1733	1894	PATHOLOGIC FRACTURE OF THE L MANDIBLE
R30M37	489D	9/10/65		9.5	150.96	13.172	3020	3952	OSTEOSARCOMA OF THE R 10TH RIB (RECURRING)
R30M39 A	489F	9/10/65		6.8	207.57	17.464	2056	3849	OSTEOSARCOMA OF THE L ISCHIUM

BEAGLE NUMBER	LITTER NUMBER	BIRTH DATE	AGE AT TERM.	AGE AT DEATH	PEAK BODY BURDEN (kBq)	(kBq/KG)	EXPOSURE DAYS	TOTAL DOSE (CENTIGRAYS)	COMMENTS
R30F42 A	499C	9/27/65		6.9	197.95	21.682	2082	4121	OSTEOSARCOMA OF THE R MANDIBLE AND R HUMERUS
R30M43	499D	9/27/65		6.1	214.97	19.906	1780	3887	OSTEOSARCOMA OF THE R SCAPULA
R30M44	499E	9/27/65		6.6	245.68	22.977	1991	4280	OSTEOSARCOMA OF THE R ISCHIUM
R30M45	499F	9/27/65		3.1	270.84	24.864	704	1819	EPILEPSY
R30F50	572A	10/03/66		6.9	142.45	18.537	2068	2870	OSTEOSARCOMA OF THE R ISCHIUM
R30F51	572B	10/03/66		7.7	111.00	13.283	2388	2859	OSTEOSARCOMA OF THE R ISCHIUM
R30F57	616C	5/21/67	8.9	8.9	88.43	16.206	2818	3107	OSTEOSARCOMA R TIBIA OSTEOSARCOMA R HUMERUS
R30F58 A	616D	5/21/67	9.8	10.2	105.45	14.319	3305	3340	OSTEOSARCOMA OF THE R RADIUS (TO FREDERICK CANCER RESEARCH CENTER)
R30F59	616E	5/21/67		7.0	136.53	18.796	2114	2952	OSTEOSARCOMA OF THE 2ND CERVICAL VERTEBRA
R30M60 A	616F	5/21/67	5.5	5.6	195.36	20.979	1626	3055	OSTEOSARCOMA OF THE L SCAPULA METASTATIC OSTEOSARCOMA
R30M61	616G	5/21/67		7.7	180.93	18.648	2381	3715	OSTEOSARCOMA OF THE L ISCHIUM
R30M64 A	624C	6/25/67		7.3	145.41	17.575	2235	3080	OSTEOSARCOMA OF THE 4TH CERVICAL VERTEBRA
R30M65	624D	6/25/67		7.9	144.30	18.056	2458	3225	OSTEOSARCOMA OF THE R MANDIBLE
R30M66 A	624E	6/25/67		8.7	138.38	18.352	2734	3613	OSTEOSARCOMA OF THE L ILIUM
FIRST RUN									
R40F01	289A	11/05/63		5.2	454.73	52.096	1479	6218	OSTEOSARCOMA OF THE L FEMUR
R40F02	289B	11/05/63		5.0	418.84	39.109	1405	5827	OSTEOSARCOMA OF THE L MANDIBLE
R40F03	289C	11/05/63		5.5	426.61	42.106	1575	6452	OSTEOSARCOMA OF THE L RADIUS
R40M04	289D	11/05/63		5.4	687.46	52.059	1527	8656	OSTEOSARCOMA OF THE R HUMERUS
R40F05	290A	11/09/63		4.7	378.88	38.184	1286	4960	OSTEOSARCOMA OF THE L ILIUM
R40F07	290C	11/09/63		6.0	349.65	36.038	1774	5684	OSTEOSARCOMA OF THE L HUMERUS
R40M09 A	290E	11/09/63		6.0	448.81	39.627	1745	6290	MALIGNANT LYMPHOMA
R40F13	312D	12/23/63		4.9	339.29	50.875	1347	6505	OSTEOSARCOMA OF THE 5TH LUMBAR VERTEBRA
R40F14	312E	12/23/63		4.8	539.46	55.611	1315	7498	OSTEOSARCOMA OF THE PELVIS
R40M15	312F	12/23/63		5.1	585.71	61.938	1438	9216	OSTEOSARCOMA OF THE L FEMUR
R40F20 A	337B	3/29/64		6.2	396.64	51.504	1829	7836	METASTATIC OSTEOSARCOMA
R40M21	337C	3/29/64		5.2	526.14	45.695	1456	7596	OSTEOSARCOMA OF THE L MANDIBLE
R40M22	337D	3/29/64		4.8	547.23	41.958	1319	6305	OSTEOSARCOMA OF THE R HUMERUS
R40M23	337E	3/29/64		5.0	619.38	45.880	1401	7359	OSTEOSARCOMA OF THE 5TH CERVICAL VERTEBRA
R40F24	408A	8/09/64		5.8	344.10	36.519	1667	6439	FIBROSARCOMA OF L MANDIBLE, OSTEOSARCOMA OF R TIBIA & L ULNA
R40F28 A	408E	8/09/64		6.1	355.94	38.036	1782	7065	OSTEOSARCOMA OF THE L TIBIA ULNA
R40M30 A	408G	8/09/64		5.0	478.04	40.589	1383	6007	OSTEOSARCOMA OF THE L HUMERUS
R40M33	433C	10/19/64		4.8	428.83	46.028	1317	6613	OSTEOSARCOMA OF THE R ISCHIUM
R40M34	433D	10/19/64		5.8	350.39	39.405	1688	6585	OSTEOSARCOMA OF THE PELVIS
R40M35	433E	10/19/64	7.2	7.2	349.28	32.449	2208	9528	OSTEOSARCOMA OF THE FRONTAL BONE
SECOND RUN									
R40F39	485D	9/01/65		5.1	475.82	43.105	1439	6109	OSTEOSARCOMA OF THE 2ND CERVICAL VERTEBRA
R40F40 A	485E	9/01/65		6.1	296.74	39.368	1798	5934	METASTATIC OSTEOSARCOMA
R40F41	486A	9/01/65		6.8	245.68	31.228	2038	5154	OSTEOSARCOMA OF THE R ILIUM

BEAGLE NUMBER	LITTER NUMBER	BIRTH DATE	AGE AT TERM.	AGE AT DEATH	PEAK BODY BURDEN (kBq)	(kBq/KG)	EXPOSURE DAYS	TOTAL DOSE (CENTIGRAYS)	C O M M E N T S
R40F48 A	531A	3/09/66		6.1	360.01	41.847	1798	6842	OSTEOSARCOMA OF THE 4TH CERVICAL VERTEBRA
R40F49	531B	3/09/66		5.0	570.91	49.469	1373	7599	OSTEOSARCOMA OF THE 2ND CERVICAL VERTEBRA
R40M50	531C	3/09/66		5.6	522.07	59.311	1600	9654	OSTEOSARCOMA OF THE 1ST CERVICAL VERTEBRA
R40M51 A	531D	3/09/66		5.0	536.13	51.874	1378	7099	OSTEOSARCOMA OF THE L HUMERUS
R40M52 A	531E	3/09/66		5.7	569.06	51.282	1649	8483	OSTEOSARCOMA OF THE L MANDIBLE
R40F53	563A	7/18/66		5.4	593.85	62.123	1547	9340	FUNGAL TURBINITIS
R40F54	563B	7/18/66		4.8	461.02	58.941	1305	6579	OSTEOSARCOMA OF THE R ACETABULUM
R40F56 A	563D	7/18/66		4.2	643.06	73.889	1092	7619	PATHOLOGIC FRACTURE OF THE R FEMUR
R40M57	563E	7/18/66		4.7	678.21	69.190	1288	9645	OSTEOSARCOMA OF THE L ISCHIUM
R40M58	563F	7/18/66		5.0	721.13	65.786	1381	9002	OSTEOSARCOMA OF THE R HUMERUS
R40F59	578A	11/15/66		5.0	700.04	83.435	1393	12481	OSTEOSARCOMA OF THE R FEMUR
R40M62	578D	11/15/66		4.8	935.73	88.393	1315	13804	OSTEOSARCOMA OF THE 5TH CERVICAL VERTEBRA
R40M63	578E	11/15/66		4.5	970.88	98.901	1198	12460	OSTEOSARCOMA OF 3RD LUMBAR VERTEBRA, PATH FRACT L HUMERUS
R40M64	578F	11/15/66		3.9	872.83	106.967	974	10054	OSTEOSARCOMA OF THE L ISCHIUM
R40M65	578G	11/15/66		4.0	1122.95	106.449	1028	12092	OSTEOSARCOMAS OF THE R & L TIBIA
R40F67	630B	7/20/67		5.5	470.27	54.686	1578	7900	OSTEOSARCOMAS OF THE L ISCHIUM & L SCAPULA
R40F68	630C	7/20/67		5.8	357.05	47.471	1670	5401	OSTEOSARCOMA L FEMUR & RADIATION OSTEODYSTROPHY L ULNA
R40F70 A	630E	7/20/67		5.3	409.22	51.800	1483	7462	METASTATIC OSTEOSARCOMA
FIRST RUN									
R50F01	283A	10/21/63		5.4	1002.33	134.162	1519	19630	PATHOLOGIC FRACTURES OF THE R HUMERUS & R FEMUR
R50F02	283B	10/21/63		4.8	964.22	120.657	1315	15660	OSTEOSARCOMA OF THE R HUMERUS
R50M03	283C	10/21/63		4.1	1045.62	124.320	1072	12920	OSTEOSARCOMA OF THE PELVIS
R50M04	283D	10/21/63		3.9	927.96	119.436	981	11382	OSTEOSARCOMA OF THE NASAL BONE
R50M05	283E	10/21/63		5.2	1222.11	140.822	1459	20994	OSTEOSARCOMA OF THE L HUMERUS
R50F06	359A	5/23/64		4.9	932.40	126.022	1340	17800	OSTEOSARCOMA OF THE R FEMUR
R50F07 A	359B	5/23/64		4.6	1054.13	134.458	1236	14070	OSTEOSARCOMA OF THE R TIBIA
R50F08 A	359C	5/23/64		4.6	1049.69	118.474	1236	15410	OSTEOSARCOMA OF THE L RADIUS
R50M09	359D	5/23/64		5.0	912.42	114.774	1387	15550	MALIGNANT MELANOMA OF THE EYE
R50M11	372B	6/12/64		4.5	1682.39	148.851	1203	20490	OSTEOMYELITIS OF FACIAL BONES
R50M12	372C	6/12/64		4.4	1488.51	158.693	1182	18830	OSTEOSARCOMA OF THE 4TH LUMBAR VERTEBRA
R50M14	372E	6/12/64		3.3	1585.08	151.552	779	13260	SACRIFICED DUE TO SEIZURES
R50F20	421D	9/20/64		5.6	1011.21	121.841	1606	18190	OSTEOSARCOMA OF THE R RADIUS & R ULNA
R50M22	421F	9/20/64		4.2	1618.75	150.738	1103	17482	OSTEOSARCOMA OF THE L TIBIA
R50M25	422C	9/20/64		4.2	1498.87	137.529	1101	17840	OSTEOSARCOMA OF THE L FEMUR
R50M26 A	422D	9/20/64		4.7	1492.58	179.598	1270	22434	OSTEOSARCOMA OF THE R RADIUS
R50M28	422F	9/20/64		5.3	1462.24	163.577	1485	24780	RADIATION OSTEODYSTROPHY, L TIBIA
R50F30	436B	11/23/64		4.5	1046.36	125.911	1193	14260	OSTEOSARCOMA OF THE 10TH TO 13TH L RIBS
R50M34	436F	11/23/64		4.0	1457.43	136.715	1038	16424	POSTERIOR PARALYSIS
R50M35	436G	11/23/64		5.2	1406.00	124.209	1449	19844	OSTEOSARCOMA OF THE L RADIUS & L ULNA

BEAGLE NUMBER	LITTER NUMBER	BIRTH DATE	AGE AT TERM.	AGE AT DEATH	PEAK BODY BURDEN (kBq)	(kBq/KG)	EXPOSURE DAYS	TOTAL DOSE (CENTIGRAYS)	C O M M E N T S
SECOND RUN									
R50F36	473A	8/07/65		2.8	1500.35	160.839	579	10014	PATHOLOGIC FRACTURES OF THE L & R MANDIBLES
R50M37	473B	8/07/65		2.3	1483.70	159.877	423	7388	APLASTIC ANEMIA
R50M38	473C	8/07/65		4.4	1507.75	137.455	1159	17940	OSTEOSARCOMA OF THE 4TH CERVICAL VERTEBRA
R50F44	564C	8/03/66		4.6	946.46	107.818	1251	14290	OSTEOSARCOMA OF THE 1ST TO 3RD LUMBAR VERTEBRA
R50F45	564D	8/03/66		3.3	1278.35	150.405	754	11014	OSTEOSARCOMA OF THE R MANDIBLE
R50M48 A	564G	8/03/66		3.8	1555.85	158.915	942	14302	OSTEOSARCOMA OF THE R FEMUR
R50M49 A	564H	8/03/66		4.9	1554.00	161.357	1352	22664	METASTATIC OSTEOSARCOMA
R50F50	604A	3/28/67		2.7	1437.08	205.868	561	10130	PATHOLOGIC FRACTURES OF THE L TIBIA & L MANDIBLE
R50F52	604C	3/28/67		1.9	1913.64	236.282	267	5176	RADIATION NEPHRITIS
R50F53	604D	3/28/67		3.0	1222.85	158.619	674	10850	PATHOLOGIC FRACTURES OF THE L TIBIA & R RADIUS
R50M56	604G	3/28/67		3.0	1607.65	188.478	673	13420	PATHOLOGIC FRACTURE OF THE R HUMERUS
R50F64 A	619C	6/02/67	4.6	4.8	1315.72	185.555	1336	21181	OSTEOSARCOMA OF THE R MAXILLA
R50F66	619E	6/02/67		4.8	1514.78	193.473	1313	23540	OSTEOSARCOMA OF THE L MAXILLA
R50M67	619F	6/02/67		3.4	2765.01	265.623	801	19650	PATHOLOGIC FRACTURES OF THE L FEMUR & L HUMERUS
R50F69	633B	7/25/67		3.6	1178.08	145.780	898	12540	UNDETERMINED (BONE MARROW INFARCTION)
R50F70 A	633C	7/25/67		4.9	1311.28	170.311	1340	20440	UNDETERMINED (PRIOR OSTEOSARCOMA AMPUTATION)
R50F71	633D	7/25/67		5.0	1175.12	137.270	1378	17900	OSTEOSARCOMA OF THE L HUMERUS
R50M72	633E	7/25/67		4.4	1336.81	157.250	1174	17840	OSTEOSARCOMA OF THE 3RD LUMBAR VERTEBRA
R50F73 A	635A	8/29/67		4.5	1032.67	155.992	1218	19280	OSTEOSARCOMA OF THE L TIBIA
R50M75	635C	8/29/67		3.1	1439.30	152.810	713	12011	ACCIDENTAL (ANESTHETIC DEATH AT LETTERMAN DURING F18 SCAN)
R50M77 A	635E	8/29/67		4.5	1443.37	171.014	1216	18910	OSTEOSARCOMA OF THE L 9TH RIB & RADIATION NEPHRITIS
R5XF01	630D	7/20/67		2.4	2234.43	247.715	756	22080	PATHOLOGIC FRACTURES OF THE R TIBIA & L HUMERUS
R5XM02	629E	7/15/67		2.3	3483.92	283.938	714	25844	OSTEOSARCOMA OF THE L TIBIA
R5XM03	629F	7/15/67		2.3	2915.60	261.257	698	22902	OSTEOSARCOMA OF THE R MANDIBLE
R5XM04	639D	9/14/67		2.9	1417.10	143.708	1000	16790	OSTEOSARCOMA OF THE L FEMUR
R5XM05	639E	9/14/67		2.7	1705.33	152.958	908	15770	OSTEOSARCOMA OF THE R FEMUR
R5XM06	639F	9/14/67		2.7	1587.67	178.377	918	17834	PATHOLOGIC FRACTURES OF THE R FEMUR, R TIBIA, & L HUMERUS
FIRST RUN									
S20F01	291A	11/12/63		14.1	370.37	34.706	4614	781	BILATERAL NEPHROSCLEROSIS
S20F06	311B	12/22/63	13.3	13.7	253.82	27.972	4447	521	TERMINATED-BCG EXPERIMENT, MAMMARY CARCINOMA
S20M09	311E	12/22/63	8.1	8.1	555.00	39.701	2422	775	MPS, SPLENECTOMY
S20F12	334C	3/26/64		15.6	364.82	43.327	5156	929	CUSHING'S SYNDROME/PITUITARY ADENOMA
S20M22	335E	3/27/64		10.3	490.62	35.816	3212	629	OSTEOSARCOMA OF THE 7TH THORACIC VERTEBRA
S20M24	335G	3/27/64		16.7	424.76	34.040	5552	808	EPILEPSY/ASPIRATION PNEUMONIA
S20F26	341B	4/03/64		12.8	293.78	31.598	4129	506	METASTATIC MAMMARY CARCINOMA
S20M33	426C	10/03/64		14.2	233.47	25.826	4655	572	CONGESTIVE HEART FAILURE
S20M35	426E	10/03/64		12.2	273.80	33.485	3906	561	ACUTE NECROTIZING PNEUMONIA, POSSIBLY ASPIRATION

BEAGLE NUMBER	LITTER NUMBER	BIRTH DATE	AGE AT TERM.	AGE AT DEATH	PEAK BODY BURDEN (kBq)	(kBq/KG)	EXPOSURE DAYS	TOTAL DOSE (CENTIGRAYS)	C O M M E N T S
SECOND RUN									
S20F37	484A	9/01/65		13.4	357.79	44.141	4339	733	METASTIC MAMMARY CARCINOMA
S20M39	484C	9/01/65		14.0	620.49	48.026	4581	1326	CONGESTIVE HEART FAILURE
S20F41	508A	11/06/65		2.1	344.10	54.279	216	106	EPILEPSY
S20F42	508B	11/06/65		15.6	505.42	61.938	5156	1176	LYMPHOSARCOMA
S20F43	508C	11/06/65		6.4	340.77	38.850	1813	423	UNDETERMINED (POSSIBLE EPILEPSY)
S20M45	508E	11/06/65		13.9	633.44	57.054	4553	1320	CHRONIC ENTERITIS
S20M46	508F	11/06/65		7.4	512.82	44.215	2172	692	UNDETERMINED (POSSIBLE EPILEPSY)
S20F48	532B	3/18/66		12.2	444.00	43.956	3928	824	CONGESTIVE HEART FAILURE
S20M49	532C	3/18/66		16.8	613.46	50.061	5604	1193	CHRONIC INTERVERTEBRAL DISC DISEASE
S20M59	584I	12/02/66		15.4	324.12	34.706	5067	803	UNDETERMINED
S20F62	603C	3/25/67		14.8	262.33	29.119	4861	395	METASTATIC TRANSITIONAL CELL CARCINOMA
FIRST RUN									
S40F02	292B	11/19/63		10.7	3328.15	328.523	3368	6058	OSTEOSARCOMA OF THE L PUBIS
S40M09	294E	11/23/63		16.5	2903.02	294.113	5471	6020	SENILE CEREBRAL ATROPHY
S40F11	328B	3/07/64		14.2	2825.69	342.102	4643	7782	ACUTE HEART FAILURE, CARDIAC INSUFFICIENCY
S40F12	328C	3/07/64		12.5	2589.26	290.598	4021	5802	FIBROSARCOMA OF THE SOFT PALATE
S40F23	331D	3/12/64		14.6	2673.62	264.735	4780	5015	PATHOLOGIC FRACTURE OF JAW
S40M27	348B	4/25/64		14.6	3237.87	443.630	4791	8531	HEMANGIOSARCOMA-BONE
S40M30	348E	4/25/64		15.5	3105.41	361.934	5134	8236	INTERVERTEBRAL DISC DISEASE
S40F34	416C	9/07/64	12.5	13.3	2354.31	252.081	4327	5633	TERMINATED-BCG EXPERIMENT/HEPATOCELLULAR CARCINOMA
SECOND RUN									
S40F36	487A	9/05/65		10.6	2575.20	286.787	3344	5282	DIABETES MELLITIS
S40F37	487B	9/05/65		12.5	2167.46	305.287	4033	3498	METASTATIC MAMMARY CARCINOMA
S40M39	487D	9/05/65		2.7	3557.18	310.393	456	1419	HEAT PROSTRATION
S40M40	487E	9/05/65		5.5	3725.90	340.474	1486	3747	CHRONIC PULMONARY DISEASE
S40M41	487F	9/05/65	12.1	12.1	3455.06	334.147	3883	6482	TERMINATED, OSTEOSARCOMA (TO FREDERICK CANCER CENTER)
S40F42	498A	9/27/65		14.2	2915.97	396.270	4637	7410	SQUAMOUS CELL CARCINOMA-GINGIVA
S40F43	498B	9/27/65		9.8	3722.20	468.790	3034	6462	METASTATIC HEPATIC HEMANGIOSARCOMA
S40F44	498C	9/27/65		2.2	3829.50	478.780	250	1151	CONVULSIONS (EPILEPSY OR CHLORDANE TOXICITY)
S40F45	498D	9/27/65		10.4	2953.34	355.829	3251	6204	IDEOPATHIC NEUROLOGIC DISEASE, ASPIRATION PNEUMONIA
S40F46	498E	9/27/65		17.4	2598.88	335.812	5812	6580	INVASIVE NASAL CARCINOMA
S40F51	544E	5/21/66		13.6	3063.23	321.789	4413	7992	FIBROSARCOMA-ZYGOMATIC ARCH
S40M57	597D	2/03/67		12.1	3785.10	344.692	3897	7549	MALIGNANT LYMPHOMA
S40M59	597F	2/03/67		13.3	3296.70	308.099	4328	6478	AORTIC THROMBOSIS-RENAL INFARCTION
S40M65	626F	7/04/67		13.8	4321.60	383.357	4517	8690	OSTEOSARCOMA, VERTEBRA
S40F66 A	639A	9/14/67		13.0	4474.04	453.731	4225	8458	METASTATIC HEMANGIOSARCOMA-BONE
S40F67	639B	9/14/67		10.4	4232.80	391.090	3252	7294	HEPATIC ABSCESSES, HEMATOMAS

SKELETAL BIOLOGY STUDIES

CELL POPULATION DYNAMICS IN CANINE CORTICAL BONE: PARTIAL DIFFERENTIAL EQUATIONS DESCRIBING THE BONE REMODELING PROCESS

S. J. Hood[1]
N. J. Parks
J. W. Brewer[2]

Data for laboratory testing of a multi-dimensional model of the cell dynamics of the bone remodeling process were obtained by taking serial sections of fluorescent- and radionuclide-labelled cortical bone in the shafts of beagle humeri. Two partial differential equations for osteoclasts and osteoclast precursor cells and an ordinary differential equation for oteoblasts are used to create a model that plots cell densities against time and distance from the point of origin of an osteon. The model was also used to predict the rate at which new bone is added to the remodeling unit. Experimental data on cell densities and the surface area to which new bone is added are consistent with predictions of the model.

INTRODUCTION

One-dimensional mathematical models of the remodelling of cortical bone have been a necessary step toward the development of a three-dimensional model of cell population dynamics in that tissue. Preliminary efforts have yielded some success in getting serial sections of fluorescent or radionuclide labelled undecalcified bone, so it will be possible now to test a 3D bone-cell dynamics model with fluorescent labels in place. Of specific interest in the evaluation of inter-radionuclide effects is the comparison of a surface area labelled with a fluorescent dye which mimics alkaline earths versus an actinide that can be visualized with high resolution--e.g., the low energy, tritium-like ^{241}Pu (E_β = 0.017 keV).

The bone remodeling process in canine cortical bone in the mid-shaft of the humerus is modeled with two forward Kolmogorov equations, which are convection-diffusion type partial differential equations, representing the osteoclast cells and the osteoclast precursor cells (Figure 1), respectively (Hood et al., 1988). The osteoblasts are modeled with an ordinary differential equation.

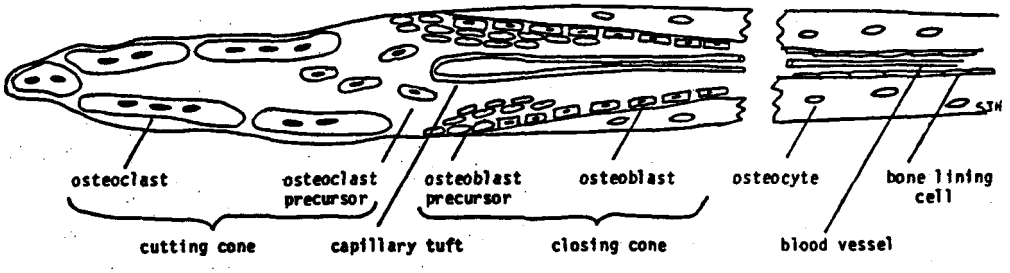

Fig. 1. Schematic diagram of cells in a single haversian canal system.

1 Present address: Thomas J. Watson Research Center, IBM Corp., Yorktown Hts., NY
2 Dept. of Mechanical Engineering, University of California, Davis

The bone remodeling system was studied experimentally by injecting beagles with three different fluorochromes to mark new, calcifying bone (Figure 2). A Videoplan microcomputer was used to measure the histomorphometric parameters that describe the bone remodeling system.

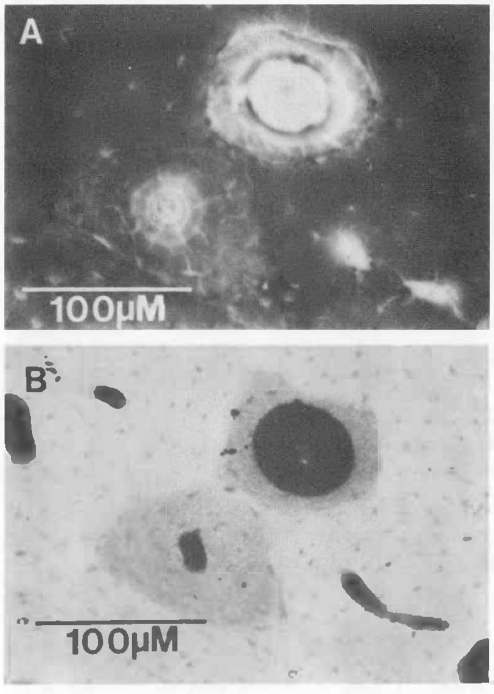

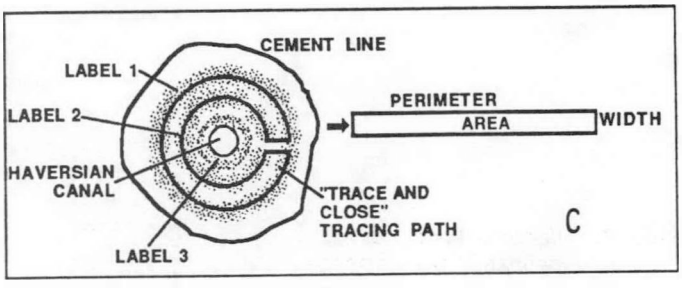

Fig. 2. Haversian canal system labelled with fluorochromes (2A) and a matching radiogram (2B) showing cement-line boundaries, with density variation. In 2C is the schematic for histomorphometrically determining the area formed per unit of time.

The mathematical solutions are in the form of probability densities (Figure 3). This figure plots cell densities (z-axis) at a range of distances from the center of any given osteon (x-axis) over time (y-axis). We interpret the tall, narrow density at time 0.08 days as indicating, first, that there is a high probability of finding an osteoclast cell at points near that position on the osteon radius and, second, that there is a rapidly decreasing probability of finding a cell as one moves away from that point. As time progresses, the probability of finding a cell at any one point decreases and the range in which one might find a cell increases. This change in the shape of the density is a result of the biological variability of the cells; some move faster through the bone than others, some move more slowly, creating a range along the osteon radius in which one might find a cell. Note that as time progresses, the most likely cell position, i.e., the peak of density, moves along the osteon radius away from the center. Since this cell population is resorbing bone, this movement corresponds to the radial enlargement of the osteon cavity.

The steady-state solution to the osteoclast equation can be interpreted as the density function for the maximum radii (cement-line radii) of the bone remodeling units. The predicted values for these radii are consistent with the experimental data (Figure 4). The solution to the osteoblast equation can be interpreted as the density of the fluorescent label sizes. These predicted densities are also consistent with the experimental densities (Figure 5). The solution of the osteoblast equation can also be used to calculate the rate at which new bone is added to the remodeling unit, the apposition rate. Apposition rate can be directly measured and is a function of label diameter (Figure 6).

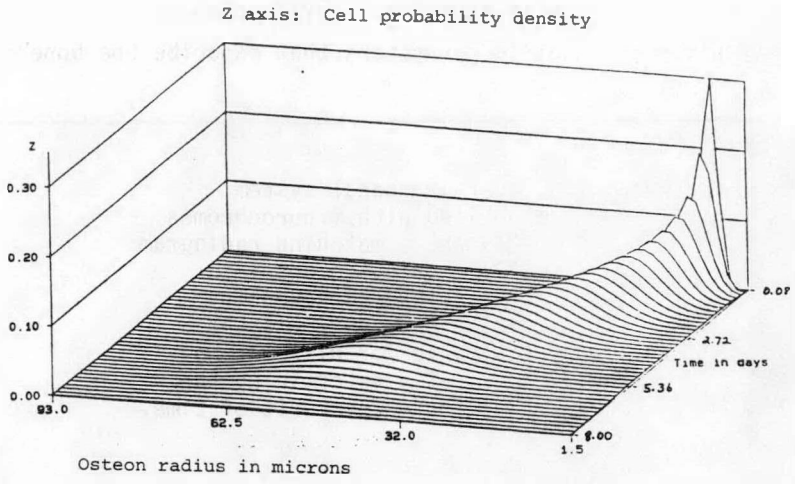

Fig. 3. Osteoclast probability density (= Z axis) in relation to time since initiation of haversian system and to distance from starting point.

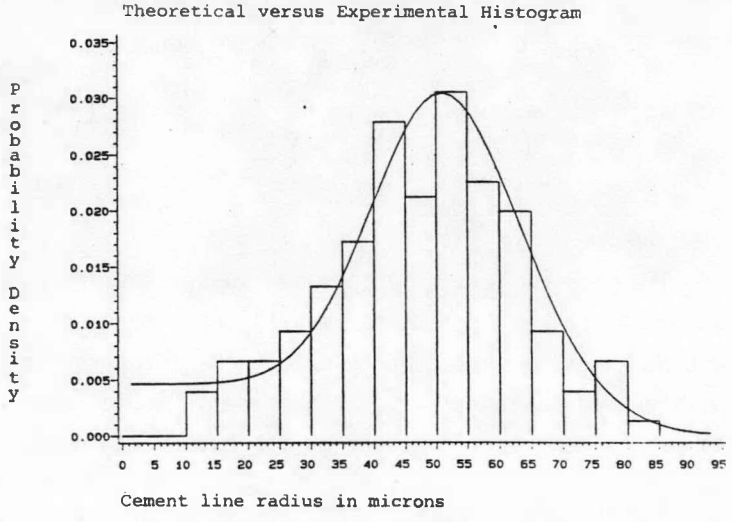

Fig. 4. Cement-line radius probability density. Curve traces theoretical values; histograms are experimental data.

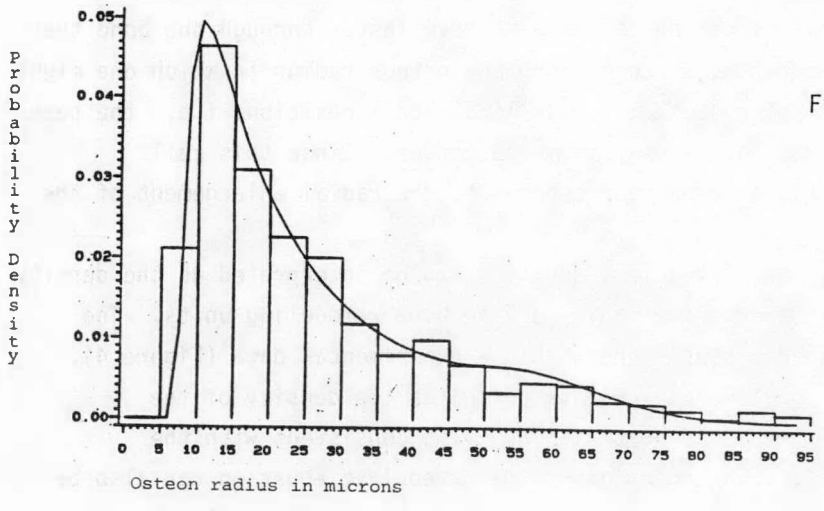

Fig. 5. Osteoblast probability density, expressed without dependence on starting time. Curve is theoretical density; histograms are experimental data.

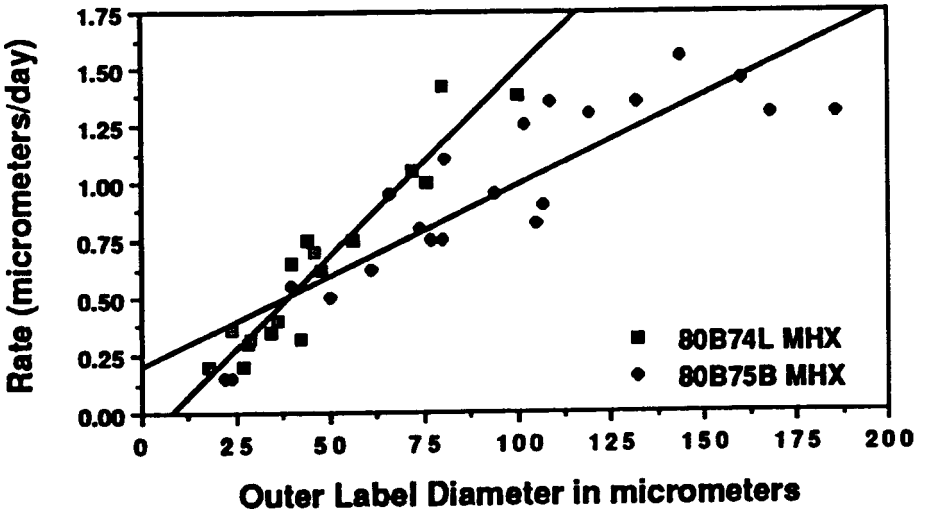

Fig. 6. Apposition rate vs. outer label diameter.

The information gained from serial sectioning and mathematical reconstruction allows us to visualize surface areas near which alkaline earths concentrate as cortical bone is rebuilt from available materials. With serial sectioning, using fluorescent and/or radioactive labels, we can follow what happens in older resting areas and in bone-forming areas of the same haversian system. An example is shown in Figure 7. Figure 7a shows a reconstruction of a single canal, whereas in 7b we see a tracing of the cement lines which formed the original outer limits of that same haversian system. Although the system shown is typically complex, the calculation of the ratio between cement-line and canal volumes is straightforward. If the two perimeter tracings were fluorescent dyes spaced at known intervals, the volume of apposition per unit time could readily be calculated. Calculations of surface areas from the serial perimeter tracings that make up the data files are also straightforward.

Fig. 7. Three-dimensional reconstruction of haversian canal system (7A) and of surrounding cement line (7B) for the same system; proximal shaft of gerbil femur.

REFERENCE

Hood, S.J., N.J. Parks, L.A. Morrin, J. Brewer. 1988. Studies in cortical bone in the Beagle: Histomorphometric analysis and mathematical model of remodeling kinetics in the humeri of young adults. Working paper, available from N. J. Parks, LEHR.

CELLULAR AND MOLECULAR STUDIES

MOLECULAR STUDIES ON RNA METABOLISM DURING MYELOID LEUKEMIC CELL DIFFERENTIATION

D. K. Getman
T. G. Kawakami

The onset of the leukemic state results from the disruption of complex regulatory mechanisms which govern hematopoietic cell growth and development. Myeloid leukemias are thought to be representative of neoplastic growth in general in that there is a loss of normal development of cells from stem cell precursors to mature descendants. Important avenues of investigation therefore concern the intracellular molecular traffic involved in proliferation and differentiation of hematopoietic cells. A wide variety of drugs induce differentiation in the HL60 cell line, including compounds which interfere with ribonucleic acid (RNA) metabolism. We have hypothesized that drug-induced differentiation in myeloid leukemic cells may be mediated through alteration of small nuclear RNAs (snRNAs). SnRNAs are short chain, highly abundant RNA molecules which control the processing of mRNA transcripts by providing the precise alignment required for intron removal and exon splicing in pre-mRNA. Alternative processing of some mRNA transcripts can produce from a single gene a range of protein products which are structurally and functionally different. SnRNAs may provide the mechanism by which the cell is able to selectively produce one final mRNA/protein product over other possible products. These particles thus would play a crucial role in controlling the pattern of gene expression during cellular events, such as differentiation. The data presented indicate that differentiation-inducing phorbol esters alter small nuclear RNA levels in HL60 myeloid leukemic cells, and that this alteration is an early event in leukemic cell differentiation.

INTRODUCTION

The onset of the leukemic state results from the disruption of complex regulatory mechanisms which govern hematopoietic cell growth and development. Radiation-induced leukemias are believed to mimic spontaneous disease in that there is a loss of coordination between cell proliferation and the maturation process.

Previous work has shown that radiation-induced myeloid leukemias have suppressed DNA synthesis and that this suppression is caused by proteins secreted into the culture medium (Kawakami et al., 1986). HPLC fractionation of culture supernatants demonstrated that both DNA inhibitory and DNA stimulatory factors are produced by these cells. Thus it appears that the failure of myeloid-lineage cells to fully differentiate in this model system is in part a result of the interaction of a number of humoral factors on the economy of the cell.

However, a complete understanding of leukemogenesis, both spontaneous and radiation-induced, cannot be attained until the growth factor-responsive subcellular events which control cell proliferation and differentiation are fully elucidated. The important avenues of investigation therefore concern the molecular traffic involved in proliferation and differentiation of hematopoietic cells.

To assess these molecular events, we have used a model system of human myeloid leukemia cells that are induced to differentiate to monocyte/macrophage cells by various

pharmacological agents. The human promyelocytic leukemia cell line HL60 was used in these studies for two reasons: First, this cell line is well characterized cytologically and biochemically, so that baseline information is available for reference; second, there is a large body of experimental data published concerning this cell line which details the effects of a wide variety of pharmacological agents on induction of differentiation in vitro. An understanding of the molecular events involved in differentiation in this human cell line can then be used to examine differentiation and maturation arrest in newly established canine myeloid leukemia cell lines.

It was hypothesized that drug-induced differentiation in myeloid leukemic cells may involve alteration of some RNA species which is involved in the differentiation process. We chose therefore to study the effect of these compounds on the expression of small nuclear RNAs (snRNAs).

SnRNAs are short chain, highly abundant RNA molecules which are complexed in the cell with a variety of proteins to form small nuclear ribonucleoproteins (snRNPs). Ten species of snRNA are known to date and are referred to as U1-U10 due to their high uridine content. There is mounting evidence that snRNPs control the processing of mRNA transcripts via their actions in RNA splicing, RNA polyadenylation, and nucleo-cytoplasmic transport of mRNA transcripts. Evidence suggests that snRNPs provide the precise alignment required for the removal of intron sequences in the RNA, followed by splicing of the exon segments together.

The excision of "non-coding" intron sequences from mRNA has been suggested as a possible site at which the regulation of gene expression occurs. This hypothesis is tenable in light of the fact that a single mRNA transcript can have a variable number of intron sequences removed, producing a range of protein products from a single gene, which are structurally and, presumably, functionally different. SnRNPs may provide the mechanism by which the cell is able to selectively produce one final mRNA/protein product over other possible products. These particles thus would play a crucial role in controlling the pattern of gene expression during cellular events such as differentiation.

RESULTS

The phorbol ester TPA (tetradecanoyl phorbol-13-acetate) was used to provide a reproducible means of inducing differentiation in HL60 cell lines. TPA is but one of a series of diterpene ester irritants found in the seeds of Croton tiglium, a shrub indigenous to India and Sri Lanka. Possessing striking carcinogenic activity, TPA was first used by Berenblum and Mottram to demonstrate the two-stage carcinogenesis model in mice, in which it functions as a promotor. More recently, TPA has been shown to activate protein kinase C and to induce leukemic cells of the myeloid lineage to differentiate to macrophages.

Figure 1 demonstrates the induction of small nuclear RNA expression which occurs with TPA treatment. HL60 cells were pulsed for one hour with the phorbol ester, after which the cells were suspended in fresh medium for an additional hour. Total cellular RNA from these cells was then isolated and analyzed by polyacrylamide gel electrophoresis and Northern blot hybridization. The blot was hybridized with a ^{32}P-labeled antisense RNA

probe containing the U6 snRNA gene, after which the blot was quantitated by an Ambis gel scanner and visualized by autoradiography. The increase in U6 snRNA levels by TPA treatment shows a clear dose response, with a plateau in the response seen at $1X10^{-7}M$. The same blot was stripped of hybridized probe and reprobed with a labeled-cDNA coding for 5s ribosomal RNA. The levels of this small RNA did not vary by more than 10%, indicating that the induction of U6 small nuclear RNA by TPA is a selective effect of this agent and not a result of a generalized increase in RNA synthesis in the cell.

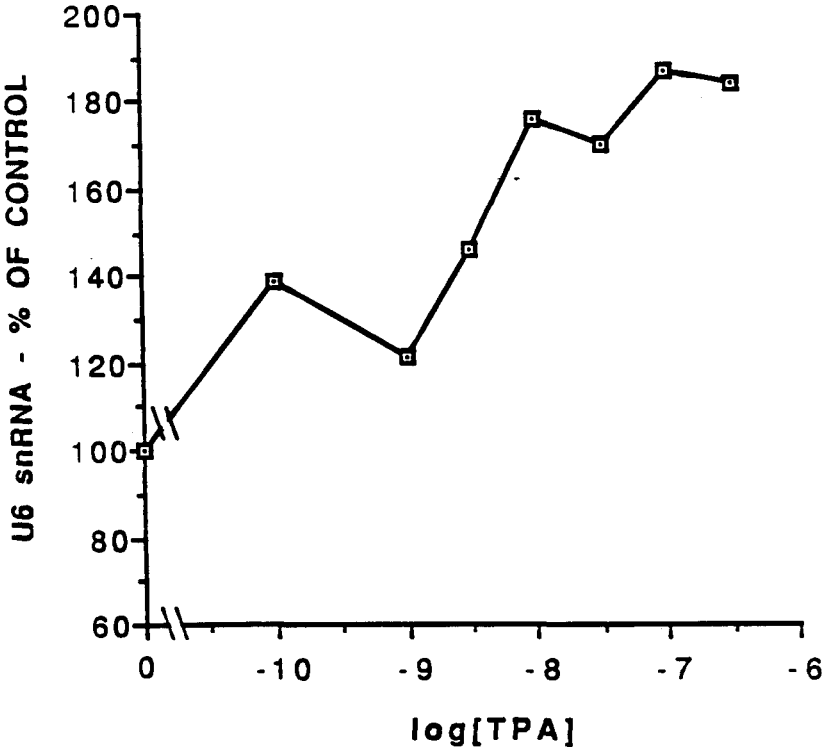

Fig. 1. Dose response of TPA at early time point in HL60L. HL60L cells were pulsed for 1h with TPA. SnRNA induction was determined in cells harvested 1h after drug removal. Points represent a single experiment shown in the autoradiographed film below.

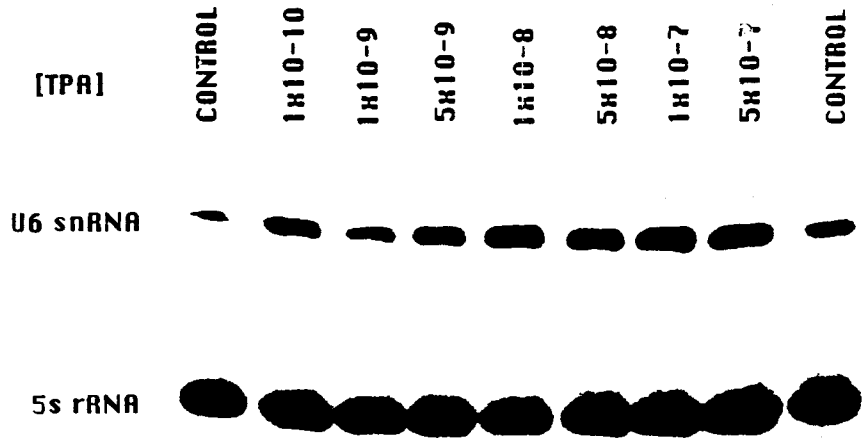

The proportion of the cell population which matured into the macrophage phenotype was also dose-dependent with TPA treatment (Figure 2). A comparison of the dose response curves for TPA-induced maturation and snRNA induction illustrates the similarity in the slopes of the curves for these two endpoints (Figure 3). The parallel relationship of the slopes suggests a similarity in mechanism of action for TPA in initiating cell maturation and snRNA expression. Since protein kinase C is believed to be the cellular receptor for phorbol esters, this provides the first indication that the expression of small-nuclear RNA molecules, and hence nuclear processing of pre-mRNA transcripts, can be influenced by intercellular messengers.

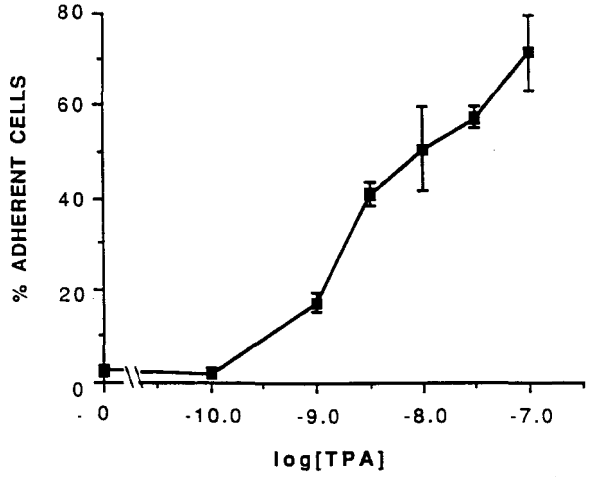

Fig. 2. TPA induces adherent macrophage morphology in HL60 cells. HL60L cells were pulsed for 1h with 1x 10^{-8}M TPA. Adherence determined after 24h as described in Methods. Each point represents mean ± S.D. of 3 separate determinations.

Fig. 3. Comparison of dose response curves of TPA-induced cell adherence and snRNA induction. HL60L Cells were pulsed for 1h with TPA for each experiment. Data are derived from Figures 1 and 2. Linear regression correlation coefficients are displayed for each curve.

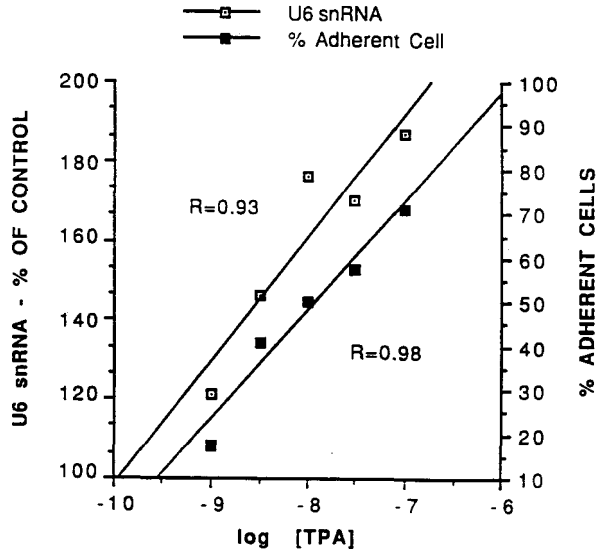

Phorbol esters are known to stimulate the phosphorylation of at least 14 different proteins via the activation of protein kinase C. This suggests that these agents influence cell metabolism by several different pathways. Thus it is of interest that 48 hours after TPA addition, snRNA levels are induced at low doses and are decreased in a dose-dependent fashion at higher doses (Figure 4). These data indicate that the expression of snRNAs may be regulated by both positively and negatively acting factors. Figure 4 also shows that the biologically inactive phorbol-13-acetate has no effect on snRNA expression.

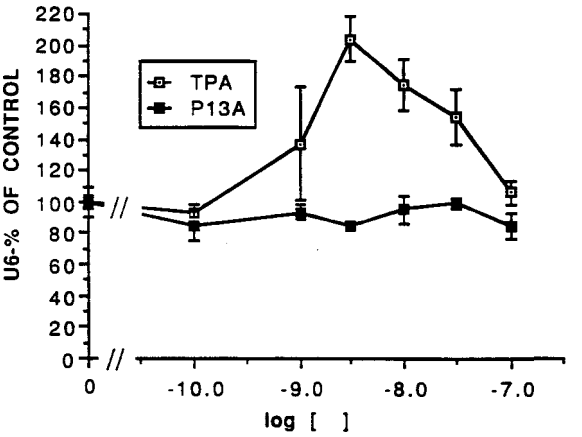

Fig. 4. Dose response of TPA and phorbol-13-acetate in HL60L. Cells were harvested at 48 h after 1 h pulse of each drug. Note that P13A is a biologically inactive phorbol ester. Points represent mean (± S.D.) of 3 separate determinations.

The TPA-induced increase in snRNA levels in HL60 cells is an early event in differentiation of the cells to the moncyte/macrophage phenotype. The time course of accumulation of snRNA transcripts shown in Figure 5 reveals a significant increase of U6 levels 30 minutes after the removal of TPA from the cell culture. This rapid response is comparable to the increase of other TPA-responsive elements in myeloid cells, including the fos and myc proto-oncogenes.

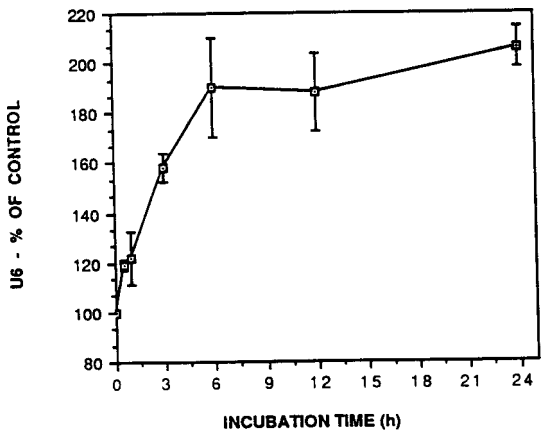

Fig. 5. Time course of 5 nM TPA induction of U6 snRNA.

Not all snRNAs respond to TPA in a similar manner. Figure 6 indicates that U1, U4 and U6 snRna levels are all increased by a 1h TPA dose of 5 nM. U3 levels did not change significantly from the control with this treatment. This difference in response to TPA between individual species of snRNA may be a function of the promoter sequences which control snRNA transcription, which in turn may reflect different functional rates for the various RNA molecules. U1, U3 and U4 snRNAs are transcribed by RNA polymerase II, while U6 is transcribed by RNA polymerase III. However, U3 snRNA is involved in ribosomal RNA processing, while U1, U3 and U4 function in the maturation of messenger RNA. The lack of induction of U3 snRNA with TPA may be a reflection of this different functional role. U1, U4 and U6 are transcribed by RNA polymerase II, while U3 is transcribed by RNA polymerase III. Small nuclear RNA gene expression may therefore be induced by TPA in a manner similar to other phorbol ester-inducible genes, in that TPA-regulated transcriptional regulatory proteins bind to specific upstream promoter and enhancer sequences to initiate RNA transcription of a particular gene. The fact that TPA induction of snRNA genes appears to be snRNA species specific would support this notion.

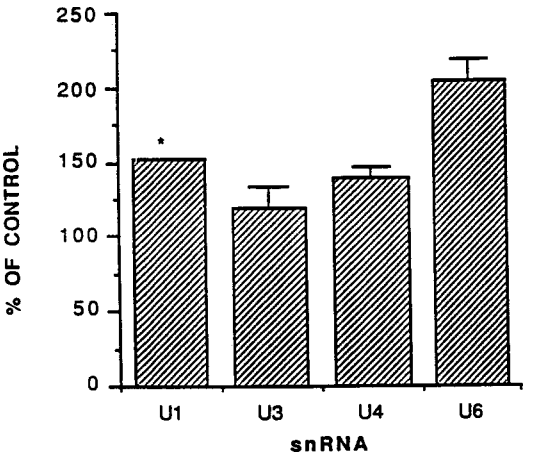

Fig. 6. Effect of TPA on different species of small nuclear RNAs. HL60L cells were pulsed for 1h with 5 nM TPA, and cells harvested 48h after drug removal. Note that U3 snRNA is not significantly different than control. Error bars represent S.D. of three separate determinations. U1 (*) represents only one experiment.

CONCLUSIONS

Thus it appears that the expression of snRNAs in differentiating HL60 myeloid leukemia cells follows a complex pattern. Cells harvested at early time points after TPA treatment show a dose-dependent induction of selected snRNA genes, while cells harvested at later time points exhibit both induction and inhibition of snRNA levels. Induction of snRNA levels by TPA in differentiating leukemic cells is also an early event in myeloid cell differentiation, occurring within one hour of addition of the drug and preceding by six to eight hours the onset of the mature macrophage phenotype.

This preliminary work therefore indicates that snRNAs may be involved in triggering the maturation process. Current efforts are directed at exploring in greater detail the temporal aspects of snRNA induction during human myeloid cell differentiation, and in relating these findings to differentiation in radiation-induced canine myeloid leukemias. It is hoped that these studies will provide some insight into the molecular control mechanisms involved in normal hematopoiesis and hence in leukemogenesis as well.

REFERENCES

Kawakami, T., G. Cain, N. Taylor, and B. Foster. 1986. In Laboratory for Energy-Related Health Research, 1985 Annual Report, UCD 472-131, pp. 52-63.

TRANSITIONAL CELL CARCINOMA IN THE LABORATORY BEAGLE

R. Culbertson
W. L. Spangler
G. R. Cain
L. S. Rosenblatt

The lifetime study of ^{226}Ra and ^{90}Sr toxicity in beagles conducted at LEHR provides a set of clinical and pathological records which are useful for the analysis of a wide range of disorders, some of which can be related to the radiation exposure, some not. We report here on an analysis of 45 cases of transitional cell carcinoma, which is a malignant neoplasm arising from the epithelium lining the urinary system. That system is considered in this study to extend from the renal pelvis to the tip of the urethra. Statistical study shows no evidence of radiation effects in this disease. Transitional cell carcinoma was fatal in 38% of the cases reported here. No clinical signs were observed in 62% of the beagles bearing this disease, which was considered to be incidental at the time of death in these cases. Neoplasms in the renal pelvis, in the trigone of the bladder plus the urethra, and in the urethra alone were found to be most serious, frequently being associated with high metastatic rates and/or resulting in fatal urinary obstruction. Both of the latter rates were above 52%. Metastasis was observed in only 32-35% of the full set of cases of transitional cell carcinoma. No sex predisposition or litter effect was observed.

INTRODUCTION

Transitional cell carcinoma is a malignant epithelial neoplasm arising from the mucosa of the urethra, urinary bladder, ureter, or renal pelvis. Previous reports document the occurrence of this neoplasm in the general canine population (Osborne et al., 1968a, 1968b; Hayes, 1976; Hayes and Fraumeni, 1977). This neoplasm frequently causes death by urinary tract obstruction, by invasive growth into adjacent tissues, and by eventual metastasis. The present report details the occurrence, clinical signs, and biological behavior of transitional cell carcinoma in a colony of experimental beagles.

MATERIALS AND METHODS

We report here on the cases of transitional cell carcinoma which were recorded in periodic clinical and radiological examinations, and in various clinical analyses that were made as part of the life-time study of chronic exposure to ^{90}Sr or ^{226}Ra that has been conducted at LEHR. In that study, animals were exposed to various dosages of the radionuclides with differing routes of administration. The last dog died in February 1986. The details of that study have been the subjects of previous publications (Raabe et al., 1981; Goldman et al., 1986). Statistical analysis of the transitional cell carcinoma data among treatment groups revealed no radiation effect, and for the purposes of this report, the animals were therefore considered as one group, regardless of experimental treatment.

RESULTS

Prevalence: Transitional cell carcinoma was documented in 45/850 (5.3%) experimental beagles. The prevalence in males was 25/425 (5.9%) and in females was 20/425 (4.7%).

Transitional cell carcinoma accounted for 45/3418 (1.3%) total neoplasms, 45/932 (4.8%) total malignant neoplasms, and 45/1800 (2.5%) total epithelial neoplasms. The incidences of transitional cell carcinoma by specific anatomical site are presented in Table 1.

Table 1. PREVALENCE, METASTATIC RATE, AND MORTALITY OF TRANSITIONAL CELL CARCINOMA BY PRIMARY SITE.

Primary Site	Male Beagles	Female Beagles
PREVALENCE		
bladder apex	1 (4.0%)	2 (10.0%)
bladder fundus	3 (12.0%)	2 (10.0%)
bladder trigone	1 (4.0%)	4 (20.0%)
bladder not otherwise specified	6 (24.0%)	5 (25.0%)
trigone and urethra	4 (16.0%)	1 (5.0%)
urethra	8 (32.0%)	4 (20.0%)
renal pelvis	1 (4.0%)	2 (10.0%)
ureter	1 (4.0%)	0 (0.0%)
TOTAL TRANSITIONAL CELL CARCINOMAS	25 (100.0%)	20 (100.0%)
METASTATIC RATE		
bladder apex	0/1	0/2
bladder fundus	1/3 (33.3%)	1/2 (50.0%)
bladder trigone	0/1	0/4
bladder not otherwise specified	0/6	1/5 (20.0%)
trigone and urethra	2/4 (50.0%)	1/1 (100.0%)
urethra	5/8 (62.5%)	2/4 (50.0%)
renal pelvis	0/1	2/2 (100.0%)
ureter	0/1	0/1
TOTAL METASTATIC RATE	8/25 (32.0%)	7/20 (35.0%)
MORTALITY		
bladder apex	0/1	0/2
bladder fundus	0/3	1/2 (50.0%)
bladder trigone	0/1	0/4
bladder not otherwise specified	0/6	1/5 (20.0%)
trigone and urethra	4/4 (100.0%)	2/2 (100.0%)
urethra	5/8 (62.5%)	2/5 (40.0%)
renal pelvis	0/1	2/2 (100.0%)
ureter	0/1	
TOTAL MORTALITY	9/25 (36.0%)	8/20 (40.0%)

n/n = observed/number at risk.

Age at Death: Animals dying of transitional cell carcinoma ranged in age from 8.3 years to 15.2 years, with a mean age at death of 12.7 years. The mean age at death for control animals in all of the experiments was 14.6 years. The mean age of males dying from the neoplasm was 12.9 years and of females was 12.5 years. The mean age at death for two dogs with transitional cell carcinoma of the renal pelvis was 8.8 years. Mean age at death for other locations fell within the range 12.2 years 15.2.

Metastasis of Primary Transitional Cell Carcinoma: Transitional cell carcinoma metastasized in 8/25 (32.0%) males and 7/20 (35.0%) females, for a sex-combined metastatic rate of 15/45 (33.3%). The metastatic rates by anatomic locations of the primary neoplasm are presented in Table 1. Metastatic lesions were detected in a variety of distant tissues, including regional lymph nodes, kidney, lung, bronchial lymph nodes, adrenal gland, colon, liver, coccygeal vertebrae, brain, heart, ovary, uterus, pancreas, spleen, and mammary gland. More widely disseminated metastatic lesions were found in females than in males.

Mortality: Transitional cell carcinoma accounted for 17/544 (3.1%) of all deaths resulting from neoplasia and was fatal in 17/45 (38.0%) beagles developing the neoplasm. The mortality rate for dogs with these neoplasms was 9/25 (36.0%) and 8/20 (40.0%) in males and females, respectively. Urinary obstruction resulted in death in 9/17 (52.9%) beagles (6/9 males and 3/8 females) dying from the neoplasm. Invasive growth and metastasis resulted in death in 8/17 (47.1%) beagles (3/9 males and 5/8 females) dying from the neoplasm. Mortality by site of the primary neoplasm is presented in Table 2.

Table 2. CAUSE OF DEATH BY PRIMARY SITE OF FATAL TRANSITIONAL CELL CARCINOMA

Site of Primary Neoplasm/Cause of Death	Male Beagles	Female Beagles
Bladder Fundus		
Metastasis	0	1/2
Bladder Not Otherwise Specified		
Metastasis	0	1/4
Trigone and Urethra		
Invasive Growth	1/4	
Invasive Growth and Metastasis	1/4	
Urinary Obstruction	2/4	2/2
Urethra		
Invasive Growth and Metastasis	1/5	1/2
Obstruction	4/5	1/2
Renal Pelvis		
Metastasis	0	2/2

n/n = specific cause of death/total mortality from transitional cell carcinoma in that part of the urinary system.

Prevalence of Transitional Cell Carcinoma by Litter: The 45 documented cases reflected transitional cell carcinoma occurring in 43 litters of beagles. Two cases of transitional cell carcinoma were noted in each of two litters. No statistically significant litter effect was observed.

Other observations: Hyperplastic lesions and neoplasms of the urinary system other than transitional cell carcinoma were found in a wide range of locations, with 41 being recorded in the kidney, 32 in the urinary bladder, 8 in the urethra and 3 in the ureter.

DISCUSSION

Transitional cell carcinoma accounted for only 1.3% of all neoplasms in the laboratory beagle, but was fatal in 38% of cases. Those neoplasms arising in the renal pelvis, those involving the trigone and urethra, and those involving the urethra alone resulted in the highest metastatic rates, the highest mortality rates, and the lowest mean ages at death. Most notably, neoplasms in the renal pelvis metastasized and killed both of the two female beagles that were so affected. Urethral neoplasms killed high percentages also, with the metastatic rate being 52.3% and mortality 68.4% (sexes combined). Those neoplasms also resulted in fatal urinary obstruction in 52.9% the cases.

Among the factors that may account for the severity of transitional cell carcinoma involving the trigone and urethra are: (1) The accessibility to major lymphatic channels (true also in the renal pelvis); (2) the relative compactness of anatomic structures in the pelvic inlet, creating opportunities for invasive growth; (3) the high likelihood of partial or complete urinary obstruction there; (4) the difficulty of surgical extirpation.

Although transitional cell carcinoma was often fatal in the beagles, clinical signs were absent, were seen as a terminal feature, or were non-specific. The difficulties in definitive diagnosis of urinary bladder neoplasms have been previously reported (Osborne et al., 1968a). No clinical signs were observed in 62% of the beagles bearing transitional cell carcinoma and the neoplasm was considered to be incidental at the time of death. Hematuria may be seen with transitional cell carcinoma, but this clinical finding may be complicated or obscured by concurrent prostatitis or cystitis. Urinary obstruction was the most consistent clinical sign in the beagles but was not evident until the neoplasm had reached sufficient size to result in at least partial obstruction of the neck of the bladder or urethra. Urinary obstruction resulting from transitional cell carcinoma was typically a terminal sign, since the neoplasms at this stage were considered to be inoperable and thus the animals were euthanized.

The duration of transitional cell carcinoma is particularly hard to determine because clinical signs are often absent or non-specific. Records exist of beagles with transitional cell carcinoma of the bladder surviving for three and six months (e.g., Anderson, 1963). We have records of the detected disease process varying in the male beagle from one day to 440 days and in the female beagle from 32 days to 55 days. Simple hematuria was associated with longer and urinary obstruction with shorter survival. No sex predisposition was noted in the prevalence of transitional cell carcinoma in the present study, nor was a statistically significant litter effect observed.

The mean age at death of fatal transitional cell carcinoma in the laboratory beagle in the present study was 12.7 years (range 8.3 years to 15.2 years), contrasting with 9.1 years in other work. The mean age at death was shortest with renal pelvic involvement (8.8 years) in the female beagle. In male beagles, involvement of both the trigone and the urethra resulted in a lower mean age at death (12.2 years) than involvement of urethra alone (13.4 years). In the female beagle, however, the mean age at death was similar for cases involving trigone plus urethra and for urethra alone (approximately 13.1 years). Those females dying of transitional cell carcinoma of the fundus or of the bladder, not otherwise specified, lived longer (14.9 years and 15.2 years, respectively).

In summary, transitional cell carcinoma is a neoplasm which always warrants a guarded to poor prognosis since urinary obstruction, invasive growth, and/or metastasis are frequent sequelae resulting in death. The clinical problem is typically compounded by the lack of specific clinical signs, by the often inaccessible location and by the inherent aggressiveness of the neoplasm. The location of the primary neoplasm may provide some insight as to the potential clinical and pathological significance of the condition.

REFERENCES

Anderson, A. C. 1963. Carcinoma of the bladder in a beagle. J. Am. Vet. Med. Assoc. 143:30-33.

Goldman, M., L. S. Rosenblatt, and S. A. Book. 1986. Lifetime radiation effects research in animals: An overview of the status and philosophy of studies at UC Davis' Laboratory for Energy-related Health Research. In R. C. Thompson and J. A. Mahaffey (eds.), Lifespan Radiation Effects Studies in Animals: What Can They Tell Us?, Proceedings of the 22nd Hanford Life Sciences Symposium, CONF-830951, pp. 53-65, NTIS, Springfield, VA.

Hayes, H. M., Jr. 1976. Canine bladder cancer: epidemiological features. Am. J. Epidemiol. 104:673-677.

Hayes, H. M., Jr. and J. F. Fraumeni, Jr. 1977. Epidemiological features of canine renal neoplasms. Cancer Res. 37:2553-2556.

Osborne, C. A., D. G. Low, and V. Perman. 1968a. Neoplasms of the canine and feline urinary bladder: Clinical findings, diagnosis, and treatment. J. Am. Vet. Med. Assoc. 152:247-259.

Osborne C. A., D. G. Low, V. Perman, et al. 1968b. Neoplasms of the canine and feline urinary bladder: incidence, etiological factors, occurrence, and pathologic features. Am. J. Vet. Res. 29:2041-2055

Raabe, O. G., S. A. Book, and N. J. Parks. 1981. Lifetime studies of ^{226}Ra and ^{90}Sr toxicity in beagles--a status report. Rad. Res. 86:515-528.

NUCLEAR MEDICAL STUDIES

COORDINATION CHEMISTRY OF THE ^{212}Pb-^{212}Bi NUCLEAR TRANSFORMATION: ALPHA-EMITTING RADIOPHARMACEUTICALS

N. J. Parks
W. R. Harris[1]
C. L. Keen[2]
S. R. Cooper[3]
S. Zidenberg-Cherr[2]
K. W. Musker[4]
P. K. Bharadwaj[5]
P. D. Schneider[6]

This project is directed at finding a way to overcome the problem of the short half-life of ^{212}Bi ($t_{1/2}$ = 1.01 h) in order that it might be used on an organic molecule as a radiopharmaceutical. A solution could be to attach its precursor, ^{212}Pb ($t_{1/2}$ = 10.6 h) to the molecule, but the problem then becomes one of finding an organic ligand that can survive the ^{212}Pb-^{212}Bi transition. Dithioethers and thiolate ligands are being examined as potentially most promising, since some of them bind strongly to both metals discriminately against possible competitors. A source of ^{212}Pb has been developed and is now automated, and ion exchange columns are being employed to assure that products are as close to the no-carrier-added state as is possible. This system also produces quantities of three bismuth radionuclides that have proven value as tracers in (1) determining binding properties of ligands and (2) following movements in the body of ligand-bound Pb and Bi. Studies of those movements show bismuth to collect primarily in kidney tissue, where significant quantities were found in the nucleus and mitochondria. In vivo and in vitro studies with labelled liposomes provide evidence that alpha particles from the ^{212}Pb/^{212}Bi transition can be effective in killing melanoma cells.

INTRODUCTION

Alpha-emitting bismuth-212 ($t_{1/2}$ = 1 h) has potential as a radiopharmaceutic agent. Its in vivo use is limited because the time required to reach the target across the vascular barrier may be longer than desirable within the constraints of this half life. Our intent is to create chemically an alpha-emitting moiety that has an effective half life of approximately 11 hours by developing coordination complexes of the ^{212}Pb ($t_{1/2}$ = 10.6 h) parent of ^{212}Bi. This moiety would need to be designed to retain the daughter bismuth radionuclide after its nuclear transformation by beta decay. Although this decay has an energy that does not, on average, lead to recoil of the ^{212}Bi daughter out of the parent complex, the high positive charge on the daughter (associated with the emission of Auger electrons and electron shake-off) can be as high as 10 to 11 in the first few attoseconds (10^{-18}) after decay. This leads to charge redistribution in a time frame of about 10-15 seconds, which is short compared to the typical bond vibration period of 10-12 seconds. This project is aimed at developing and testing the efficacy of electron-rich coordination complexes that can withstand the charge redistribution process and retain the ^{212}Bi daughter.

1 Department of Chemistry, University of Missouri
2 Department of Nutrition, University of California, Davis
3 Inorganic Chemistry Laboratory, The University at Oxford, UK
4 Department of Chemistry, UCD
5 LEHR and Department of Chemistry, UCD
6 Department of Surgery, Medical School, UCD

Other aspects of the project are: 1) Experiments to determine which organs and tissues these forms of bismuth are deposited in and 2) studies to determine precisely where the ^{212}Bi may end up within the cells. Organ location is significant in terms of putting the radiopharmaceutical adjacent to tumors as well as determining potential radiotoxic effects on various organs and tissues if the ^{212}Bi is not effectively chelated and goes to non-target sites. Information on location inside cells is important in anticipating effects of both the recoil atoms and the alpha particle on key chemical constituents of the cell and its nucleus.

Bismuth radionuclides show promise, also, as tracers, particularly in studies of the binding properties of possible carriers and of the movement and localization of this element in the body. Both of these types of tracer studies are essential preliminaries to the development of radiotherapeutic applications. Two such isotopes are ^{205}Bi (15.31 d) and ^{206}Bi (6.24 d).

The study has been organized to address five problems that grow out of these concerns:

(1) Finding a way to produce no-carrier-added (NCA) ^{212}Pb, which is the precursor to ^{212}Bi. An important aspect of this work is the development of sources of the bismuth radiotracers with half lives longer than 1 h.

(2) Designing, synthesizing, and characterizing chelating agents which will retain both ^{212}Pb and ^{212}Bi under physiological conditions and permit attachment to an antibody or a specific ligand.

(3) Evaluating intramolecular chemical effects of the nuclear transformation, which is to say, possible damage to the ligand from the transition of ^{212}Pb to ^{212}Bi. In this case, the work has had to start with the development of new experimental techniques.

(4) Finding where bismuth goes in the body and determining how it is bound to proteins so that binding constants of synthetic chelating agents can be selected to match.

(5) Screening new ligands for Pb-Bi administration, using bismuth binding constants measured in the other work.

Since it was initiated in 1985 this project has attracted some very capable people, working in a wide variety of fields, and we are already able to report considerable progress, primarily in radioengineering and organic chemistry.

RADIOCHEMICAL ENGINEERING

The collaboration with the Crocker Nuclear Laboratory at UCD has given us the ability not only to produce the needed ^{203}Pb from natural lead but also to produce $^{205,206}Bi$ in sufficient quantities that these radionuclides can be used as tracers in continuing biological and chemical studies (Lagunas-Solar et al., 1987). Automated methods that reduce both personnel exposure and the number of radiochemists required have since been

developed. ^{203}Pb and the various bismuth radionuclides, which are readily detectable gamma-emitters, have become the mainstay of the experiments with chemical and biological kinetics of (NCA) Bi under physiological conditions.

A ^{228}Th-based generator system for ^{212}Pb and ^{212}Bi has been developed. In this system, precipitated ^{228}Th colloids are supported in filter assemblies through which carrier gases transport ^{220}Rn to liquid nitrogen traps constructed from Teflon™. The ^{220}Rn serves as the source of ^{212}Pb and ^{212}Bi in this system.

ORGANIC CHEMISTRY

Early efforts have focussed on the search for ligands that would (1) bind strongly to both Pb and Bi in aqueous media and in a wide range of pH's and (2) bind those metals discriminately against transition metals. Two groups which showed promise in these respects were the dithio ethers and the trisuccinyl-substituted compounds. The latter group proved not only to be difficult to synthesize but had troublesome general physical properties as well.

Work on alternative groups began with the synthesis of two new classes of thioethers, designated 24S6 and L. Thioethers have a high affinity for lead and show promise of surviving the nuclear transformation from lead to bismuth. Spectroscopic structural analysis of their bonding with transition metals--particularly nickel (II), about which much is already known--permitted us to determine that lead atoms would not fit into the cavity as well as theory suggested. Experiments which showed a low affinity of these ligands for the Pb(II) ion confirmed this prediction. Study of a wide range of thioether complexes indicates that stability constants for Pb(II) decrease with increasing positive charge on the complex. This has led us to design new chelating agents for Pb(II), based upon incorporation of three anionic thiolate groups as well as three neutral binding groups (amines or thioethers). In fact we are opening up the crown to allow the metal to be complexed. The next step has been to close the molecular structure somewhat in an effort to gain the high stability needed for survival in physiological fluids.

The next generation of ligands combines thiolate-based donor groups, with their high affinity for metal ions such as Pb(II), with complexes that will have sufficient steric encumbrance to shut down oligomer formation. Formation of oligomers is promoted by the tendency of thiolate ligands to bridge two metal ions. Again, Ni(II) coordination chemistry is providing the benchmark for understanding the properties of these compounds as potential chelators of Pb and Bi. Bharadwaj, Arbuckle and Musker report in this publication on some unusual characteristics of a representative of a similar group, a dithiocarbamate, which has also been considered for use as a ligand.

CHEMICAL EFFECTS OF NUCLEAR TRANSFORMATION

First steps have been taken in the development of new methods for studying the effects on the coordination complex of the decay of ^{212}Pb to ^{212}Bi. Quantities of the metals are 10 orders of magnitude lower than those which are typically seen in macroscopic studies, so we have adapted methods from research on chemical effects of nuclear

transformations (CENT) and "hot atom chemistry." One special problem has been that our NCA materials react with the stainless steel, glass, and titanium components of the available radio-high performance liquid chromatography (HPLC) equipment. The separation of inorganic ions and coordination complexes through electrophoresis can, in principle, provide a solution to the problem, but we have found the process too slow to meet our general needs. Radioscanners are being developed now to provide greater speed. Another option for eliminating these reactions is to construct the radio-HPLC system entirely from fluorocarbon polymer. Progress continues toward that end.

CELLULAR RADIOBIOLOGY OF ALPHA PARTICLES

In vitro and in vivo melanoma models are being used to relate alpha energy deposition from intracellular ^{212}Pb-^{212}Bi to response distribution (Hill et al., 1986). Liposomes that have been labelled with radiotracers and with fluorescent dyes are being used in cell culture systems to carry the ^{212}Pb-^{212}Bi into the cell. An early phase of the in vivo work is described below (Hill et al., this report). One aspect of the in vitro work has developed into a study of the effectiveness of intracellular radiation, in cell culture, for killing melanoma cells. This radiobiology work provides the benchmark against which the efficacy of radiotherapeutic alpha emitter molecules will be tested.

DISTRIBUTION OF BISMUTH IN THE BODY

The whole-body clearance, organ distribution, and subcellular distribution of no-carrier-added and carrier-added intraperitoneally administered bismuth radio tracer (^{205}Bi-^{206}Bi) has been determined in Sprague-Dawley rats. Clearance rate kinetics are being determined using several chemical forms of the tracer (Zidenberg-Cherr et al., 1987, and below in the present report). That work has provided definitive evidence that bismuth does indeed enter subcellular organelles. Specifically, the nucleus and mitochondria had 30-50% and 10-25%, respectively, of activity in kidney tissue in this study. The kidneys were the main sink for radiotracer, with uptake ranging from 20-50% of total body activity. Special attention is being given to association of bismuth there with metallothionein-like proteins, which have been proposed to function in the cellular detoxification of heavy metals.

REFERENCES

Hill, A., P.D. Schneider, K.C. Chelton and N.J. Parks. 1986. Murine model for intracellular therapeutic radiation of melanoma. Surgical Forum 37: 425-427 (Extended Abstract).

Lagunas-Solar, M.C., O.F. Carvacho, L. Nagahara, A. Mishra and N.J. Parks. 1987. Cyclotron production of no-carrier-added ^{206}Bi (6.24 d) and ^{205}Bi (15.3 d) as tracers for biological studies and for the development of alpha-emitting radiotherapeutic agents. Int. J. Radiat. and Appl. Isotopes 38(2): 129-137.

Zidenberg-Cherr, S., N.J. Parks and C.L. Keen. 1987. Tissue and subcellular distribution of bismuth radiotracer in the rat: Considerations of cytotoxicity and microdosimetry for bismuth radiopharmaceuticals. Radiat. Res. 111: 119-129.

LIQUID SCINTILLATION SYSTEMS FOR BETA SPECTROSCOPY: APPLICATIONS IN DOSIMETRY OF ^{90}SR AND ^{90}Y

A. C. Mishra
N. J. Parks

We have demonstrated that commercially available liquid scintillation counters are adequate for obtaining useful information about the variation of beta spectral shapes as a function of attenuation. A gel scintillation system that permitted the approximation of point source geometry worked well. The spectral shapes predicted by the Fermi equations were reasonably matched with experimental spectra of sources with geometry close to a point source. For energies in the range of 50 to 2300 keV, we found sufficient linearity of the energy scale and uniformity of detection limits for the direct output of the instrument to be experimentally useful. The gel scintillation system has been used to directly measure the energy distribution of the beta flux coming out of bone samples and incident on the soft tissue of dogs fed ^{90}Sr–^{90}Y from in utero to 540 days of age.

INTRODUCTION

Estimates of radioactivity content are frequently desired when destructive preparation of the sample is precluded. In this project, variation of energy as a function of attenuation was examined with a conventional liquid scintillation spectrometer, and results are compared with those obtained by other techniques, as reported in the literature. We used glass and aluminum as attenuators, separately and in combination, and we observed spectra from sources arrayed in two ways within a commercially available liquid scintillator gel--first as point sources and second in uniform mixture within the mass of gel.

The results, as reported in Mishra and Parks (1987), confirmed and extended the observations given in the 1984 Annual Report (Parks and Mishra, 1985). New material included (1) added data on attenuation of beta energy from ^{32}P, using our experimental conditions, for comparison with the prior reports; (2) more detailed comparison (Figure 1) of beta spectra from two parts of the lower jaw of a strontium-fed beagle with the model (Equation 1), and (3) description of the relationship between beta energy and depth of the radionuclide (Table 1, Figure 2).

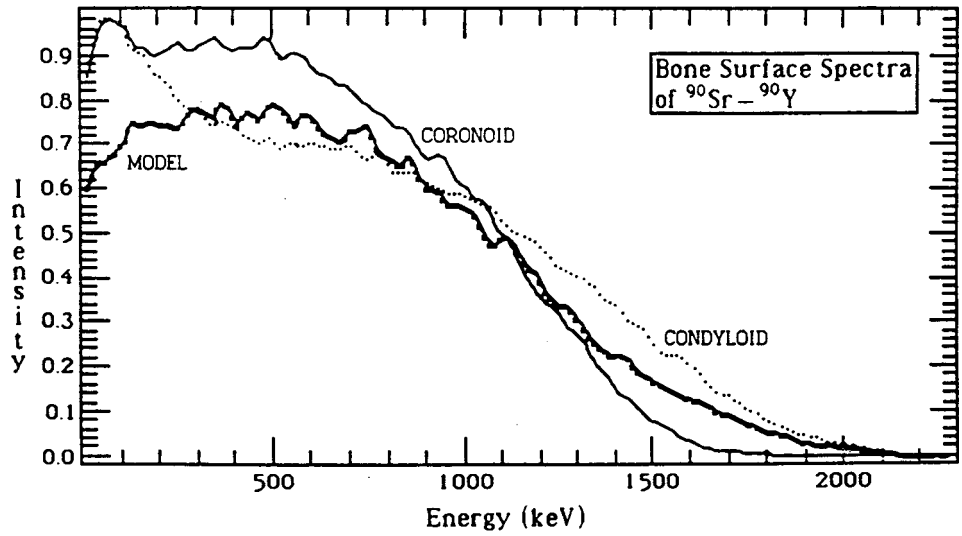

Fig. 1. Comparison of ^{90}Sr-^{90}Y labeled coronoid and condyloid processes of a beagle mandible with that of a semi-empirical model.

Equation 1: $(\text{Intensity})_{i,att} = (\text{Intensity})_{i,0}(att+1)^{b}(\exp [-k*att])$

where channel number i = 1-256, and attenuation (att), in units of mg/cm^2, has the range 0-472; b and k are obtained by fitting equation 1 to the data.

Table 1. Correction factors for surface equivalent (CFUD) intensity as a function of uniform distribution thickness, and the correction factors for surface equivalent (CFLS) intensity of a source localized at a uniform depth from the surface.

Attenuation (mg/cm^2)	CFUD	CFLS
15	1.60	2.01
30	1.86	2.45
45	2.06	2.83
60	2.23	3.21
75	2.40	3.60
90	2.56	4.01
105	2.71	4.43
120	2.86	4.87
135	3.00	5.33
150	3.15	5.81
165	3.29	6.30
180	3.43	6.81
195	3.57	7.33
210	3.71	7.87
225	3.85	8.42
240	3.99	8.99
255	4.13	9.57
270	4.27	10.2
285	4.40	10.8
300	4.54	11.4
315	4.67	12.0
330	4.81	12.7
345	4.95	13.3
360	5.08	14.0
375	5.21	14.6
390	5.35	15.3
405	5.48	16.0
420	5.61	16.7
435	5.75	17.4
450	5.88	18.2
465	6.01	18.9
480	6.14	19.6

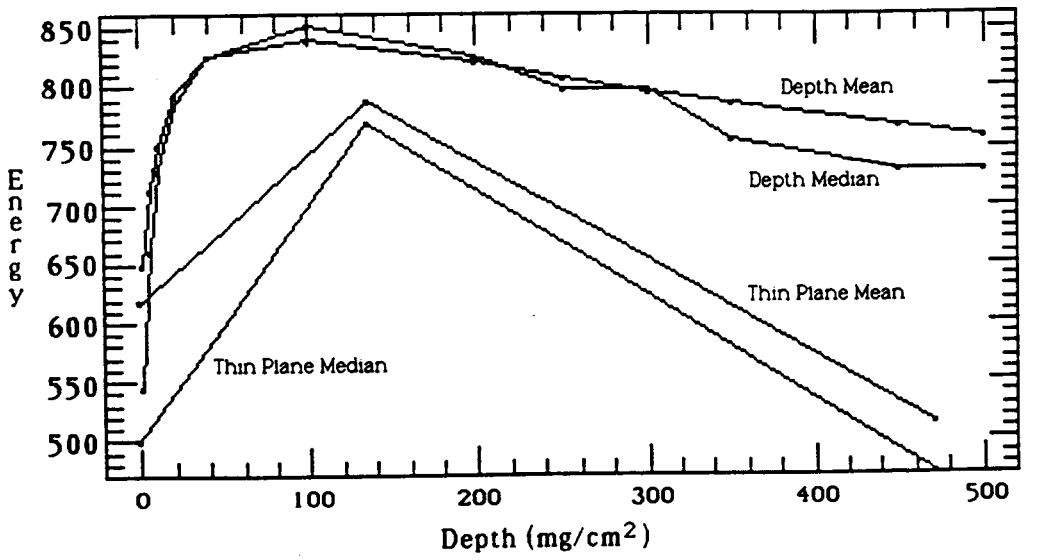

Fig. 2. Relationship of mean and median energy as a function of depth for a uniform pattern of distribution (upper lines) and for an infinitely thin plane (lower lines).

Depth is expressed in this case as two different independent variables--depth for uniform distribution of the radionuclide within a mass of bone and depth for an infinitely thin plane, approximating the surface separating bone laid down before and after cessation of feeding of our experimental beagles with ^{90}Sr-^{90}Y. The mean and median energies for the beta flux emanating from the surface of the condyloid bone are 662 and 607 keV, respectively, whereas those for the coronoid are 493 and 440 keV, respectively. These values provide a convenient indication of variation in the beta flux at surfaces of radiolabelled bone and consequent variation of radiation dose to adjacent soft tissue. In the case of a bone sample such as the coronoid process of the mandible, which has a mean energy of 493 keV, we know from Figure 1 that most of the activity is buried deeply enough to decrease the mean energy from the 620 keV of an unattenuated source. We also know from Figure 2 that the activity is not uniformly distributed because the mean energy calculated for uniform distributions is always greater than 600 keV.

This mean energy information can be augmented with information about the spectral shape to show that some activity is mainly on the surface. All of the information that can be obtained without destroying the sample is typically useful as a selection method for suitable samples for subsequent procedures such as detailed autoradiographic or histomorphometric analysis of radiation-induced tissue perturbations.

REFERENCES

Mishra, A. C. and N. J. Parks. 1987. Beta spectroscopy with liquid scintillation systems: Applications in dosimetry of ^{90}Sr and ^{90}Y. Int. J. Radiat. Appl. Instrum., Part A, 38:455-461.

Parks, N. J. and A. C. Mishra. 1985. Beta spectroscopy with gelled emulsion scintillation. In 1984 Annual Report, Laboratory for Energy-related Health Research, UCD 472-131, pp. 116-120.

TISSUE AND SUBCELLULAR DISTRIBUTION OF BISMUTH RADIOTRACER IN THE RAT: CONSIDERATIONS OF CYTOTOXICITY AND MICRODOSIMETRY FOR BISMUTH RADIOPHARMACEUTICALS

S. Zidenberg-Cherr[1]
N. J. Parks
C. L. Keen[1]

The whole-body clearance, organ distribution, and subcellular distribution of no-carrier-added and carrier-added intraperitoneally administered bismuth radio tracer (a combination of 15.3 d ^{205}Bi and 6.24 d ^{206}Bi) has been determined in Sprague Dawley rats. Differences in clearance rate kinetics were observed for this study with administration of neutral solutions of tracer in carbonate buffer as compared to other studies with other chemical forms. The final organ distribution was not strongly dependent on administered chemical form. We provide definitive evidence that bismuth does indeed enter subcellular organelles such as the nucleus and mitochondria, which had 30-50% and 10-25%, respectively, of activity in kidney tissue. The kidneys were the main sink for radiotracers, with uptake ranging from 20-50% of total body activity. The calculated energy deposition by recoil nuclei after alpha emission of potentially therapeutically useful ^{212}Bi (60.2 m) was found to equal or exceed the alpha energy deposition per organelle if the source is inside the cell nucleus or mitochondria.

INTRODUCTION

There is a growing interest in the use of immunochemically targeted radiotherapeutic agents labeled with alpha-emitting radionuclides. This stems from the recognition that the short range of alpha particles (60-100 μm) coupled with their high linear energy transfer (ca. 100 keV/μm) offers the possibility of greatly improved precision in the delivery of cytotoxic radiation doses within cellular dimensions.

Recently Kozak et al. (1986) reported that they had successfully conjugated the alpha-emitting radionuclide ^{212}Bi ($t_{1/2}$ = 60.2 m) to anti-Tac, a murine monoclonal antibody directed to the human interleukin 2 (IL-2) receptor, and they concluded that the ^{212}Bi anti-Tac conjugate should be well suited for use as a therapeutic agent. A particularly attractive feature of ^{212}Bi as a cytotoxic agent is that each mCi (37 MBq) decays to innocuous quantities (0.03 pmol; ca. $2x10^{11}$ atoms) of stable ^{208}Pb within 10 hours.

However, the in vivo fate and radiological consequences of alpha-emitting cytotoxic agents in nontarget tissues and organs are not well understood. Questions pertaining to sequestration of the intact targeting conjugate or chelate in healthy tissue and to loss of the radionuclide to naturally occurring chelates need to be answered. We are investigating the physiochemical pathways and cellular sequestering sites of ^{212}Bi complexes and longer-lived complexes that initially incorporate the ^{212}Pb ($t_{1/2}$ = 10.6 h) parent of ^{212}Bi.

We began with the hypothesis that some dissociation of radiobismuth from ligands which incorporate Bi directly or that initially incorporate radiolead will occur in vivo, and we have constructed an array of experiments which provide (1) a tissue and subcellular distribution map for the locus of putative radiobiological effects, (2) estimates of organ

1 Department of Nutrition, University of California, Davis

distribution and (3) evidence that prior exposure to macroscopic amounts of Bi influences the subcellular distribution of radiobismuth tracer.

The subcellular distribution of Bi has been examined because the electronic energy imparted to a recoiling ^{208}Tl daughter nucleus from the alpha decay of ^{212}Bi is dissipated in a range of only a few hundred molecular bonds. Much the same thing occurs in alpha decay of ^{212}Po ($t_{1/2}$ = 0.3 μsec), a ^{212}Bi daughter formed by competing beta decay. The dose to molecules in the affected volume is estimated at ca. 30,000 Gy.

The chemical changes induced by nuclear transformations involving these activities (beta decay, electron capture, and conversion electron emission) range from mild to catastrophic. The probability of death or functional impairment for mammalian cells in which radioactive transitions occur is dependent on the spatial and temporal characteristics of the energy transfer (among other variables) to the molecular environment represented by the cell nucleus, mitochondria, cytoplasm, and membrane. When it occurs, cell death is attributed to effects on DNA.

In the case of the ^{212}Bi decay chain leading to stable ^{208}Pb, there are two possible beta decays and two possible alpha decays. This particular combination is guaranteed to produce an energetic recoil nucleus 100% of the time and similarly localized energy deposition from electron emission 20% of the time (ICRP 1983). Consequently, the specific intracellular or epicellular location of ^{212}Bi and daughter atoms at the time of decay is expected to be an important determinant of radiobiological effects.

For the present investigation, the 60-min half period of ^{212}Bi was a distinct inconvenience because of the time required to perform dissections and to separate subcellular fractions. Consequently, we employed cyclotron-produced ^{205}Bi ($t_{1/2}$ = 15.3 day), ^{206}Bi ($t_{1/2}$ = 6.24 day), or mixtures of the two as a no-carrier-added (NCA) tracer of Bi distribution. This material was used in two groups of animals--one with naturally occurring levels of the element in body fluids and tissues and another that had been pharmacologically challenged with macroscopic amounts of bismuth. The latter were sufficient to raise the in vivo concentrations 10-1000 times the natural levels.

MATERIALS AND METHODS

Preparation of No-Carrier-Added (NCA) Bismuth Tracer

Approximately 200 mg of electrolytically produced lead was irradiated with 40 MeV protons at the University of California, Davis, cyclotron facility, producing microcurie (37 kilobecquerels) quantities of ^{205}Bi ($t_{1/2}$ = 15.3 day) and ^{206}Bi ($t_{1/2}$ = 6.24 day).

A prompt separation of nonradioactive lead by ion exchange allowed the ingrowth of NCA ^{203}Pb (51 h) on an anion exchange column which retained Bi ions but quantitatively passed Pb ions (Lagunas-Solar et al., 1987) All experiments were carried out with mixtures of ^{205}Bi and ^{206}Bi tracers. For simplicity, the tracer will be referred to hereafter simply as ^{205}Bi.

Animal Methods

Female Sprague-Dawley rats were injected intraperitoneally every other day for 7 days with 3 mg Bi/kg body weight (exposed) or with the same volume of saline (non-exposed).

Twenty-four hours after the last cold Bi or saline injection, rats were injected with NCA ^{205}Bi, providing approximately 500 kBq per rat.

Blood was collected, counted, and centrifuged to obtain red blood cell and plasma fractions; radioactivity was determined in both fractions. Liver, kidneys, brain, heart, femur, pancreas, spleen and muscle were removed and counted immediately. Whole-body retention was derived from complete accounting for all radioactivity in the carcass, organs, and excreta at the time of sacrifice. Carcass activities were obtained with a small bulk counter (Parks et al., 1979). Macroscopic bismuth concentrations were determined after wet ashing the specimens with 16N nitric acid (recovery of added metals 98-100%). Tissue concentrations of Bi were determined by atomic absorption spectrophotometry of bismuthine gas produced with a hydride generator. Bismuth was detected at 223.1 nm.

Livers and kidneys were homogenized and subcellular fractions were obtained by differential centrifugation, resulting in the isolation of nuclear, mitochondrial, and cytosolic fractions. Liver and kidneys were used for subcellular studies because these two tissues have been reported to contain the highest concentrations of Bi.

RESULTS

Results of whole-body retention measurements are given in Table 1. By 2 hours postinjection, rats had sequestered approximately 55% of the activity administered. At 2-24 h, urinary excretion accounted for approximately 40% of the activity excreted, while the remainder of the radioactivity was found in the feces. In animals previously exposed to Bi, maximum tissue concentrations of 15 ppm (μg/g tissue) were found in the kidneys, 0.1-1 ppm in liver, and an order of magnitude less in other tissues. Nonexposed animals had an ambient Bi background on the order of one part per billion by weight.

Table 1. Whole-body retention and excretion of no-carrier added ^{205}Bi[a] in Sprague-Dawley rats not previously exposed (NE) and previously exposed (E) to 4 injections of 3 mg of bismuth/kg body wt. in tartrate solution.

Time	ID	(Exposure Code)	Whole Body[b]	Urine	Feces
2 h	1	(NE)	60	31	9
	2	(NE)	70	24	6
	3	(E)	57	43	-
6 h	4	(NE)	58	42	-
	5	(NE)	58	41	1
	6	(E)	53	49	-
24 h	7	(NE)	51	44	5
	8	(NE)	61	36	3
	9	(E)	53	44	3
	10	(E)	36	11	53
	11	(E)	66	30	4

[a] Given intraperitoneally as a bicarbonate solution buffered to physiological pH.
[b] Values are expressed as the percentage activity administered.

Tissue distribution of radiobismuth is expressed in terms of percent administered dosage (PCA) and percent administered dosage per gram tissue. Relative to other tissues, the kidneys contained the most radioactivity at all time points measured (Table 2). The same was true on a per gram basis. When expressed as radioactivity per gram tissue weight, muscle and bone were found to concentrate Bi less than other tissues. Muscle and bone account for approximately 40 and 10% of body weight, respectively. The absolute muscle content ranged from 2 to 7% of the total radioactivity administered, whereas bone concentrated between 5 and 15%. Average activity in bone was only 5% of the total by 24 hours post-injection, suggesting that the Bi is not being incorporated into the bone matrix.

Table 2. Distribution of NCA ^{205}Bi tracer as percent of administered activity among organs and body fluids in Sprague-Dawley Rats not previously exposed (NE) and previously exposed (E) to 4 injections of 3 mg of bismuth/kg of body wt. in tartrate solution.[a]

ID:	1	2	3	4	5	6
(Exposure Code)	(NE)	(NE)	(E)	(NE)	(NE)	(E)
TIME:	2 h	2 h	2 h	6 h	6 h	6 h
Carcass	18.8	13.8	20.6	25.3	8.61	16.4
Blood	0.25	0.22	0.82	0.22	0.10	0.20
Heart	0.07	0.07	0.04	0.04	0.02	0.03
Brain	0.02	0.01	0.01	0.01	0.03	0.01
Spleen	0.35	0.12	0.15	0.21	0.12	0.15
Kidney	26.4	49.2	21.5	22.1	38.0	17.0
Liver	2.79	3.17	5.20	2.54	1.97	2.45
Pancreas	0.57	0.84	0.50	0.07	0.22	0.08
Stomach	0.56	0.71	0.45	0.18	0.20	0.33
Intestine	9.3	1.44	6.62	1.07	1.98	1.21
Colon	1.28	0.57	2.48	7.05	6.17	13.9
Feces	9.00	6.19	0.01	0	1.04	0
Urine	31.1	23.8	42.6	41.6	0.68	48.6
Bladder	0.04	0.04	-	0.02	0	0.03

[a] Given intraperitoneally as a bicarbonate solution buffered to physiological pH.

Subcellular Distribution of Radiobismuth

Kidney. Between 30 and 50% of the recovered radioactivity was found in the nuclear fraction of the cell (Table 3). Similar percentages of activity were found in the cytosol. The remaining activity (10-20%) was localized in the mitochondria. From 0.25 h to 6 h post-injection, Bi-exposed rats had a higher percentage of activity (nonexposed rats) in the nuclear fraction of the cell.

Liver. Subcellular distribution of radiobismuth in the liver differed from that of the kidney (Table 3). At 0.25 h, nuclear and cytosolic fractions were similar and contained about 40 to 50% of recovered activity. Later on, the fraction of radioactivity increased in the nuclear and mitochondrial fraction and decreased in the cytosolic portion of the cell.

Table 3. Subcellular distribution[a] of radiobismuth in the liver and kidney of Sprague-Dawley rats with and without prior exposure to 4 injections of 3 mg bismuth/kg body weight in tartrate solutions.

		Kidney			Liver		
	Time	Nuclear	Mito-chondria	Cyto-plasm	Nuclear	Mito-chondria	Cyto-plasm
Nonexposed	.25 h	32.0(3.2)	16.0(3.6)	52.0(3.6)	39.0(2.4)	18.5(0.9)	42.5(0.9)
Exposed	.25 h	49.0(1.0)	11.0(1.3)	40.0(1.3)	40.0(18.4)	13.0(2.6)	47.0(2.6)
Nonexposed	2 h	28.8(15)	17.2(5.7)	54.0(6.8)	35.6(11.4)	29.6(16.9)	37.0(2.6)
Exposed	2 h	58.8(2.9)	9.7(3.6)	31.5(5.7)	48.6(2.3)	22.5(2.5)	26.0(2.4)
Nonexposed	6 h	37.0(4.0)	14.3(8.8)	84.7(7.4)	47.8(4.3)	22.0(6.0)	27.5(3.9)
Exposed	6 h	50.4(1.4)	8.3(3.1)	41.3(1.8)	46.5(4.5)	34.1(9.0)	22.0(3.2)
Nonexposed	24 h	49.5(10)	12.0(4.5)	34.2(11)	53.5(4.4)	18.0(11)	29.0(3.6)
Exposed	24 h	51.3(7.4)	23.0(5.3)	26.0(6.6)	53.0(3.0)	24.7(7.1)	22.0(2.4)

[a] Value represents the mean percent ± (SD) in each cellular fraction expressed as the % activity recovered; 3 animals per group except for 2h E group of 5 and 24 h NE group of 4. The % total body activity (± SD) recovered in livers at 0.25 h for NE group was 3.3(1.3), for E group was 3.0(1.2). The % total body activity recovered in the kidneys at 0.25h for NE group was 16.3(10.0), for E group was 12.8(8.5); at 24 h for NE group was 22.7(12.8), for E group was 30.7(17.3).

DISCUSSION

Our results show differences from those reported by a number of other investigators whose work suggests that chemical form, route of entry, and systemic carrier concentrations determine the actual quantities of tracer in tissues at a given time. Specifically, Vienet et al. (1983) report a kidney:liver percent activity ratio (KLA ratio) of 2.0 at 72 h post-exposure, using intravenously injected Bi NCA radiotracer. Russ et al. (1975) injected NCA Bi radiotracer intraperitoneally and report a median KLA ratio ranging from 30 to 75. Our ratio range was 8.7-19.3 for nonexposed animals at 2-6 h. The previously exposed animals gave KLA ratios of 4.1 and 6.9 at 2 and 6 h, respectively. Szymanska et al. (1977) obtained KLA ratios of 6.4 and 16.3 by injecting ^{206}Bi-labelled $BiCl_3$ subcutaneously at macroscopic levels (2.5 mg Bi/kg) for 1 and 5 days, respectively. A lower dosage (0.5 mg Bi/kg) gave a ratio of 26.9.

At similar times post-administration, different chemical forms of Bi introduced by various routes give different KLA ratios, which indicates different rates of sequestration or elimination. However, kidneys were the main sequestering site in all cases. Increasing nonradioactive Bi levels to 15 to 20 ppm (μg/g tissue) did not "block" kidney Bi tracer uptake; nor did it reduce tracer concentrations to the levels found in other organs. The nonradioactive Bi levels that we and others have employed do not appear to be in the toxic range (Urizar and Vernier, 1966).

Subcellular Distribution

The majority of the recovered radioactivity in both the kidney and the liver (representing high uptake and low uptake of the radionuclide, respectively) was distributed between the cytosolic and nuclear fractions. Other studies have reported that Bi binds to

low-molecular-weight proteins within the cytosol, where it is possible that Bi may induce the synthesis of proteins with metallothionein-like properties. Metallothioneins are low molecular weight (<8,000 MW) cysteine-rich proteins which have been proposed to function in the cellular detoxification of heavy metals. In addition, these proteins may serve as storage sites and as donors of essential metals into apo-metalloproteins. We are currently investigating the influence of initial cellular Bi concentration on the molecular localization of Bi taken up from picogram dosages.

Our results show that Bi can cross the blood brain barrier. This is consistent with earlier reports and suggests that the cases of encephalopathy which have been reported following continual administration of Bi compounds may be due to a direct effect of the element on brain cells.

Microdosimetric Factors

The short range of the recoil nucleus (R_n) energy loss means its energy will be distributed at the organelle level in the same way as the parent atom. On the other hand, the alpha particle energy will be approximately isotropically distributed because its range is several cell diameters and the portion of alpha energy seen (on a statistical basis for a large population of decays) by each organelle will be proportional to that organelle's volume (Table 4).

Table 4. Bismuth-212 decay: Recoil nucleus and alpha particle energy distribution fraction, energy per organelle, and energy density (eV/atom) predicted for the kidney of rats exposed (E) and non-exposed (NE) to carrier bismuth (4 injections of 3 mg/kg body wt.).

	Energy Distribution fraction per organelle			Energy per Organelle (keV)			Energy density (eV/atom)[c]		
	R_n[a]		α[b]	R_n		α		R_n	α
Kidney	(E)	(NE)	(E and NE)	(E)	(NE)	(E and NE)			
Nucleus	0.52	0.34	40/5,041	83.2	54.4	63.6	Median	250	32
Mitochondria	0.11	0.16	1/5,041	17.6	25.6	1.6	Range	200-300	20-40
Cytoplasm	0.37	0.50	5,000/5041	59.2	80.0	7,934.9			

[a] Median of data sets; energy of recoil is 36% (117 keV) and 65% (169 keV).

[b] Based on cytoplasmic:nuclear:mitochondrial volume ratio of 5,000 μm^3:40 μm^3:1 μm^3 The sum of volumes is cell volume; α energy is 36% (6,070 keV) and 65% (8,780 keV).

[c] A weighted mean of the ^{212}Bi and daughter ^{212}Po recoil (160 keV) and α energies (8 meV) are used for this calculation; energy density estimates include energy that would be removed by scattered electrons and are an upper limit.

If the energy distribution fraction (EDF) per organelle for R_n is multiplied by a nominal E_{recoil} value of 160 keV, and the EDF per organelle for an alpha energy of 8,000 keV, we get the values shown on the right hand side of Table 4, suggesting that the energy per organelle from R_n is typically the same, or higher than that from alphas, except for cytoplasm. The large volume of cytoplasm accounts for it receiving most of the alpha energy.

The energy density segment of Table 4 estimates the energy in eV/atom of local environment by dividing the available energy per particle by the pathlength in typical bond length units of 0.25 nm and adopting the convention that, on average, there is one atom per bond. Irrespective of the descriptive convention, the energy density for R_n is about 10-fold higher than for alphas.

In summary, the present study shows that if radiobismuth is released from a radiopharmaceutic ligand prior to its reaching a given target, uptake into kidneys and liver will occur rapidly. This underscores the importance of developing a chelate with high affinity for Bi such that it allows for minimal release of the element to these tissues. Secondly, this study shows that prior exposure to Bi influenced the subcellular distribution liver and kidney uptake of the element. Thus, the Bi status of a patient receiving Bi nuclides in radiotherapy treatment may be an important factor in determining possible secondary tissue damage. Finally, the data indicate that the deposition of highly localized energy by recoil nuclei after alpha decay may be the most radiobiologically important factor because the parent radionuclide concentrates in the sensitive subcellular organelles, cell nuclei, and mitochondria.

REFERENCES

ICRP. 1983. *Radionuclide transformations: energy and intensity of emissions.* ICRP Publication 38, International Commission on Radiological Protection, Report Task Group of Committee 2, Pergamon Press, Oxford.

Kozak, R. W., R. W. Atcher, O. A. Gansow, R. M. Friedman, J. J. Hines and T. A. Waldman. 1986. Bismuth-212-labeled anti-TAC antibody and particle-emitting radionuclides as modalities for radioimmunotherapy. Proc. Nat. Acad. Sci. USA 83:474-478.

Lagunas-Solar, M. C., O. F. Carvacho, L. Nagahara, P. Mishra and N. J. Parks. 1987. Cyclotron production of no-carrier-added ^{206}Bi (6.24 d) and ^{205}Bi (15.3 d) as tracers for biological studies and for the development of α-emitting radiotherapeutic agents. Int. J. Appl. Radiat. Isot. 38:129-137.

Parks, N. J., J. A. Schwind, and E. A. Hinz. 1979. An automatic sample changer and microprocessor controlled data router for a small bulk-sample counter. Health Phys. 36:458-462.

Russ, G. A., R. E. Bigler, R. S. Tilbury, H. Q. Woodard and J. S. Laughlin. 1975. Metabolic studies with radiobismuth. 1. retention and distribution of ^{206}Bi in the normal rat. Radiat. Res. 63:443-454..

Szymanska, J. A., E. M. Mogilnicka, and B. W. Kaszper. 1977. Binding of bismuth in the kidneys of the rat: The role of metallothionein-like proteins. Biochem. Pharmacol. 26:257-258.

Urizar, R. and R. L. Vernier. 1986. Bismuth nephropathy. JAMA 198: 187-189.

Vienet, R., P. Bouvet and M. Istin. 1983. Cinetique et Distribution du ^{206}Bi chez le Rat et le Lapin: un Modele. Int. J. Appl. Radiat. Isot. 34:747-753.

STRUCTURE OF A NOVEL NEUTRAL LEAD(II) COMPLEX WITH DIPROPYLDITHIOCARBAMATE

P. K. Bharadwaj[1]
B. W. Arbuckle[2]
W. K. Musker[2]

The synthesis and X-ray structure of a tetramer of Pb(II) with the dipropyldithiocarbamate ligand is described, continuing the examination of potential carriers for use as pharmaceuticals that might survive the decay of ^{212}Pb to ^{212}Bi. This compound crystalizes in the triclinic space group $P\bar{1}$. The structure consists of a sulfur-bridged neutral tetrameric species where each Pb(II) ion is pentacoordinated.

INTRODUCTION

There is much interest in determining when the size of the ligand causes the typical coordination geometry of a metal to change to give a species having either a higher or lower coordination number. For simple ligands, substituents on the atom next to the donor can be increased in size, but with 1,1-dithio ligands the substituents on the atom at least two atoms away from the donor must be increased in size to achieve the desired result. Pb(II) complexes of both dimethyldithiocarbamate and diethyldithiocarbamate have been prepared and found to be monomeric with a distorted, four-coordinated, square pyramidal geometry. However, a weak intermolecular interaction with an adjacent molecule occurs, giving an overall coordination number of six to the Pb(II) ion. For the dimethyldithiocarbamate group this distance is an average of about 3.50 Å. When the length of the hydrocarbon chain is increased by one methylene group, the coordination number of Pb(II) changes from four to five, resulting in a novel tetrameric species. The work is part of a research program to develop an α-emitting radiopharmaceutical that binds strongly to Pb(II) and Bi(III). Crystalline dipropyldithiocarbamate complexes of both Pb(II) and Bi(III) have now been prepared and we report here the structure of the lead complex. Structural elucidation of the Bi(III) complex is in progress.

METHODS

The ligand was synthesized following a published procedure (Jones et al., 1957) as the potassium salt. An aqueous solution of $Pb(NO)_3 \cdot 6H_2O$ was allowed to react with an aqueous solution of the ligand. Single crystals of $[Pb(C_{14}H_{28}N_2S_4)]_2$ were obtained on slow evaporation of an acetone solution.

A crystal of the title compound was mounted at the end of a glass fiber and all diffraction measurements were made at 130(1)k with a Syntex $P2_1$ diffractometer. Details of data collection and refinement are presented in Table 1.

The structure was solved by the heavy atom method and refined on F using full matrix, least-squares techniques with the SHELXTL (version 5.1) program package. Views of the structure are given in Figures 1 and 2. Atomic parameters are given in Bharadwaj, Arbuckle and Musker (1988).

1 LEHR and Department of Chemistry, University of California, Davis
2 Department of Chemistry, UCD

Table 1. CRYSTAL AND REFINEMENT DATA

Formula	$2(C_{14}H_{28}N_2S_4Pb)$
Formula weight (a.u.)	1119.66
a (A)	9.576(2)
b (A)	14.151(4)
c (A)	16.175(4)
α (°)	104.84(2)
β (°)	102.26(2)
γ (°)	90.62(2)
V (A^3)	2065(1)
Space group	$P\bar{1}$
Z	2
No. of reflections used to determine cell constants	15($9.65 < \theta < 13.55$)
Diffractometer	Syntex $P2_1$
Temperature (K)	130(1)
Radiation used	graphite monochromated Mo Kα (0.71073 A)
D_{calc} (g cm^{-3})	1.80
Crystal dimensions (mm)	0.13 X 0.16 X 0.18
Linear absorption coefficient (cm^{-1})	84.31
Data collection method	ω-scan
2θ range (°)	$0 < 2\theta < 50$
ω-scan range (°)	1.0
Scan rate (°)	variable
No. of standard reflections	2
% Variation in standard intensity	<0.1
Octants collected ($+h, \pm k, \pm l$)	11, ±16, ±18
R(Merge)[a]	0.0001
No. of data used in refinement	5323 ($F_o > 3\sigma(F_o)$)
Data:parameter ratio	~14
Weighting scheme[b]	$w = 1/[(\sigma^2(F_o) + gF_o^2]$
Systematic absences	none
Final GOF	1.35
Final R_f	0.030
Final R_{wf}	0.032
Final largest shift/e.s.d.	0.013
Highest peak[c] in final difference map (e/A^3)	1.67

[a] R(merge) = $(\Sigma(N\Sigma(\text{weight}(F(\text{mean}) - F)^2))/\Sigma((N-1)\Sigma\text{-}(\text{weight}FF)))^{1/2}$, where the inner summations are over the N equivalent reflections averaged to give F(mean) and the outer summations are over all unique observed reflections. [b] g was refined by fitting $(F_o - F_c)^2$ to $(\Sigma^2(F) + \text{abs}(g)FF)/K$ (where K is a scale factor) to put weight on an approximately absolute scale. For the present structure g = 0.00018. [c] Large peaks near the Pb atoms may be due to inadequate absorption corrections.

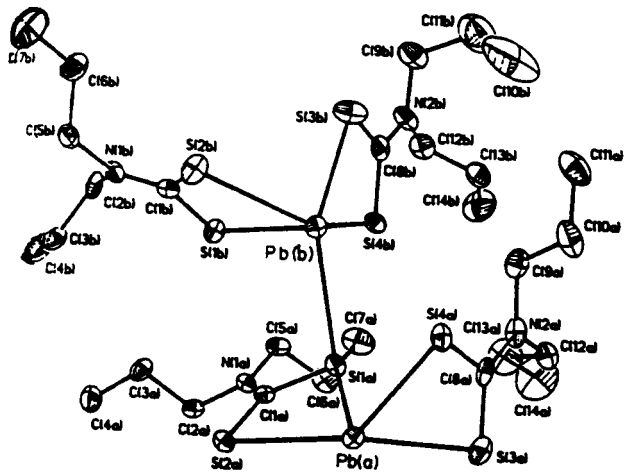

Fig. 1. View of the title compound showing the atom numbering scheme. H atoms are omitted for clarity. Thermal cilipsoids are drawn at the 50% probability level.

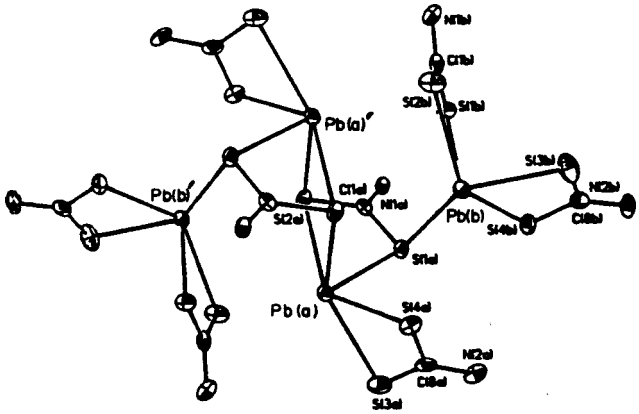

Fig. 2. View of the tetramer. Alkyl groups have been omitted for clarity. Thermal ellipsoids are at the 50% probability level.

RESULTS AND DISCUSSION

The structure of the Pb(II) complex consists of neutral discrete tetrameric species (Fig. 2; a and a'; b and b'), where each Pb(II) atom in the tetramer is pentacoordinated. Only a and b are present in the asymmetric unit; a' and b' are related by a center of inversion. Several transition complexes of 1,1-dithio ligands are known where S acts as a bridge between two metal ions, but this structure is the first example in which a Pb(II) ion is involved. When 1,1-dithio ligands act as chelates, they make four-membered rings which are under strain. One way to relieve the strain is by making the M-S bonds slightly unequal in length. However, the extent of the asymmetric binding found in this molecule also suggests that the lone-pair on Pb(II) is stereochemically active.

Normally, with 1,1-dithio ligands, Pb(II) makes a distorted, four-coordinate, pyramidal PbS_4 unit and then increases its coordination number to six by weakly binding to two sulfur atoms on the adjacent molecule. In the present structure, the combined effects of an additional methylene group and the lone pair on Pb(II) have distorted the coordination geometry even further, causing a considerable gap in the PbS_4 coordination sphere. However, only one sulfur atom, S(1a), from the nearest neighbor comes close enough to bind to Pb(b) (Pb(B)...S(1a) = 3.268(6) Å). Thus, the Pb(b) achieves only five-coordination (Figure 1).

REFERENCES

Bharadwaj, P.K., B.W. Arbuckle and W.K. Musker. 1988. Inorg. Chim. Acta 142: 243-246.

Bharadwaj, P.K. and W. K. Musker. 1987. Inorg. Chem. 26: 1453-1455.

Jones, R.G., E. Bindschadler, G.A. Richards, G.A. Martin, J.R. Thirtle and H. Gilman. 1957. J. Am. Chem. Soc. 79: 4921.

MURINE MODEL FOR INTRACELLULAR THERAPEUTIC RADIATION OF MELANOMA

A. S. Hill[1]
P. D. Schneider[1]
K. C. Chelton[2]
N. J. Parks

Mice were used to model the delivery of the radioisotope, ^{212}Pb, to tumors via liposome IV injection as a test of therapeutic effects from intracellular alpha irradiation. The ^{212}Pb was complexed to albumin and built into liposomes formed by reverse-phase evaporation. Flank tumors of mice which had been injected with melanoma from cell culture contained 10% of the liposomes two hours after their injection. This was comparable to the fraction taken up by the liver, which is the major organ of liposome uptake. Uptake of liposomes exceeded the uptake of free fluorescein dye and of albumin-complexed ^{131}I. Melanoma cells treated in this way do not form flank tumors, suggesting possible therapeutic use targeting metastatic melanoma.

INTRODUCTION

A theoretically attractive but untested approach to the treatment of malignancy is targeted intracellular alpha particle irradiation. A model for intracellular delivery of alpha irradiation to melanoma has been developed in mice. Liposome encapsulation and subsequent intracellular release of radioactivity is utilized to study intravenous (IV) delivery to flank tumors. In vitro studies have confirmed avid intracellular uptake of liposomes by melanoma (Potter et al., 1984). Intravenous injection of liposome-entrapped fluorescent dye and radioisotopes in flank tumor-bearing mice is used to test delivery in vivo. The therapeutic effect from intracellular alpha irradiation can be tested for melanoma cells treated in vitro or in vivo.

MATERIALS AND METHODS

The alpha emission from the $^{212}Pb/^{212}Bi$ isotope pair functionally provides 10.6-hour half-life alpha radiation (6 to 8 MeV). ^{212}Pb obtained from a thorium generator was complexed with albumin (HSA) at 0.05 mg/mL. Large, unilamellar liposomes (350 to 500 nm in diameter) containing this complex were formed by reverse-phase evaporation (Szoka and Papahadjopoulos 1978). Alternatively, carboxyfluorescein or ^{131}I-neogalactosyl-albumin (NGA) was encapsulated. B16 F10 melanoma maintained in cell culture was subcutaneously injected (10-5 cells) to give rise to 1-g flank tumors in 30 synergistic C57 B16 mice. Two hours after IV injection of liposomes organs were sampled to determine the organ distribution of liposome contents in the tumor-bearing mice. Organs and tumors were analyzed by dye extraction and fluorescence spectroscopy or scintillation counting.

RESULTS AND DISCUSSION

The delivery of liposome contents to the melanoma is compared to hepatic uptake in Table 1. Liver is the major site of uptake of liposomes, and liver uptake is a quantitative benchmark of tissue targeting for IV injections of liposomes. The fraction

1 Department of Surgery, University of California, Davis Medical Center
2 Tomales Psychotherapy Training Program, Santa Rosa

of the injected dose per gram internalized by flank tumors represents 10% of the infused liposomes, while hepatic uptake appeared to be related to the volume infused IV. Liposome encapsulation enhanced tumor uptake in comparison to injections of free dye or radioisotopes in each case tested. Treatment of melanoma cells in vitro with ^{212}Pb-labeled albumin liposomes at an intracellular dose of approximately 60 cGy/10^7 cells has rendered the cells incapable of forming flank tumors. The possible therapeutic application of nonspecific targeting to metastatic melanoma is supported by this evidence for liposome delivery of alpha emitter in vivo. Preliminary therapeutic in vitro application of intracellular ^{212}Pb to melanoma shows an antineoplastic effect. The pronounced dose effect and limited range of alpha particles (0.6 to 2 mm) makes $^{212}Pb/^{212}Bi$ an attractive isotope for therapeutic use with currently available targeting vehicles.

Table 1. UPTAKE OF LIPOSOME CONTENTS BY MELANOMA VS. LIVER.

	Fraction of injected dose/g		
	Liver	Tumor	Liposome volume injected
Carboxygluirescein			
Free	0.012 ± 0.001	0.033 ± 0.018	
Liposome	0.097 ± 0.022	0.047 ± 0.043	0.018 ± 0.01 mL
^{131}I-NGA			
Free	0.085 ± 0.029	0.074 ± 0.008	
Liposome	0.091 ± 0.006	0.134 ± 0.018	0.08 ± 0.01 mL
^{212}Pb-albumin			
Free	(Not Done)	(Not Done)	(Not Done)
Liposome	0.268 ± 0.021	0.130 ± 0.030	0.25 ± 0.013mL
Mean liposome uptake per 100 µL injected	0.092	0.014	

Values expressed as mean ± SEM

REFERENCES

Potter, D. A., C. M. Gorschboth and P. D. Schneider. 1984. Liposome uptake by melanoma: In vitro comparison with hepatocytes. J. Surg. Res. 39:157-163.

Szoka, F. and D. Papahadjopoulos. 1978. Procedure for preparation of liposomes with large internal aqueous space and high capture by reverse-phase evaporation. Proc. Natl. Acad. Sci. USA 75:4194-4198.

RADIOLOGICAL IMPACTS

THREE-DIMENSIONAL DOSE-RESPONSE MODELS OF COMPETING RISKS AND NATURAL LIFESPAN

O. G. Raabe

Three-dimensional dose-rate/time/response surfaces for chronic exposure to carcinogens, toxicants and ionizing radiation dramatically clarify the separate and interactive roles of competing risks. The three dimensions are average dose rate, exposure time, and risk. Illustrations that employ mathematical stripping and computer graphics show the contributions with the passage of time of the competing risks of death from radiation pneumonitis/fibrosis, lung cancer, and natural aging consequent to the inhalation of plutonium-239 dioxide by beagles. Radiation pneumonitis predominates at high dose rates and lung cancer at intermediate dose rates. Low dose rates result in spontaneous deaths from natural aging, yielding a type of practical threshold for lung cancer induction.

INTRODUCTION

The adverse biological responses resulting from the chronic exposure of people or laboratory animals to toxic, carcinogenic, or radioactive materials depend on the temporal pattern of dose to sensitive cells, tissues, or organs. The manifestation of these responses depends also on the complex relationship of risks associated with the different possible competing effects as a function of elapsed time of exposure. The common use of two-dimensional dose versus response functions can obscure the importance of time both upon the cumulative dose and upon the occurrence of different effects and can blur the relationships of the competing risks. In this study a three-dimensional modeling scheme was developed using computer graphics to elucidate more clearly these three-dimensional relationships, including the effect of competing risks. By utilizing a mathematical stripping procedure, we have investigated the occurrence of specific effects such as cancer with respect to time and dose. As an example, these methods were applied to the evaluation of the fatality risk distributions for systemic injury and cancer that result from chronic irradiation of the lung by alpha particles after inhalation of aerosols of plutonium-239 dioxide ($^{239}PuO_2$) by beagles utilizing data from Battelle Pacific Northwest Laboratories.

METHODS

Mathematical analysis: The cumulative risk for a single effect, $F(t,\overline{D})$, which is a function of elapsed time, t, and average absorbed radiation dose rate, $\overline{D}$, is the independent probability (values between zero and one) of an individual succumbing to the specified response (e.g., dying of lung cancer), assuming that there are no other possible effects. Likewise, the probability density, $f(t,\overline{D})$, is the fraction of all individuals originally at risk who succumb per unit of time (e.g., per day) after exposure begins. Thus, if T is the time from exposure to death from a specified cause and there are no other causes of death, then the probability of dying at a given average dose rate before or at a specified time, t, is given by:

$$\Pr[T \leq t] = F(t,\bar{D}) = \int_0^t f(t,\bar{D})\partial\theta \tag{1}$$

where $t = A - E$, with A the age of the individuals at risk and E their age at the beginning of the exposure.

When several separate risk distributions, F_i, are superimposed in the time and dose-rate space, the occurrence of one cause of death, i, is a fraction, Ω_i, of individuals who succumb to that cause at a specific average dose rate. For example, effect $i = 1$ could be spontaneous deaths associated with natural lifespan, effect $i = 2$ could be deaths associated with a specific form of toxicant-induced cancer, and effect $i = 3$ could be deaths from systemic injury induced by exposure to the toxicant. Thus, if T_i is the time from exposure to death from a specified cause, i, and there are three causes of death, then the probability of occurrence of one type of death ($i = 1$, for example) at a given average dose rate before or at a specified time, t, is given by:

$$\Pr[T_1 \leq t, T_2 > T_1, T_3 > T_1] = \Omega_1(t,\bar{D}) = F_1 - \int_0^t [F_2 + F_3 - F_2F_3]f_1\partial\theta \tag{2}$$

where the subscripts 1, 2, and 3 refer to three separate independent risk distributions, and death is the common endpoint.

The distribution of deaths associated with natural lifespan is a mixture of the various causes, including various forms of both communicable and non-communicable diseases, and is commonly represented utilizing the Gompertz function. This risk distribution describes a hazard rate, $f_1/(1.0-F_1)$, that increases exponentially with time. The Gompertzian cumulative risk from an age E until a time $t = A - E$ is given by:

$$F_1(t) = 1.0 - \text{EXP}[h_0 e^{\psi E}(1.0 - e^{\psi t})/\psi] \tag{3}$$

where h_0 is the hazard rate at birth, ψ is the exponential coefficient, and $e^{\psi E}$ is a constant introduced to displace the time axis to $t = 0$ at the beginning of exposure rather than at birth.

For the purposes of this investigation, the three-dimensional lognormal power function was used in the same manner as previously applied to radiation-induced bone cancer (Raabe et al., 1980; Raabe et al., 1981; Raabe et al., 1983; Raabe, 1984) and to radiation toxicity (Raabe and Goldman, 1979). The lognormal model involves a basic dose-rate/time/response relationship given by:

$$t = K\,\bar{D}^{-S} \tag{4}$$

where $\bar{D}$ is the average dose rate of toxicant or ionizing radiation to the organ or tissue at risk, t is the elapsed time to death (or other endpoint) after initial exposure, K is a characteristic parameter associated with level of risk and exposure conditions, and S is the negative slope of the logarithmic form of the function. At any given $\bar{D}$, both K and t are lognormally distributed with geometric standard deviation, σ_g. This relationship defines a three-dimensional lognormal dose-rate/time/response surface for a specific effect such that:

$$Z = (\ln t - \ln K_m + S \ln \bar{D})/\ln \sigma_g \tag{5}$$

where K_m is the fitted median risk value of K, σ_g is the observed geometric standard deviation of K values for the individual cases, and Z is the standardized normal deviate, which is equal to zero at the median risk ($F = 0.5$). Hence, the cumulative risk for a lognormal dose-rate/time/response distribution for effect j can be calculated for each $\overline{D}$ and t by numerical integration of the standardized normal distribution:

$$F_j(t,\overline{D}) = F_j(Z) = \int_{-\infty}^{Z} \frac{1}{\sqrt{(2\pi)}} e^{-y^2/2} dy \qquad (6)$$

A separate lognormal risk distribution ($j = 2$ to i) can be used for each effect.

Response relationship for inhaled plutonium-239 dioxide: The three-dimensional dose-response model is demonstrated here by means of an example which concerns the principal deleterious responses associated with chronic α particle irradiation of the lung, utilizing data obtained from published reports of two separate, carefully controlled, lifetime studies of the inhalation toxicity of inhaled $^{239}PuO_2$ aerosols in purebred beagles. These studies were conducted by Bair, Park and their co-workers at Battelle Pacific Northwest Laboratory in Richland, Washington (Bair and Willard, 1962; Park et al., 1962; Park et al., 1972; Park et al., 1985) and were sponsored by the U.S. Department of Energy (and the predecessor Atomic Energy Commission). The first study involved single 10- to 30-minute nose-only exposures of beagles that varied in age from about 6 to 43 months (Bair and Willard, 1962; Park et al., 1962; Park et al., 1972). These exposures occurred between 1959 and 1961. The second study involved single 5- to 30-minute nose-only exposures of beagles that varied in age from about 14 to 21 months (Park et al., 1985). The exposures occurred between 1970 and 1972.

The independent variable in the dose-response relationships in this example is the average concentration of the plutonium in lung tissue, and the corresponding gravimetric-average absorbed radiation energy per unit time. The time-weighted average radiation dose rate, $\overline{D}$, was calculated in relation to total lung mass (1.16% of total body mass for beagles, including normal lung volume of circulating blood) for the 5.15 MeV ^{239}Pu α particles for the period extending from exposure to death, using the lung burden and retention of plutonium for each dog.

Beagle deaths at high doses were associated with cardiopulmonary insufficiency from acute radiation pneumonitis and pulmonary edema at early times, from pulmonary fibrosis at later times, and a combination at intermediate times. For simplicity, this progression of lung injury is herein inclusively called "radiation pneumonitis." The lognormal dose-rate/time/response model for these radiation pneumonitis/fibrosis deaths for beagles exposed to aerosols of $^{239}PuO_2$ has been described previously by a lognormal function having $S = 1.0$ (Raabe and Goldman, 1979), and those results were used without change. Lung cancers in beagles caused by α particles from ^{239}Pu are usually described as bronchiolo-alveolar carcinomas, but some other malignant neoplasms may also occur. The parameters of the distributions were calculated by least-squares fit of Eq. 2 using the logarithms of average dose rate (centigray/day) and time to death (days). This fitting was done separately for the radiation pneumonitis cases at high dose rates and for lung cancer cases at intermediate dose rates.

To obtain a lifespan risk distribution, a life-table analysis was performed for 178 similar purebred beagles from the University of California, Davis, colony of control dogs. The Gomperzian parameters were estimated by the least-squares fit of the function using the logarithm of the hazard rate versus age.

RESULTS

The parameters and associated confidence limits of the risk distributions are summarized in Tables 1 and 2, showing satisfactory fits to the data. The results of this analysis are shown in two dimensions in Figure 1, with each beagle being coded by cause of death or recorded as alive (at the time of the data summary). The loci of the medians of the three independent risk distributions are shown as separate lines. In this two-dimensional plot the third dimension, the combined risk distribution, is reflected by the clustering of the individual cases.

Table 1. FITTED PARAMETERS OF THE LOGNORMAL DOSE-RATE/TIME/RESPONSE SURFACE DESCRIBING THE INDEPENDENT RISK OF RADIATION-INDUCED LUNG CANCER DEATHS AND RADIATION PNEUMONITIS/FIBROSIS DEATHS FOR BEAGLES FROM INHALED ^{239}Pu.*

Response	K_m [GSE]	S [SE]	σ_g	n	r [95% conf.][b]	χ^{2c}
Pneumonitis	4,300 [1.06]	1[a]	1.35	24	0.95 [0.87-0.98]	1.01 (p<0.31)
Lung Cancer	2,250 [1.03]	0.29 [0.02]	1.21	66	0.86 [0.76-0.91]	1.28 (p<0.26)

* Where S is the negative slope (standard error, SE) and σ_g is the geometric standard deviation of K values about the median K_m (geometric standard error, GSE) for beagles with correlation coefficient, r (with 95% confidence range), and chi-square (χ^2) with one degree of freedom based upon dose rate in cGy/day (or rad/day) and time post-exposure in days.

a Assumed value of S based upon overall data from Raabe and Goldman, 1979.

b A t test of the hypothesis of zero correlation leads to p<0.00001.

c To test the hypothesis that the data are lognormal, four groups of equal probability were formed at the boundaries of Z = -0.6749, 0, and 0.6749, yielding one degree of freedom since n, K_m, and σg are from the data (for the given S values); values of χ^2 smaller than 2.7 are expected in 90% of such tests.

Table 2. FITTED PARAMETERS OF THE GOMPERTZ FUNCTION FOR THE LIFESPAN OF 178 UNEXPOSED BEAGLES FROM THE DAVIS COLONY FOR A LEAST-SQUARES FIT OF TEN HAZARD RATES* OBTAINED FROM A LIFE-TABLE ANALYSIS USING THE COORDINATES OF TIME AND LOGARITHM OF HAZARD RATE.†

$h_0(day^{-1})$ [GSE]	$\psi(day^{-1})$ [SE]	n	r [95% conf.][a]	χ^{2b}
2.037×10^{-6} [1.45]	1.104×10^{-3} [0.093×10^{-3}]	10	0.97 [0.86-0.99]	3.26 (P<0.071)

* Equally spaced in time between 900 and 6300 days of age.

† Where h_0 is the coefficient (geometric standard error, GSE), ψ is the slope (standard error, SE) for values with correlation coefficient, r (with 95% confidence range), and chi-square (χ^2) with one degree of freedom.

a A t test of the hypothesis of zero correlation leads to p<0.00001.

b To test the hypothesis that the original data are Gompertzian, four groups of equal probability were formed at the boundaries of age of 4580 days, 5373 days, and 6000 days, yielding one degree of freedom since n, h_0, and ψ are from the data (for the given S values); values of χ^2 smaller than 4.9 are expected in 97% of such tests.

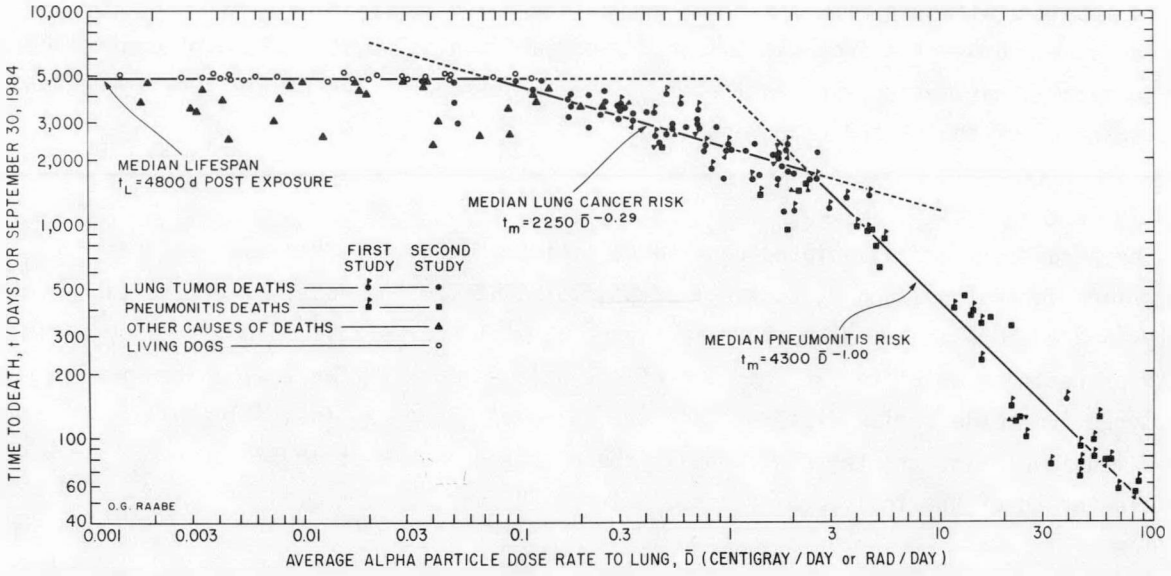

Fig. 1. Two-dimensional presentation of the three-dimensional dose-rate/time/response relationships with the experimental data for radiation-pneumonitis deaths, lung cancer deaths, and other deaths in beagles exposed to aerosols of $^{239}PuO_2$, showing time from exposure to death for each individual dog versus average dose rate to lung from & particle irradiation and showing fitted median risk functions; response magnitude is indicated by the clustering of the data points.

A three-dimensional representation of the combined risk probability density distribution, $f_c(t,\bar{D})$, derived from Figure 1, is illustrated in Figure 2, showing the relationships of the three independent risk distributions. The resulting combined cumulative risk, $F_c(t,\bar{D})$, is illustrated in the first panel of Figure 3, showing the regions of predominance of the three effects.

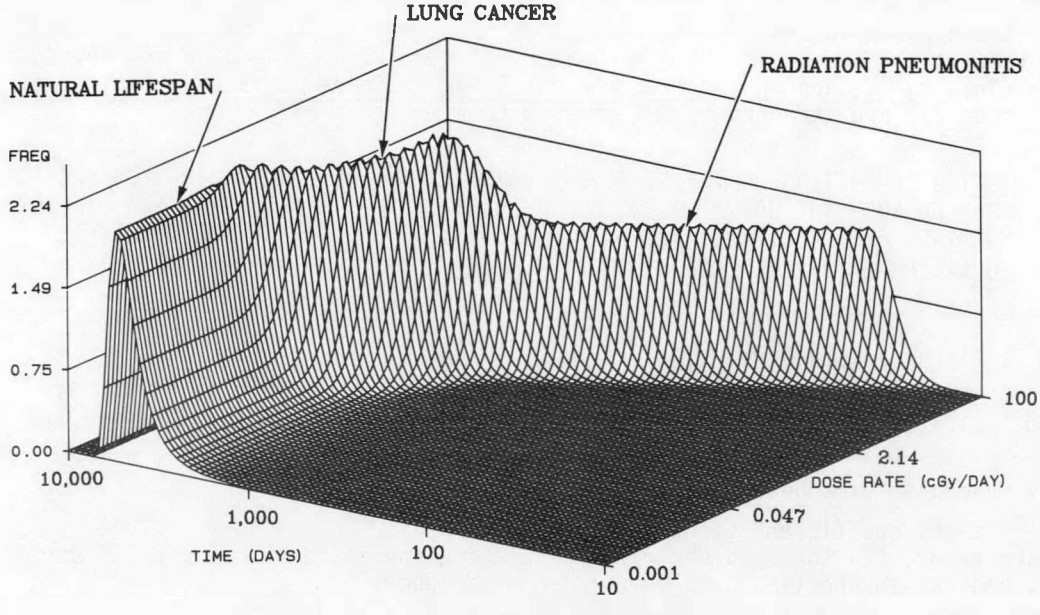

Fig. 2. Three-dimensional representation of the dose-rate/time/response relationships of Figure 1 given as the combined probability density distribution frequency, $f_c(t,\bar{D})$, utilizing the fitted risk functions for deaths from radiation pneumonitis, lung cancer, and causes associated with the natural lifespan for beagles with lung burdens of $^{239}PuO_2$. [Time post-intake & average dose rate to lung.]

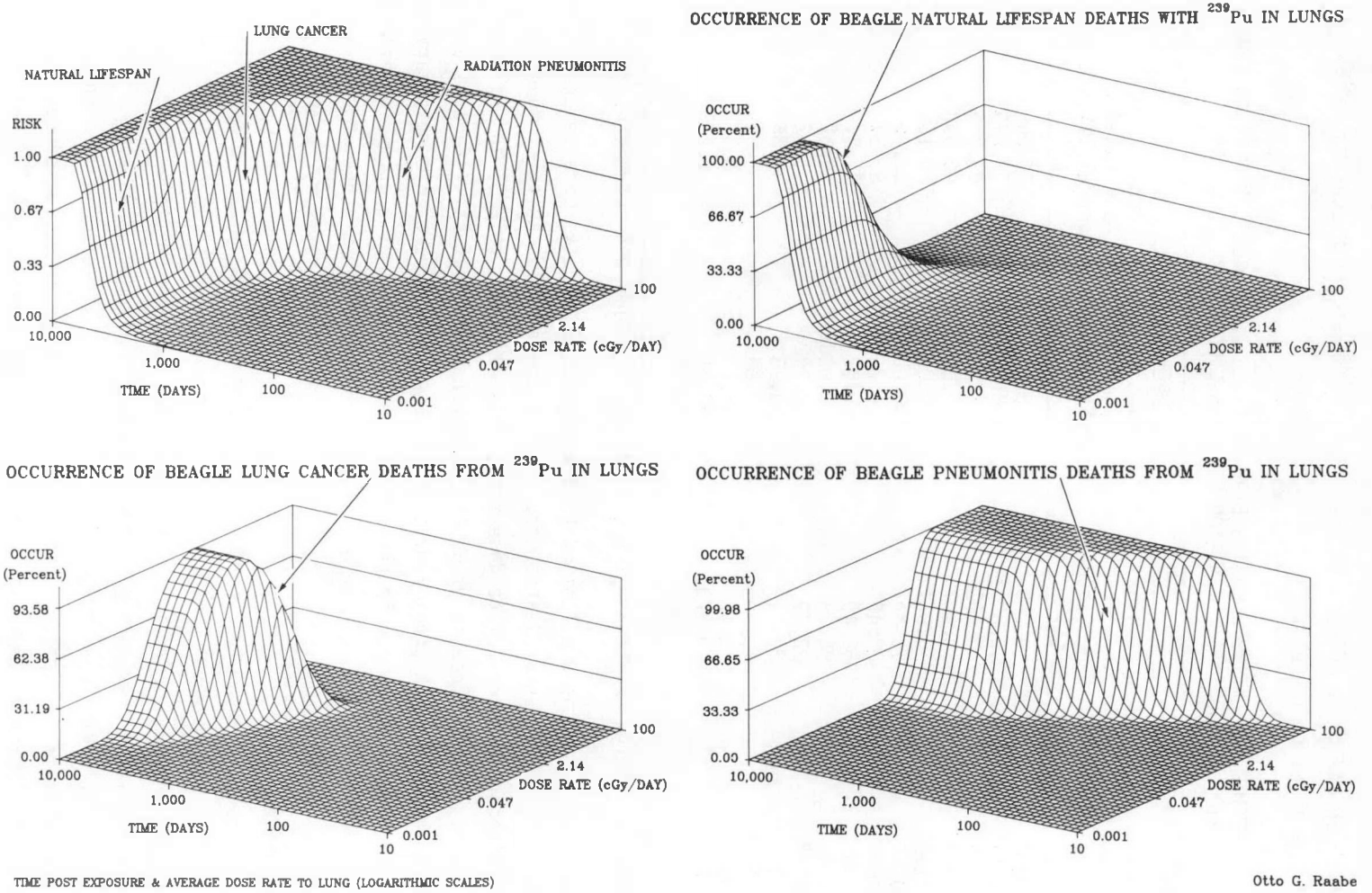

Fig. 3. Three-dimensional representation in the first panel of the dose-rate/time/response relationships of Figures 1 and 2 given as the cumulative distribution, $F_{\mathcal{C}}(t,\overline{D})$, of the combined risk of dying from radiation pneumonitis, lung cancer, or from causes associated with natural lifespan for beagles with lung burdens of $^{239}PuO_2$, and in successive panels the separate occurrence percentages, Ω_i, for these three separate effects.

The actual occurrence of each fatal effect for a specific average dose-rate (as the percentage of all individuals initially at risk that succumb to that effect) depends upon the interrelationship of the competing risks. Competing risks are accounted for using mathematical stripping (Equation 2), and the resultant occurrence percentages are shown separately for each of the three effects in the remaining panels of Figure 3. Selected numerical values are given in Table 3.

Table 3. LIFETIME CUMULATIVE OCCURRENCE PERCENTAGES IN BEAGLES EXPOSED TO INHALED $^{239}PuO_2$ AEROSOLS AS A FUNCTION OF AVERAGE DOSE RATE TO LUNG*

Dose Rate, $\bar{D}$ (cGy/day)	Deaths		
	Radiation-Induced Lung Cancer (%)	Radiation Lung Pneumonitis/ Fibrosis (%)	Other Causes Associated with Natural Lifespan (%)
0.0010	0.000	0.00	100.00
0.0017	0.0001	0.00	99.9999
0.0024	0.001	0.00	99.999
0.0060	0.107	0.00	99.893
0.0100	0.804	0.00	99.196
0.0278	12.54	0.00	87.46
0.0600	38.46	0.00	61.54
0.100	58.49	0.00	41.51
0.215	80.38	0.0001	19.62
0.60	92.79	0.192	7.02
1.00	92.41	3.23	4.36
2.15	60.10	37.94	1.96
6.00	3.93	95.60	0.463
10.00	0.273	99.50	0.229
100.00	0.00	99.98	0.0178

* Calculated utilizing Equation 2 integrated over all time post-exposure.

Radiation pneumonitis deaths are limited to the highest dose rates because at intermediate dose rates lung cancer deaths occur before pneumonitis can fully develop. Lung cancer predominates at intermediate dose rates (Figure 3 and Table 3) and is seen to be low both at low dose rates (because of deaths associated with natural lifespan) and at high dose rates (because of deaths from radiation pneumonitis). There is a necessary minimum latent period for lung cancer in these experiments because of a competing effect that does not involve cancer; lung cancer does not occur earlier than about 1000 days post-exposure because of the lung cancer rate is masked at higher doses by deaths associated with pneumonitis.

The independent risk of fatal lung cancer always approaches unity with time (all are ultimately susceptible and succumb) when there are no other causes of death (Equations 5 and 6); however, at lower dose rates it takes longer to reach any specified level of risk, and this varying latent period may exceed the natural lifespan. As time elapses, the occurrence (dependent risk) may approach a constant that is much less than unity (Equation 2). This results in a practical threshold for cancer induction since, at low dose rates, Ω_2 does not approach unity with increasing time, even though F_2 does. For example, the independent lognormal risk distribution (Equations 5 and 6) for fatal lung cancer at an average ^{239}Pu dose rate of 0.0017 centigray/day predicts an incidence in beagles of 3% at ten thousand days post exposure. Beagles live about 6,500 days at

most, so the expected lifetime occurrence is only 0.0001% (1 per million) because of the limitation of natural lifespan (Equation 2 and Table 3). Similar but appropriately scaled relationships can be applied to human risk distributions.

DISCUSSION

The results of the beagle lung cancer study show the usefulness of the three-dimensional graphical analysis of the dose-rate/time/response relationships. The method has proved useful when several risks from chronic exposure to toxic materials or to ionizing radiation must be described and evaluated and also when the roles of the competing risks from different responses need to be elucidated. A key result of this study was to show that the risk of cancer cannot be adequately described in two dimensions. The three dimensional representation shows a mountain-like peak rising late in time out of a plane (Figure 3). This cannot be detected using a two-dimensional graph.

The variable, lifetime average dose rate, $\overline{D}$, used in this analysis was evaluated retrospectively, but must be estimated prospectively for risk assessment purposes. If the exposure conditions and appropriate toxicokinetic models are available, the average dose rate can be described as a function of time and incorporated into the three-dimensional analysis.

To apply these methods to human risk assessment, an appropriate Gompertzian function must be used that describes the normal lifespan of people, and the dose-response functions must be properly scaled to human levels, either by utilizing actual human data or by scaling from experimental animal data using appropriate response ratios.

REFERENCES

Bair, W.J. and D.H. Willard. 1962. Plutonium Inhalation Studies IV. Mortality in dogs after inhalation of $^{239}PuO_2$. Radiation Research 16:811-821.

Park, J.F., D.H. Willard, S. Marks, J.E. West, G.S. Vogt and W.J. Bair. 1962. Acute and chronic toxicity of inhaled plutonium in dogs. Health Physics 8:651-657.

Park, J.F., W.J. Bair and R.H. Busch. 1972. Progress in beagle dog studies with transuranium elements at Battelle-Northwest. Health Physics 22:803-810.

Park, J.F. and staff members of Pacific Northwest Laboratory. 1985. Pacific Northwest Laboratory Annual Report for 1984 to the DOE Office of Energy Research: Part 1, Biomedical Sciences, Battelle Pacific Northwest Laboratory, Richland, Washington; Available from NTIS, U.S. Department of Commerce, Springfield, VA 22161.

Raabe, O.G. 1984. Comparison of the carcinogenicity of radium and bone-seeking actinides. Health Phys. 46:1241-1258.

Raabe, O.G. and M. Goldman. 1979. A predictive model of early mortality following acute inhalation of PuO_2 aerosols. Radiation Research 78:264-277.

Raabe, O.G., S.A Book and N.J. Parks. 1980. Bone cancer from radium: Canine dose response explains data for mice and humans. Science 208:61-64.

Raabe, O.G., N.J. Parks, and S. A. Book. 1981. Dose-response relationships for bone tumors in beagles exposed to ^{226}Ra and ^{90}Sr. Health Physics 40:863-880.

Raabe, O.G., S.A. Book and N.J. Parks. 1983. Lifetime bone cancer dose-response relationships in beagles and people from skeletal burdens of ^{226}Ra and ^{90}Sr. Health Physics 44(Suppl. 1):33-48.

A RADIOBIOLOGICAL PERSPECTIVE ON THE CHERNOBYL ACCIDENT

M. Goldman

Radiological impacts beyond the 30-kilometer radius of the "near field" of the 1986 accident at the Chernobyl nuclear power plant will be largely attributable to two radioisotopes of cesium contained in the plume. Cesium is not strongly retained in the human body, having a biological half-life there of about 3 months. Between 1 and 2.4 million curies (3.7-8.9 Bq) were released--one third each to the European Soviet Union, to Central and Western Europe and to the remainder of the Northern Hemisphere. Of the total dose commitment, one-half was delivered in the first year and the rest will be received over the next five decades. Risk of health effects is distributed equally between Soviet and non-Soviet Europe, with little of it being borne by the larger region. Fatal cancers and cases of genetic effects and mental retardation (a consequence of fetal exposure) due to this radiation are unlikely to be numerous enough to be detected against the background of cases normally manifest in the population. Carefully designed epidemiological studies of exposed populations, particularly the 24,000 people from the evacuation zone, could yield valuable information on scaling of risk assessments from high-dose, high-rate situations to these lower-dose exposures. Amelioration of dose rates for latent health effects, which is known from animal experiments only, and could range from two to ten-fold, would also be a worthy subject for study. Data on the occurrence of myelogenous leukemia among the evacuees might be particularly valuable in this regard.

INTRODUCTION

More than a year has passed since the destruction of the Unit 4 reactor at the Chernobyl nuclear power plant. If the health toll were to be limited to the 31 rescue and fire-fighting personnel, it would be recorded as a very severe "industrial accident," somewhat analogous to a coal mine cave-in or a large construction site collapse. The fact that the fatalities were due to massive radiation doses, complicated by thermal and radiation burns, raises this tragedy to a special position, however (USSR SCUAE, 1986). Not since the atom bombings of Hiroshima and Nagasaki has the world confronted such a radiation toll. We now probably have enough information to attempt to put the potential for future health effects from Chernobyl's radioactive releases into perspective (Goldman, 1987).

Many people who were in the high-fallout area are concerned that their present and future exposure to radiation has not been accurately described. Others point out that the expected latent effects are likely to be so few in number as to be largely obscured by the normal mortality of the maturing population.

Outside of the "near-field" region (that is, outside a radius of 30 kilometers), almost all of the radiological impact can be ascribed to exposure to the volatile radionuclides, radioiodine and radiocesium, which were efficiently transported through the atmosphere. Iodine-131 (8-day half-life) dominated early concern Because of its relatively high concentration in the "far-field" Chernobyl plume and its efficient entry into our food web, concentrating in the thyroid after ingestion. However, it now appears that the radiocesium, with its wide distribution, its 30-year half-life, its beta-gamma dose

potential, and its ubiquitous distribution throughout all tissues (it is a potassium congener), poses the dominant threat to the population. Two major radiobiological factors need to be considered--actual radiation dose absorbed into tissues and the establishment of "radiation risk coefficients."

Radiocesium deposited on surfaces can present an external dose to people, but these exposures lessen as the radiocesium is washed away, as it leaches into soil, and as it decays. However, radiocesium deposited on plants, washed into waterways, and absorbed from soil into crops can be ingested and is uniformly distributed throughout the body to produce an internal radiation dose. Cesium is not strongly retained and has a biological half-life in the body of about 3 months. Practically speaking, the lifetime dose from exposure to Chernobyl's cesium is now about half completed. Most of the remaining half will be added in the next 2 years and will be complete in about a decade.

Estimates of the amount of radioactive cesium that were released from Chernobyl range from about 1 million to about 2.4 million curies (8.9×10^{16}Bq) (Goldman, 1987; Cambray et al., 1987). The 2.4-million curie value is consistent with measurements made near Chernobyl and in locations as much as 10,000 kilometers away. This amount represents almost half of the radiocesium present in the reactor at the time of the accident. At present, it appears that about one-third of the radiocesium released is in the European Soviet Union, one-third in central and western Europe, and one-third in Asia and the rest of the Northern Hemisphere. The collective population dose commitment in these regions for the next 70 years can be estimated at about 120 million person-rem (1.2 million person sieverts), which is the sum of all individual doses. About half of this collective dose has already been delivered. It is the accurate determination of the dose values that will permit the ultimate assessment of the health impact of the Chernobyl releases on the population of the earth.

Several radiation effects are involved in the "radiation risk coefficient." Most publicized is the risk of fatal cancers. The available data base from the atom bombings of Japan, from studies of large medical radiation dosage, and from other sources provides a rough estimate of 1×10^{-4} to 2×10^{-4} fatal cancers per rem, or 1×10^{-2} to 2×10^{-2} per sievert (USNAS, 1980). An absolute-risk model permits us to predict that if 1 million people each received 1 rem, about 100 to 200 additional fatal cancers would ultimately be added to the approximately 190,000 spontaneous cancers that would be expected. A newer model (USNRC, 1985) that is mainly predicated on a relative risk projection, which remains proportional to the age-specific cancer mortality rate, yields a little larger risk value for very low doses, viz., 2.3×10^{-4} fatal cancers per rem (= 2.3×10^{-2} per sievert). It is not likely that any epidemiological study could ever detect such small increments and, given the statistical variation in the data, we cannot rule out a zero increment.

Another radiation risk coefficient could be developed for genetic effects, which could be serious in heavily irradiated populations, according to some predictions. There are no human epidemiological data supporting such effects, but we know from observations on animals and plants that such effects are manifested on the basis of exposure of the reproductive cells. It is currently estimated that less than 2000 such cases will be

induced (almost all in Europe and the European part of the Soviet Union) and added to the 50 million that normally manifest in the population. As with the cancer fatality risk, it is unlikely that any ill health from genetic effects will be detected.

Otake and Schull (1984) recently used data from Hiroshima and Nagasaki to focus on a third latent radiation effect, that of possible severe mental retardation in children in who were in the 8th to 15th week of gestation at the time of irradiation. The size of the absorbed doses, the dose rate, and other factors make it difficult to transfer their model directly to the Chernobyl situation. If one were to do so, as many as 700 cases may have been induced from exposure to Chernobyl's radiation and added to the 70,000 cases that normally would be expected in the European population during 1986. If pregnant women were not immediately evacuated from the 30-kilometer "exclusion zone" around the accident site, the initially reported doses (USSR SCUAE, 1986) were sufficient to cause a doubling of the risk to this specific group (from a normal expectation of about 13 to a total of about 30).

Almost without exception, radiation risk assessments are based on analyses of populations that received high doses, usually delivered at high rates. Experimental data from animals give evidence of consistent dose rate amelioration of latent health effects. For the population doses and rates under consideration from the Chernobyl accident, I would expect that this amelioration might lead to latent health effects two to ten times less than the established models would predict.

Myelogenous leukemia is a rare disease that is relatively easily induced by whole body irradiation and has a relatively short latent period of 2 to 5 years. If the doses were received at a high enough rate by the 24,000 evacuees, and if the current risk models are correct, one might find about 26 excess cases of myeloid leukemia in the next 2 to 8 years, with the increase starting about 50 months after the accident. Almost none would normally be expected. Animal studies of this disease suggest that the risk is dose-rate dependent. There is reason to believe, too, that a dose rate reduction factor could have been operative in this situation, in which case almost no excess is likely to be detected. There is not yet a proven method by which we can accurately scale the latency and dose rate factors derived from experiments on short-lived animals to human risks. Thus it is of particular importance that a carefully designed epidemiologic study of people from the "evacuation zone" be mounted soon.

The Chernobyl accident thus provides us with some radiobiological challenges. There is a real opportunity to advance our understanding of the role of dose rate and latency by careful study of the Soviet evacuated population, exposed workers, and rescue personnel. Furthermore, for two of the latent health effects, there is a reasonable chance that significant information could be available in the next two to four years. The accurate finding of no or many fewer effects than expected, on the basis of today's models for radiation risk assessment, would have a major impact on the degree of conservatism that one might include in radiation regulations for the public.

The analysis in the Department of Energy report presents latent health risk expectations for the entire Northern Hemisphere (Goldman et al., 1987). Because of the

non-threshold nature of the models, the higher average population density in central and western Europe compared to the European part of the Soviet Union, and the distribution of population doses, the authors of the report estimated that about 50 percent of the risk would be in the European part of the Soviet Union. The lower doses, multiplied by much higher population densities, places most of the remaining 50 percent of the global risk in central and western Europe. For example, the global fatal cancer risk increment of up to 28,000 from Chernobyl's radioactive material is estimated to increase the spontaneous expectation of over 600 million by no more than 0.004 percent.

For most of these populations, the individual doses range from a fraction of a year's background radiation to 2 to 4 years' worth. On an individual basis, the associated risks are minuscule. It is the size of the population over which the dose is distributed that has received the most attention. The irony may be that even in the highest exposed groups there may never be any demonstrable deleterious effects, whereas in the lesser exposed, larger, and more distant populations, attention will be focused on any clusters of health effects that show up in the next decades. The question will be whether these effects could be a consequence of the Chernobyl accident. On the basis of what we know now, the answer is "not likely."

REFERENCES

Cambray, R.S. et al. 1987. Nucl. Energy 26: 77.

Goldman, M. 1987. Chernobyl: A radiobiological perspective. Science. 287: 622-623.

Goldman, M. et al. 1987. Health and environmental consequences of the Chernobyl nuclear power plant accident. Report DOE/ER-0332, Department of Energy, Washington, DC.

Otake, M. and W.J. Schull. 1984. Br. J. Radiol. 57: 409.

U.S. National Academy of Sciences. 1980. The effects on populations of exposure to low levels of ionizing radiation. National Academy Press, Washington, D.C.

U. S. Nuclear Regulatory Commission. 1985. Health effects model for nuclear power plant accident consequence analysis. Report NUREG/CR-4214, Government Printing Office, Washington, D.C.

U.S.S.R. State Committee on the Utilization of Atomic Energy. 1986. The accident at the Chernobyl nuclear power plant and its consequences. International Atomic Energy Agency meeting, 25 to 29 August 1986, Vienna.

PUBLICATIONS AND PRESENTATIONS

Bharadwaj, P. K., and W. K. Musker. 1987. A 1,1-Dithiocarboxylate Ligand with an Easily Derivatizable Group. Synthesis and Structure of Tris[2-(ethylamino)-cyclopent-1-ene-1-dithiocarboxylateo]bismuth(III). J. Inorganic Chem. 26(9): 1453-1455.

Book, S. A., L. S. Rosenblatt, and M. Goldman. 1986. Lifetime effects of long-term exposures to strontium-90 and radium-226 in beagle dogs. In: R. C. Thompson and J. A. Mahaffey (eds.), Lifespan Radiation Effects Studies in Animals: What Can They Tell Us? Proceedings of the 22nd Hanford Life Sciences Symposium, CONF-830951, pp. 646-659, National Technical Information Service, Springfield, VA.

Goldman, M. 1987. Chernobyl: A radiobiologic perspective. Science 238: 622-623.

Goldman, M., R. Catlin, L. Anspaugh, et al. 1987. Health and Environmental Consequences of the Chernobyl Nuclear Power Plant Accident. DOE/ER-0332, 300 p.

Goldman, M., L. S. Rosenblatt, and S. A. Book. 1986. Lifetime radiation effects research in animals: An overview of the status and philosophy of studies at UC Davis' Laboratory for Energy-Related Health Research. In: R. C. Thompson and J. A. Mahaffey (eds.), Lifespan Radiation Effects Studies in Animals: What Can They Tell Us?, Proceedings of the 22nd Hanford Life Sciences Symposium, CONF-830951, pp. 53-65, National Technical Information Service, Springfield, VA.

Hill, A., P. D. Schneider, K. C. Chelton, and N. J. Parks. 1966. Murine Model for Intracellular Therapeutic Radiation of Melanoma. Surgical Forum Volume 37: 425-427 (Extended Abstract).

Lagunas-Solar, M.C., O. F. Carvacho, L. Nagahara, A. Mishra and N. J. Parks. 1987. Cyclotron Production of No-Carrier-Added ^{206}Bi (6.24 d) and ^{205}Bi (15.31 d) as Tracers for Biological Studies and for the Development of Alpha-Emitting Radiotherapeutic Agents. Int. J. Appl. Radiat. Isotopes 38(2): 129-137.

Mishra, A. C. and N. J. Parks. 1987. Beta spectroscopy with liquid scintillation systems: applications in dosimetry of ^{90}Sr and ^{90}Y. International Journal of Applied Radiation and Isotopes 38: 455-461.

Morgan, J. P. and L. S. Rosenblatt. 1987. Canine hip dysplasia: Significance of pelvic and sacral attachment. California Veterinarian, 12-16.

Morgan, J. P., R. R. Pool and T. Miyabayashi. 1987. Primary joint disease in the shoulder of the Beagle dog. Journal of the American Veterinary Medical Association 190(5): 531-540.

Raabe, O. G. 1987. Three-dimensional dose-response models of competing risks and natural life-span. Fundamental and Applied Toxicology 8: 465-473.

Raabe, O. G. 1986. Use of three-dimensional lognormal dose-response surfaces in lifetime studies of radiation-induced cancer. In: R. C. Thompson and J. A. Mahaffey (eds.), Lifespan Radiation Effects Studies in Animals: What Can They Tell Us?, Proceedings of the 22nd Hanford Life Sciences Symposium, CONF-830951, pp. 320-342, National Technical Information Service, Springfield, VA.

Rosenblatt, L. S., S. A. Book, and M. Goldman. 1986. Effects of x-irradiation of young female beagles on life span and tumor incidence. In: R. C. Thompson and J. A. Mahaffey (eds.), Lifespan Radiation Effects Studies in Animals: What Can They Tell Us?, Proceedings of the 22nd Hanford Life Sciences Symposium, CONF-830951, pp. 629-645, National Technical Information Service, Springfield, VA.

Zidenberg-Cherr, S., N. J. Parks, and C. L. Keen. 1987. Tissue and subcellular distribution of bismuth radiotracer in the rat: considerations of cytotoxicity and microdosimetry for bismuth radiopharmaceuticals. Radiation Research 111(1): 119-129.

Cain, J. L., G. R. Cain, E. Feldman, and B. Lasley. Induction of fertile estrus in the dog. 5th Annual ACVIM Forum. San Diego, California. May, 1987.

Goldman, M. The Chernobyl Accident. Atomic Industrial Forum, Boston, Massachusetts. October 6, 1986.

Goldman, M. The Accident at Chernobyl. Grappling with Risk Assessment Conference. Sponsored by U.C. Toxic Substances Research and Teaching Program, U.C. Division of Agricultural and Natural Resources, California Department of Health Services, and U.S. Forest Service; Granlibakken, Lake Tahoe, California. October 6, 1986.

Goldman, M. The Accident at Chernobyl: Biomedical and Environmental Impact. Laboratory for Energy-Related Health Research, University of California, Davis, California. November 5, 1986.

Goldman, M. The Accident at Chernobyl. Health Physics Society, San Diego Chapter, San Diego, California. November 6, 1986.

Goldman, M. The Accident at Chernobyl. Rio Grande Health Physics Society, Santa Fe, New Mexico. November 7, 1986.

Goldman, M. Keynote Address. Society for Risk Analysis, Boston, Massachusetts. November 11, 1986.

Goldman, M. The Accident at Chernobyl. American Nuclear Society, Bethesda, Maryland. November 15, 1986.

Goldman, M. Health and Environmental Consequences in Exposed Populations: DOE/OHER Chernbyl Committee Report. The Commission of the European Communities. Brussels, Belgium. February 3-5, 1987.

Goldman, M., L. R. Anspaugh and R. J. Catlin. Radiobiological significance of the Chernobyl accident. Eighth International Congress of Radiation Research, Edinburgh, Scotland, July 19-14, 1987.

Meyers, F.J., P.H. Gumerlock, S.P. Kokoris, B. Foster, and T. G. Kawakami. Detection of an Activated c-N-ras Oncogene in Radiation-induced Canine ANLL. Genetics Department Symposium, Lake Tahoe, CA. July, 1987.

Raabe, O. G., Regional Deposition and Pulmonary Distribution of Inhaled Monodisperse Aerosol Particles in Small Laboratory Animals. University of California, Davis, CA, November 12, 1986

Raabe, O. G., Basis for Particle size-selective sampling for Beryllium. Advances in Air Sampling, sponsored by the American Conference of Government Industrial Hygienists. Invited speaker, Asilomar, Pacific Grove, CA, February 15-17, 1987.

Raabe, O. G. Risk Estimation for Bone Cancer from ^{226}Ra Utilizing Three-dimensional Response Surfaces. 32nd Annual Meeting of the Health Physics Society, Salt Lake City, Utah, July 5-10, 1987.

Raabe, O. G., Some Aspects of the Radium/Strontium Toxicity Studies at the University of California, Davis. Department of Energy Special Meeting on Beagle Life Span Studies, June 14-16, 1987, Salt Lake City, UT (Invited Speaker).

LABORATORY FOR ENERGY-RELATED HEALTH RESEARCH PERSONNEL

LABORATORY FOR ENERGY-RELATED HEALTH RESEARCH
PERSONNEL

Administrative Staff

James W. Overstreet	Director
Otto Raabe	Associate Director for Science
Cecilia Bauernhuber	Management Services Officer

Clerical

[1]Charles Baty	Administrative Assistant	Debbie Hicks	Secretary
Pamela Carroll	Sr Word Proc Specialist	Donna Madding	Secty/Receptionist
[1]Laura Creely	Principal Clerk	Diane Schroeder	Financial Assistant
Cathy Diaz	Administrative Assistant		

Professional Staff

Gary Cain	Sr. Veterinarian	Leon Rosenblatt	Biostatistician
M. Roger Culbertson	Pathologist	John Schwind	Electronics Engin
Marvin Goldman	Radiologist	William Spangler	Pathologist
Thomas Kawakami	Cancer Biologist	Russell White	Clin Veterinarian
Joe Morgan	Radiologist	[1]Teresa Wolfe	Asst Veterinarian
Norris Parks	Radiochemist	Sheri Zidenberg-Cherr	Assoc Res Nutritionist
Roy Pool	Pathologist		

Technical Staff

Mohammed Al Bayati	[2]SRA-Aerosol	Steven Maslowski	An Resources Mgr
[1]Martha Conard	SRA-Histology	Lynne Morrin	SRA-Clin Lab Science
Norman Cone	SRA-Toxicology	[1]Susan Munn	SRA-Clin Lab Science
[1]Bradley Foster	SRA-Biochemistry	Maximita Nasr	SRA-Biochemistry
Fiorella Gielow	SRA-Radiochemistry	[1]David Silberman	SRA-Chemistry
John Henderson	SRA-Toxicology	Sophie Soo	SRA-Bone Pathology
Debra Johnson	SRA-Biochemistry	Roger Sullivan	SRA-Pathology
Tom Kellner	RA-Toxicology	Steve Teague	SRA-Aerosol
[1]A. Kimi Klein	SRA-Exptl Hematol	Dale Uyeminami	SRA-Aerosol

---

[1]Terminated
[2]Staff Research Associate
[3]Associated Western University Staff (summer only)

Data Processing

Victor Pietrzak	Programmer/Analyst

Laboratory Services

Donald Ballard	Sr Lab Mechanician	[1]Evelyn Profita	EH&S Officer
Steve Eckberg	EH&S Officer	Patrice Rodgers	EH&S Officer
Carl Foreman	EH&S Officer		

Animal Technicians

Scott Hammond	Asst Animal Tech	Lisa Reis	Asst Animal Tech
Rafael Montoya	Asst Animal Tech	[1]Kiyo Senda	Pr Animal Tech
[1]Carol Rasmussen	An Health Tech		

Postdoctoral Scientists

Parmal Baradwaj
[1]Takayoshi Miyabayashi

Graduate Students

Awanish Mishra

[3]AWU Staff

Jamie Anderson
Ross Morgan
Jennifer Nystrom
Cynthia Stevens
Barry Taylor

Student Assistants

[1]Scott Folwarkow
Hosna Mogaddedi
Barry Taylor

ADVISORY COMMITTEE AND COLLABORATORS

ADVISORY COMMITTEE AND COLLABORATORS

University of California Advisory Committee

A G Hendrickx Chairman	Anatomy
E L Barrett	Food Science & Technology
T A Cahill	Physics
R D Cardiff	Medical Pathology
G DeNardo	Radiology

Extramural Collaborators

L Anspaugh	Radiation Effects	Lawrence Livermore Laboratory, Livermore
S A Book	Epidemiological Studies	Department of Health Services, Berkeley
P K Bharadwaj	Chemistry	India Institute of Technology, Kampur, India
R Catlin	Radiation Effects	Electric Power Research Institute, Menlo Park
R A Champlain	Oncology/Hematology	University of California, Los Angeles
K C Chelton	Radiobiology	Tomales Psychotherapy Training Program, Santa Rosa
S R Cooper	Chemistry	Inorganic Chemistry Laboratory, The University of Oxford, UK
T Feinstat	Gastroenterology	Laurel Hills Medical Center, Sacramento
T E Fritz	Radiation Effects	Argonne National Laboratory, Illinois
R P Gale	Oncology/Hematology	University of California, Los Angeles
W R Harris	Chemistry	University of Missouri, St. Louis, Missouri
S J Hood	Skeletal Studies	Thomas J. Watson Research Center, IBM, Corp., Yorkton Heights, New York
W S S Jee	Skeletal Studies	University of Utah, Salt Lake City, Utah
A T Keane	Center for Human Radiobiology	Argonne National Laboratory, Illinois
D W Later	Chemical Methods & Kinetics	Battelle Northwest Laboratories, Richland, Washington
J F Remsen	Biochemistry	California Dept. of Food and Agriculture Sacramento
R Schlenker	Skeletal Studies	Argonne National Labororatory, Illinois
T Seed	Division of Biological/ Medical Research	Argonne National Laboratory, Illinois
J N Stannard	Radiobiology	University of California, San Diego

University of California, Davis, Collaborators

B Arbuckle	Chemistry
J W Brewer	Mechanical Engineering
A R Buckpitt	Vet Pharmacology & Toxicology
R D Cardiff	Medical Pathology
A Hendrickx	Calif Primate Research Center
A S Hill	Surgery, UCD Medical Center
R S Holdstock	Environmental Health & Safety
D Hsieh	Environmental Toxicology
D Katz	Medical Reproductive Biology
C Keen	Nutrition
J Knaak	Calif Dept Food Agriculture
L Wiley	Medical Reproductive Biology
F J Meyers	Medical Hematology/Oncology
J P Morgan	VM Radiological Sciences
J E Moulton	Veternary Pathology
K W Musker	Chemistry
R R Pool	Pathology
P Schneider	Surgery, UCD Medical Center
B W Wilson	Avian Sciences
S Zidenberg-Cherr	Nutrition

AUTHOR INDEX

AUTHOR INDEX